

ANALYSIS ON THE POTENTIAL IMPLICATIONS OF A TERRORIST ATTACK AT  
U.S. SPENT NUCLEAR FUEL STORAGE FACILITIES

By

Derek Joe Favret

Thesis

Submitted to the Faculty of the  
Graduate School of Vanderbilt University  
in partial fulfillment of the requirements

for the degree of

MASTER OF SCIENCE

in

Physics

August, 2006

Nashville, Tennessee

Approved:

Professor Michael G. Stabin

Professor Frank L. Parker

# TABLE OF CONTENTS

	Page
LIST OF TABLES .....	iv
LIST OF FIGURES .....	vi
LIST OF ABBREVIATIONS .....	x
Chapter	
I. INTRODUCTION .....	1
II. BACKGROUND .....	3
The U.S. Commercial Nuclear Reactor Complex .....	3
Probability of an Attack on a Spent Fuel Pool .....	17
Radionuclides of Concern in Spent Fuel Accident .....	25
Cesium-137 .....	29
Strontium-90 .....	38
Chernobyl Accident .....	40
Environmental Effects .....	43
Human Exposure Effects .....	45
Exclusion Zone .....	51
Dispersion Modeling .....	53
Radiation Exposure Modeling .....	58
Determination of Environmental Cleanup Goals .....	62
Regulations Pertaining To Remediation .....	63
NRC Regulations .....	64
EPA Regulations .....	65
Other Regulations .....	66
Approaches to Remediation .....	66
NRC/EPA Memorandum of Understanding .....	69
III. METHODS AND MATERIALS .....	71
Chernobyl Exclusion Zone Characterization .....	71
Site Selection .....	72
Dispersion Modeling .....	73
Radiation Exposure Modeling .....	76

IV. RESULTS .....	79
Chernobyl Exclusion Zone Characterization .....	79
Site Selection .....	81
Dispersion Modeling .....	83
Rural Scenario .....	83
Urban Scenario .....	88
Radiation Exposure Modeling .....	92
Rural Scenario .....	92
Urban Scenario .....	102
V. DISCUSSION .....	109
Human Health Effects .....	110
Environmental Effects .....	118
Psychosocial and Economic Impacts .....	122
VI. CONCLUSION .....	128
REFERENCES .....	131

## LIST OF TABLES

Table	Page
2-1 Fission products formed in nuclear reactor core .....	27
2-2 Causes of the Chernobyl Accident .....	42
2-3 Current estimate of Chernobyl radionuclide release .....	42
2-4 Acute Radiation Syndromes .....	45
2-5 RESRAD family of codes .....	57
2-6 Consultation Triggers for Residential and Commercial/Industrial Soil Contamination .....	70
3-1 HPAC parameter descriptions .....	75
3-2 RESRAD scenario pathways .....	77
3-3 RESRAD default parameters .....	77
4-1 Five smallest populations within 30-km of U.S. reactor sites .....	82
4-2 Five largest populations within 30-km of U.S. reactor sites .....	83
4-3 HPAC parameter values utilized in rural and urban scenarios .....	83
4-4 Monthly dispersion results in rural scenario .....	86
4-5 Radiological dispersion results in rural scenario .....	87
4-6 Monthly dispersion results in urban scenario .....	90
4-7 Radiological dispersion results in urban scenario.....	91
5-1 Protective Action Guidelines .....	111
5-2 Countermeasures to reduce external and internal exposure .....	113
5-3 ICRP Risk Coefficients.....	116

5-4	Comparison of released activities for select radionuclides.....	118
5-5	Radionuclide Surface Soil Action Levels for Rocky Flats .....	124

## LIST OF FIGURES

Figure	Page
2-1	Locations of nuclear power plants in the United States .....3
2-2	Nuclear reactor vessel .....4
2-3	Power-producing side of a NSSS .....7
2-4	Cross-sectional view of a PWR .....8
2-5	PWR steam generator .....9
2-6	Cross-sectional view of a BWR .....10
2-7	Layout of spent fuel pool and transfer system for a typical PWR .....11
2-8	Schematic section through a PWR reactor .....12
2-9	Layout of spent fuel pool and transfer system for a typical BWR .....12
2-10	Schematic section through a G.E. Mark I BWR reactor .....13
2-11	Spent fuel pool .....14
2-12	PUREX reprocessing plant .....17
2-13	Fission product curve .....26
2-14	$^{137}\text{Cs}$ decay scheme .....30
2-15	Annual average $^{137}\text{Cs}$ deposition in the midwestern U.S. and average annual $^{137}\text{Cs}$ level in the Chicago adult diet .....33
2-16	Average whole body $^{137}\text{Cs}$ activity in Norwegian reindeer herders .....34
2-17	$^{90}\text{Sr}$ decay scheme .....39
2-18	Chernobyl-4 Reactor .....43
2-19	Radioactive contamination in areas around Chernobyl reactor .....44
2-20	Chernobyl Exclusion Zone .....52

2-21	Plume dispersion showing Gaussian distributions in horizontal and vertical directions .....	54
2-22	RESRAD environmental pathways .....	60
2-23	RESRAD pathway model .....	61
2-24	Depiction of radiation and chemical paradigm for cancer risk management .....	68
4-1	Terrestrial density of $^{137}\text{Cs}$ contamination at Chernobyl .....	80
4-2	Terrestrial density of $^{90}\text{Sr}$ contamination at Chernobyl .....	80
4-3	$^{137}\text{Cs}/^{90}\text{Sr}$ activity ratio in soil at Chernobyl .....	81
4-4	30-km zones around U.S. reactor sites .....	82
4-5	HPAC dispersion in rural scenario .....	86
4-6	Estimates of TEDE at 2 days, rural scenario .....	87
4-7	Estimates of TEDE at 6 days, rural scenario .....	88
4-8	HPAC dispersion in urban scenario .....	90
4-9	Estimates of TEDE at 2 days, urban scenario .....	91
4-10	Estimates of TEDE at 6 days, urban scenario .....	92
4-11	Annual dose from radionuclide contamination within $3.7 \text{ GBq m}^{-2}$ contour, rural scenario .....	93
4-12	$^{134}\text{Cs}$ dose contribution within $3.7 \text{ GBq m}^{-2}$ contour, rural scenario .....	93
4-13	$^{137}\text{Cs}$ dose contribution within $3.7 \text{ GBq m}^{-2}$ contour, rural scenario .....	94
4-14	$^{90}\text{Sr}$ dose contribution within $3.7 \text{ GBq m}^{-2}$ contour, rural scenario .....	94
4-15	$^{106}\text{Ru}$ dose contribution within $3.7 \text{ GBq m}^{-2}$ contour, rural scenario .....	95
4-16	$^{125}\text{Sb}$ dose contribution within $3.7 \text{ GBq m}^{-2}$ contour, rural scenario .....	95
4-17	Annual dose from radionuclide contamination within $0.37 \text{ GBq m}^{-2}$ contour, rural scenario .....	96

4-18	$^{134}\text{Cs}$ dose contribution within 0.37 GBq m <sup>-2</sup> contour, rural scenario .....	97
4-19	$^{137}\text{Cs}$ dose contribution within 0.37 GBq m <sup>-2</sup> contour, rural scenario .....	97
4-20	$^{90}\text{Sr}$ dose contribution within 0.37 GBq m <sup>-2</sup> contour, rural scenario .....	98
4-21	$^{106}\text{Ru}$ dose contribution within 0.37 GBq m <sup>-2</sup> contour, rural scenario .....	98
4-22	$^{125}\text{Sb}$ dose contribution within 0.37 GBq m <sup>-2</sup> contour, rural scenario .....	99
4-23	Annual dose from radionuclide contamination within 0.037 GBq m <sup>-2</sup> contour, rural scenario .....	99
4-24	$^{134}\text{Cs}$ dose contribution within 0.037 GBq m <sup>-2</sup> contour, rural scenario .....	100
4-25	$^{137}\text{Cs}$ dose contribution within 0.037 GBq m <sup>-2</sup> contour, rural scenario .....	100
4-26	$^{90}\text{Sr}$ dose contribution within 0.037 GBq m <sup>-2</sup> contour, rural scenario .....	101
4-27	$^{106}\text{Ru}$ dose contribution within 0.037 GBq m <sup>-2</sup> contour, rural scenario .....	101
4-28	$^{125}\text{Sb}$ dose contribution within 0.037 GBq m <sup>-2</sup> contour, rural scenario .....	102
4-29	Annual dose from radionuclide contamination within 3.7 GBq m <sup>-2</sup> contour, urban scenario .....	103
4-30	$^{134}\text{Cs}$ dose contribution within 3.7 GBq m <sup>-2</sup> contour, urban scenario .....	103
4-31	$^{137}\text{Cs}$ dose contribution within 3.7 GBq m <sup>-2</sup> contour, urban scenario .....	104
4-32	$^{90}\text{Sr}$ dose contribution within 3.7 GBq m <sup>-2</sup> contour, urban scenario .....	104
4-33	Annual dose from radionuclide contamination within 0.37 GBq m <sup>-2</sup> contour, urban scenario .....	105
4-34	$^{134}\text{Cs}$ dose contribution within 0.37 GBq m <sup>-2</sup> contour, urban scenario .....	105
4-35	$^{137}\text{Cs}$ dose contribution within 0.37 GBq m <sup>-2</sup> contour, urban scenario .....	106
4-36	$^{90}\text{Sr}$ dose contribution within 0.37 GBq m <sup>-2</sup> contour, urban scenario .....	106
4-37	Annual dose from radionuclide contamination within 0.037 GBq m <sup>-2</sup> contour, urban scenario .....	107
4-38	$^{134}\text{Cs}$ dose contribution within 0.037 GBq m <sup>-2</sup> contour, urban scenario .....	107



4-39	$^{137}\text{Cs}$ dose contribution within $0.037 \text{ GBq m}^{-2}$ contour, urban scenario .....	108
4-40	$^{90}\text{Sr}$ dose contribution within $0.037 \text{ GBq m}^{-2}$ contour, urban scenario .....	108
5-1	Comparison of NRC and EPA Remediation Criteria .....	121

## LIST OF ABBREVIATIONS

ANL	Argonne National Laboratory
ALARA	As Low As Reasonably Achievable
ARARs	Applicable or Relevant and Appropriate Requirements
Bq	Becquerel
BWR	Boiling Water Reactor
cSv	centi-Sievert
CBRNE	Chemical, Biological, Radiological, Nuclear and High Explosives
CFR	Code of Federal Regulations
CERCLA	Comprehensive Environmental Response, Compensation, and Liability Act
Ci	Curie
DNA	Defense Nuclear Agency
DTRA	Defense Threat Reduction Agency
DoD	Department of Defense
DOE	Department of Energy
DCFs	Dose Conversion Factors
EPA	Environmental Protection Agency
GBq	Giga-Becquerel
GWt	Giga-Watt thermal
Gy	Gray
HPAC	Hazard Prediction and Assessment Capability
HEAST	Health Effects Assessment Summary Tables

IAEA	International Atomic Energy Agency
ICRP	International Commission on Radiation Protection
ITRC	Interstate Technology and Regulatory Council
kBq	kilo-Becquerel
LNT	Linear No-Threshold
LTR	License Termination Rule
MCLs	Maximum Contamination Limits
MCi	Mega-Curie
MeV	Mega-Electron Volts
MWt	Mega-Watt thermal
MOU	Memorandum of Understanding
MTU	Metric Tons of Uranium
$\mu$ Ci	micro-Curie
$\mu$ Sv	micro-Sievert
mrem	milli-roentgen equivalent man
mSv	milli-Sievert
nCi	nano-Curie
NCRP	National Council on Radiation Protection
NCP	National Contingency Plan
NUREG	NRC technical report
NEA	Nuclear Energy Agency
NRC	Nuclear Regulatory Commission
NSSS	Nuclear Steam Supply System

pCi	pico-Curie
PUREX	Plutonium Uranium Extraction
PWR	Pressurized Water Reactor
PB	Prussian Blue
RDD	Radiological Dispersal Device
RASCAL	Radiological Assessment for Consequence Analysis
RBMK	Reactor Bolshoy Moshchnosty Kanalny
RESRAD	Residual Radiation
SDWA	Safe Drinking Water Act
SCIPUFF	Second-order Closure Integrated Gaussian Puff
TMI	Three Mile Island
tU	tons Uranium
TEDE	Total Effective Dose Equivalent
UIAR	Ukrainian Institute of Agricultural Radiology
UN	United Nations
UNSCEAR	United Nations Scientific Committee on the Effects of Atomic Radiation
WHO	World Health Organization

## CHAPTER I

### INTRODUCTION

On 11 September 2001, the world learned of the great lengths to which terrorists are now prepared to go to attack their enemies. Attacks using aircraft, land- or water-based forces, vehicle bombs, and even chemical, biological, or radiological weapons, once believed to be only remotely possible, are now considered realistic threats. Today, attacks on the U.S. commercial nuclear power industry are also considered a realistic threat. A successful attack, or sabotage, at a nuclear facility would potentially cause a devastating release of radioactive material into potentially heavily populated or major agricultural areas. While many people focus their concerns on the vulnerability of reactors themselves, an increasing number of experts are concerned with the spent fuel storage facilities, or spent fuel pools (SFPs). SFPs are a cause for concern because they are more vulnerable than the reactor containment vessels and contain much more radioactive material than the reactor core.

The purpose of this study is to analyze the potential consequences of an incident in which a SFP is targeted for terrorist activity and significant quantities of radioactive materials were released into the environment based on a worst-case scenario. Utilizing the HPAC and RESRAD modeling codes, radioactive contamination levels are generated and resulting dose/risk projections were obtained, for an attack on a rural and urban SFP which results in a zirconium fire. The environmental impacts are studied in comparison with the levels of contamination measured in the latest 30-km exclusion zone characterization at Chernobyl. Additionally, radiation dose levels for personnel remaining in the contaminated

areas are analyzed to estimate the radiation health effects that may be experienced prior to the institution of countermeasures or other protective measures. Lastly, U.S. regulatory standards, as they may apply to a terrorist attack on a SFP, are reviewed to analyze the differences between NRC and EPA approaches to determining environmental cleanup goals.

## CHAPTER II

### BACKGROUND

#### The U.S. Commercial Nuclear Reactor Complex

As of 2003, there were 103 commercial nuclear reactors operating in 31 states (Figure 2-1), all of which are classified as light-water reactors. Of these, 34 are BWRs and 69 are PWRs (Alvarez, 2003).



Figure 2-1: Locations of nuclear power plants in the United States. Circles represent sites with one reactor, squares represent plants with two, and stars represent three. Open symbols represent sites with at least one shutdown reactor (Alvarez, 2003).

In fossil-fueled power plants, water is heated by the burning of coal, oil, or natural gas and is converted to steam which drives a turbine-generator to produce electricity. In a nuclear power plant, fission energy released in the reactor produces steam, either directly in

the reactor or in auxiliary heat exchangers called steam generators, that drives the turbine-generator to produce electricity.

Figure 2-2 presents a generic drawing of the principle components of a nuclear reactor vessel, along with corresponding radiation shield and containment. The central region of the reactor vessel is called the core and contains the fuel, the moderator, and the coolant. The fuel includes the fissile isotope  $^{235}\text{U}$  and the fissionable isotope  $^{238}\text{U}$  responsible for both the criticality of the reactor and the release of fission energy.

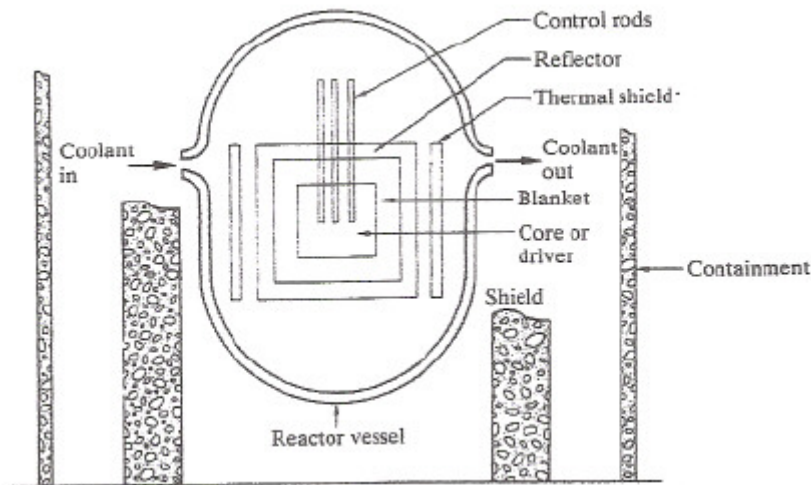


Figure 2-2: Nuclear reactor vessel (Lamarsh, 2001).

Fissioning occurs when a nucleus of a large mass number atom (referred to as a “heavy nucleus”) obtains enough energy to split in two, thus becoming more stable. For this to occur, the additional energy introduced to a nucleus by a neutron causes an altering of the attractive forces between the protons and neutrons and thus deforms the nucleus to the point where the system begins to split in two. In a reactor, energy must be supplied rapidly enough to sustain a chain reaction. This is accomplished through neutron production and absorption. When a neutron is absorbed in a heavy nucleus, the resulting isotope is formed in an excited



state at an energy level equal to the kinetic energy of the incident neutron plus the binding energy of the neutron in the isotope. If this binding energy alone is greater than the critical energy of fission (i.e. the energy required to produce a fission event) of the isotope, then fission can occur with neutrons having little or no kinetic energy. For example, when a  $^{235}\text{U}$  isotope absorbs a neutron, it becomes a  $^{236}\text{U}$  isotope. The binding energy of this neutron in  $^{236}\text{U}$  is 6.4 MeV while the critical energy of fission is only 5.3 MeV. Therefore, a neutron with no kinetic energy absorbed in  $^{235}\text{U}$  will induce a fission event, making  $^{235}\text{U}$  a fissile isotope. However, when a  $^{238}\text{U}$  isotope absorbs a neutron with no kinetic energy, the resulting isotope has a binding energy of 4.9 MeV. With a critical energy of fission of 5.5 MeV, this isotope will not undergo fission. Thus,  $^{238}\text{U}$  is considered fissionable, and not fissile, because a neutron with kinetic energy greater than 0.6 MeV is required to induce a fission event (Lamarsh, 2001).

The moderator is used to “slow down” fast neutrons to thermal energies and the coolant is used to remove heat energy from the core and other parts of the reactor where heat energy may be produced. In light-water reactors, water is utilized as both the moderator and coolant. Water is ideal because it is readily available at low cost and has thermodynamic properties that are well understood.

A “blanket” surrounds the core as shown in Figure 2-2. The blanket is used in breeder reactors for conversion of fissionable material to fissile material. As this study focuses on light-water reactors currently employed in the U.S., aspects of the breeder or converter reactors are beyond the scope of this report.

Also surrounding the core, the reflector performs a function as its name implies. A wall of moderating material is placed around the core to return neutrons to the core after one or more collisions.

Control rods are movable pieces of neutron-absorbing material and are used to control the rate of reaction in reactors. Since they absorb neutrons, any movement of the rods affects the multiplication factor of the system. The multiplication factor is defined as the measure of the rate of neutron production compared to the rate of loss in the system (Cember, 1996). A multiplication factor of 1.0 ensures a system is critical. When this factor increases, the system will become supercritical. When the factor decreases, the system will become subcritical and eventually die out.

As stated previously, most of the fission energy released in a reactor is used to produce steam, either directly in the reactor or in steam generators. The reactor or reactor-steam generator combination is called the NSSS. The NSSS serves the same function as the steam boiler in a conventional fossil-fuel plant.

Figure 2-3 illustrates the process of how steam generated in the reactor drives steam turbines, coupled to generators, to produce electricity. Turbines consist of a series of bladed wheels affixed to an axle, which rotates at high speed as steam at high temperature and pressure strikes the blades (Lamarsh, 2001). Spent steam passes into a condenser where it is cooled and condensed to water. From there, the condensed water is eventually returned back to the NSSS as feedwater.

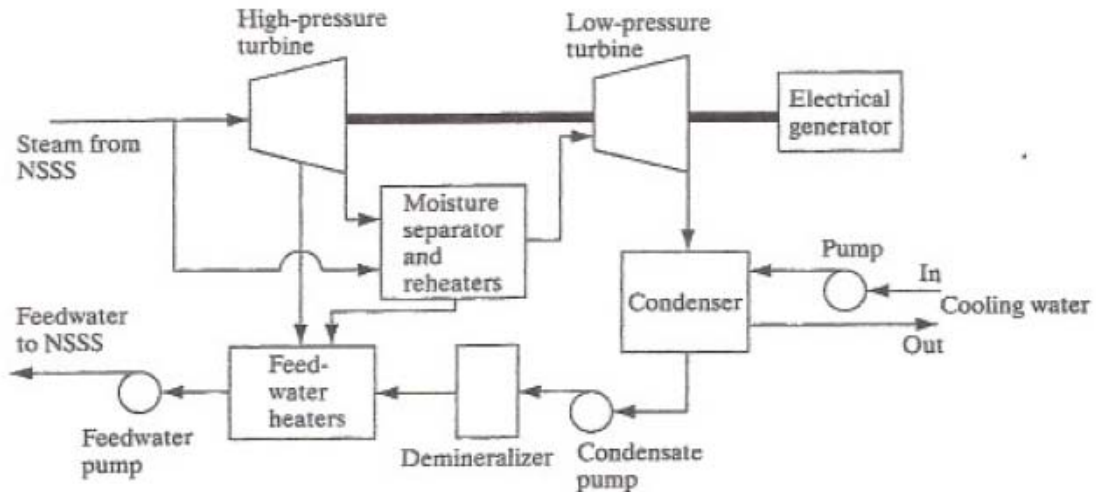


Figure 2-3: Power-producing side of a NSSS (Lamarsh, 2001).

Today, light-water reactors are the most widely used reactors in the world for producing electric power and are used exclusively for U.S. commercial reactors as either PWRs or BWRs.

Figure 2-4 provides a cross-sectional view of a PWR. As illustrated, water enters the vessel at a temperature of approximately 290°C (554°F), flows down around the outside of the core where it serves as a reflector, passes upward through the core where it is heated, and then exits from the vessel with a temperature of approximately 325°C (617°F). This water is maintained at a high pressure (approximately 2250 psi) and will not boil (Lamarsh, 2001).

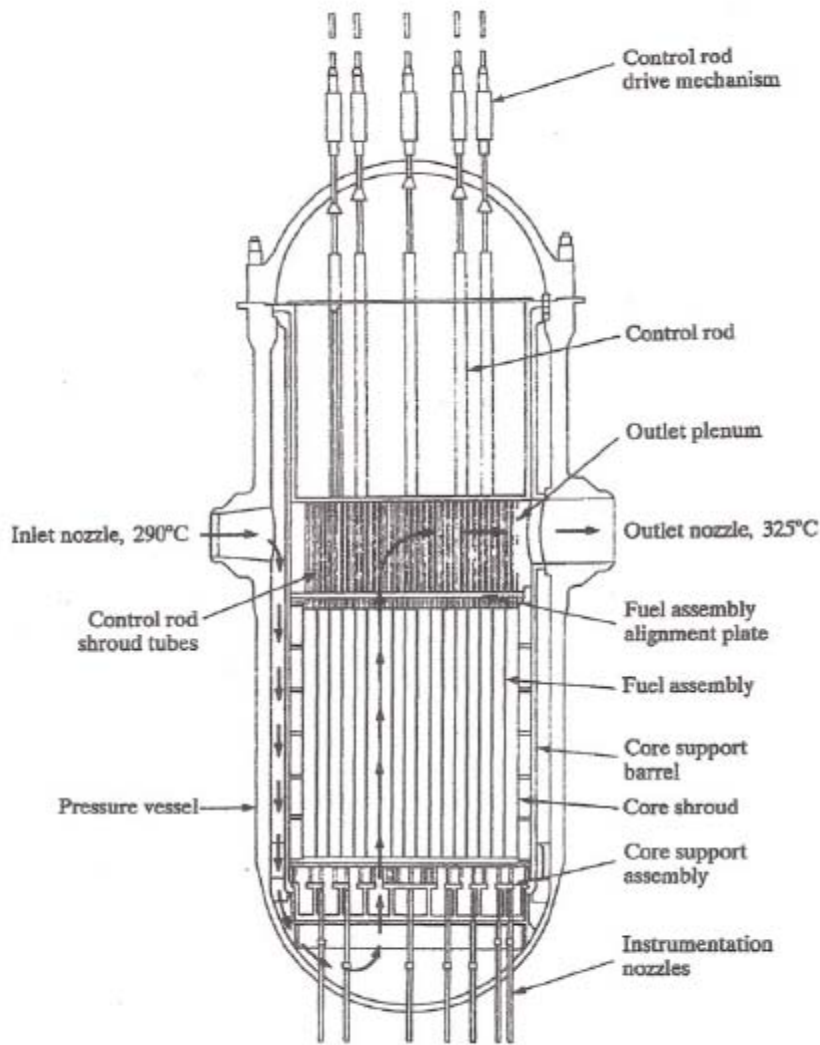


Figure 2-4: Cross-sectional view of a PWR (Lamarsh, 2001).

Because the water does not boil in the reactor, steam must be produced in steam generators (see Figure 2-5). High temperature and pressure water is passed through several thousand tubes in “U” shapes. The outer surfaces of these tubes are in contact with lower pressure and cooler water, causing it to boil and produce “wet” steam in the evaporator section of the generator. The wet steam passes into the steam drum section where it is dried before exiting to the turbines.

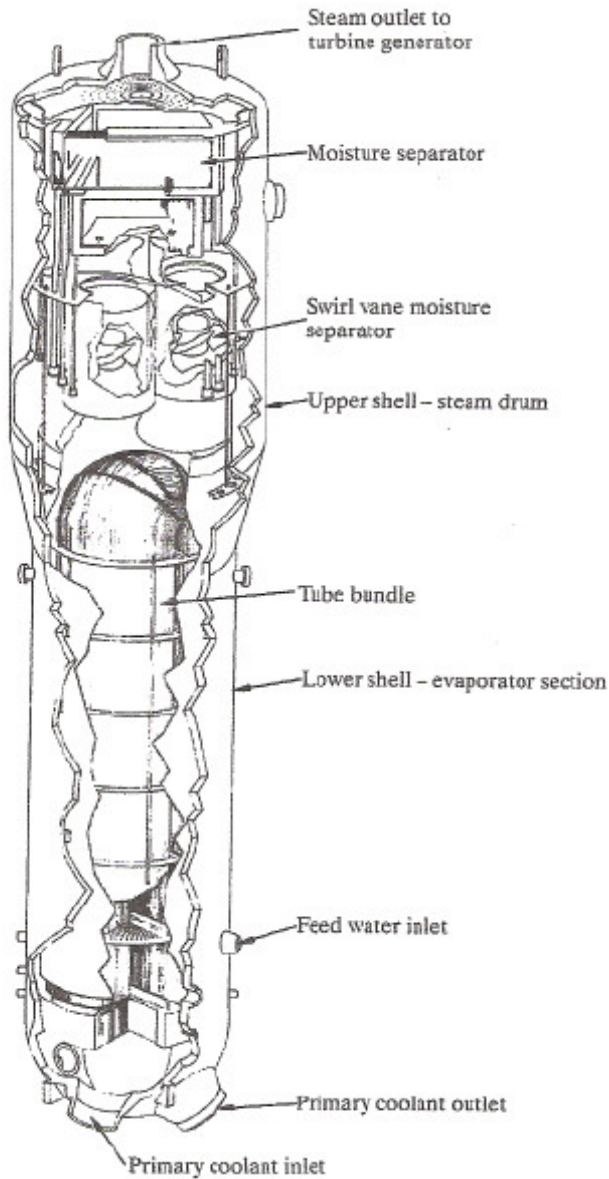


Figure 2-5: PWR steam generator (Lamarsh, 2001).

A cross-sectional view of a BWR is included in Figure 2-6. As depicted, water passes upward through the reactor core where a portion of the coolant becomes vaporized. The mixture of steam and liquid water is separated in the steam separator. The steam is further separated in the dryer. All wet liquid from the steam separator and dryer mix with

feedwater returning from the condenser to the core. The dry steam exits the reactor via the steam line to the turbines as discussed previously.

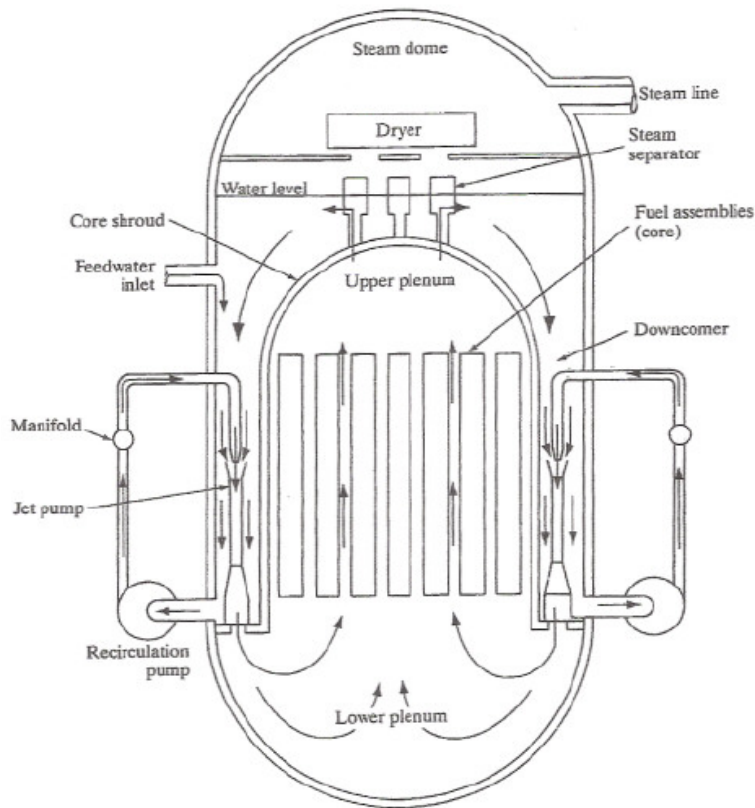


Figure 2-6: Cross-sectional view of a BWR (Lamarsh, 2001).

Due to the design differences of PWRs and BWRs, there are a variety of advantages and disadvantages of each. For instance, less water is pumped through a BWR per unit time because more heat can be absorbed as latent heat (i.e. heat necessary to vaporize a liquid) in a BWR than as sensible heat (i.e. heat only changes the temperature of a fluid) in a PWR. Secondly, the water passing through a BWR core becomes slightly radioactive and thus all components of the steam utilization system must be shielded. The pressure necessary in a BWR is only one-half the value required in a PWR so reactor vessel walls are not required to

be as thick. Lastly, the power density is smaller in a BWR so the overall dimensions of the reactor vessel must be larger than required in a PWR.

In all reactors, the nuclear fuel elements must be periodically removed from the core and replenished with new fuel so that criticality will be sustained, due to the fissioning of uranium during reactor operations. When this occurs, a reactor is shut down to transfer fuel to spent fuel pools. About one-third of the fuel in the core is replaced during each refueling cycle although some operations commonly offload the entire core into the SFP (NAS, 2006).

Although SFPs have a variety of designs, almost all are located outside of the containment structure holding the reactor vessel. Figures 2-7 and 2-8 illustrate SFP layouts for PWRs outside the reactor vessel. Figure 2-9 illustrates a layout for a SFP located outside the reactor vessel in a BWR while Figure 2-10 illustrates a SFP located inside a reactor vessel.

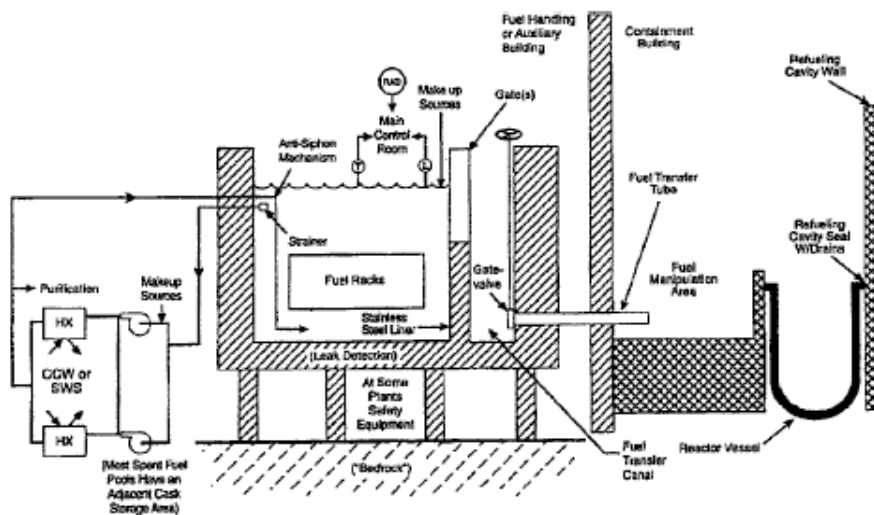


Figure 2-7: Layout of spent fuel pool and transfer system for a typical PWR (Alvarez, 2003).

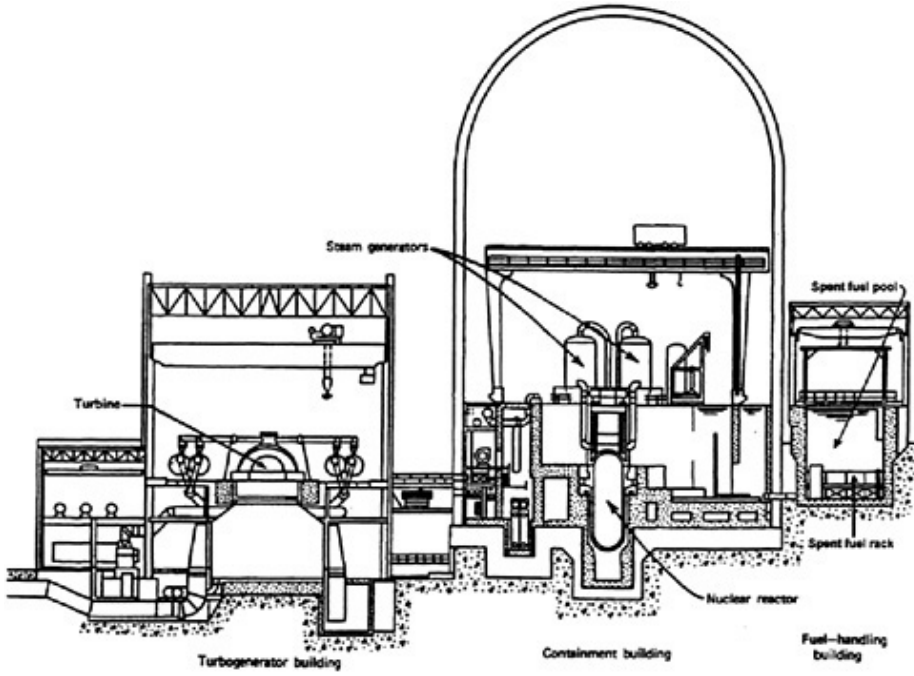


Figure 2-8: Schematic section through a PWR reactor (NAS, 2006).

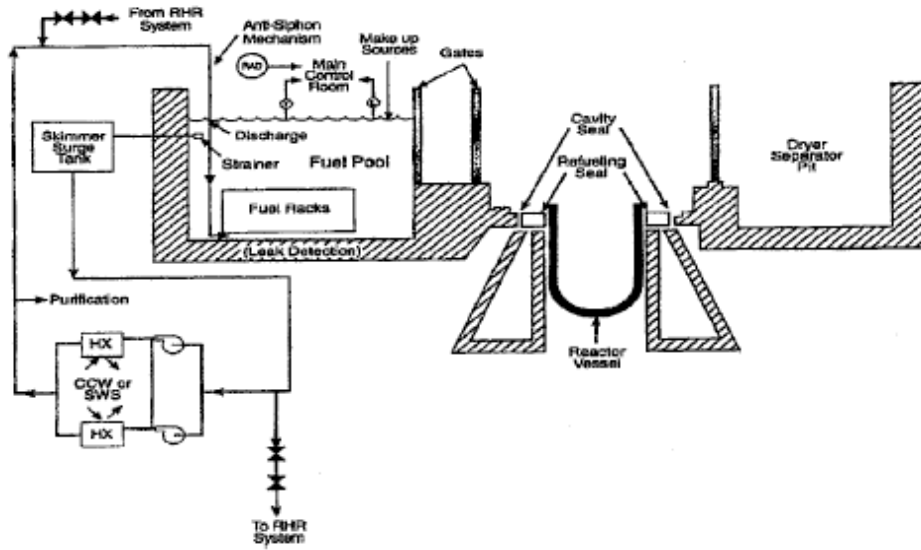


Figure 2-9: Layout of spent fuel pool and transfer system for a typical BWR (Alvarez, 2003).



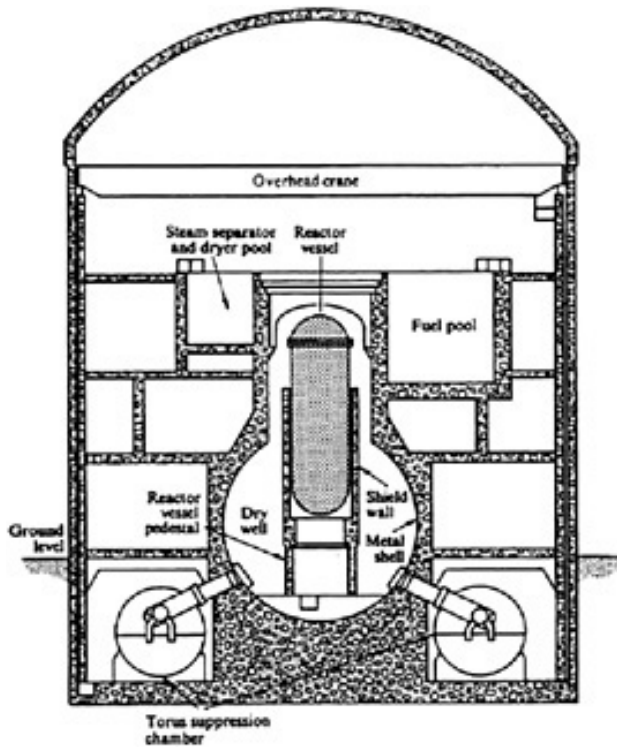


Figure 2-10: Schematic section through a G.E. Mark I BWR reactor (NAS, 2006).

Whether located inside or outside the containment facility, SFPs are designed to withstand a variety of insults, mostly naturally occurring events such as earthquakes and tornado-propelled debris. Nearly all are constructed as a “pool within a pool” with a stainless steel inner pool situated within a steel-reinforced concrete outer pool but are open to the surrounding structure at its surface (see Figure 2-11). SFPs within the reactor building are typically constructed with about 2 feet of reinforced concrete. For SFPs located outside the containment structure (see Figure 2-8), one or more walls may be located on the exterior wall of an auxiliary building that is located adjacent to the containment building. The enclosing superstructure above the pool are typically steel, industrial-type buildings designed to house cranes used to move reactor components, spent fuel and spent fuel casks (NAS, 2006). For

added safety, there are no drains or low-level pathways to allow water to exit the pool.

Typical pool depths are between 12 and 15 meters with a total volume of 4,000 to 5,000 m<sup>3</sup>.

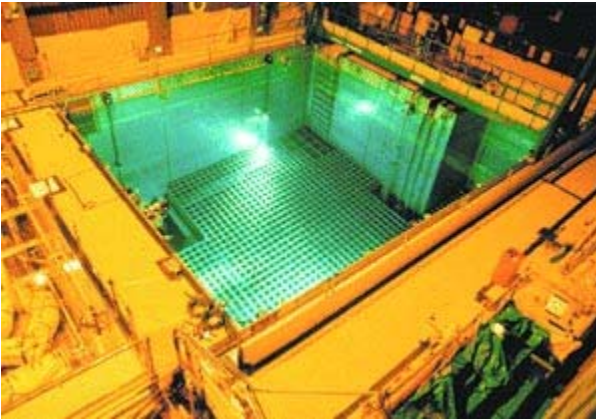


Figure 2-11: Spent fuel pool (NRC, 2003).

Spent fuel is stored in 4-meter high racks near the bottom of the pool which results in approximately 30 feet of water above. Racks have feet to provide space between their bottoms and the pool floor. There is also space between the sides of racks and the steel pool liners for circulation of water.

As depicted specifically in Figures 2-8 and 2-10 above, the general elevation of the spent fuel pool matches that of the vessel containing the reactor core. PWR designs use comparatively shorter reactor vessels that are closer to ground level. In contrast, BWR vessels are taller, resulting in a more elevated SFP.

All of these factors (i.e. location with respect to ground level, presence of surrounding shielding structures, etc.) contribute to the general vulnerability of the SFP to terrorist attack.

Over the past four decades, approximately 50,000 MTU of spent fuel have been generated. A typical nuclear power plant generates about 20 MTU per year with the entire industry generating approximately 2000 MTU per year. Of all the spent fuel generated to

date, approximately 87% is stored in SFPs with the remaining stored in dry storage. SFPs exist at all sites with operating nuclear power reactors and at 8 sites where reactors are no longer operating (i.e. reactors that have been shut down or decommissioned) (NAS, 2006).

Each year, about one third of the core fuel is discharged into the SFP. A hypothetical one GWt PWR core contains about 80 tU fuel. A pool with a 15-year storage capacity will hold about 300 tons of spent fuel. Assuming a  $^{137}\text{Cs}$  inventory at shutdown of  $3.70\text{E}6 \text{ GBq tU}^{-1}$  ( $0.1 \text{ MCi tU}^{-1}$ ) and a burn-up of  $50,000 \text{ MWt-day tU}^{-1}$  (INESAP, 2005), a pool with 300 tons of 10 year old spent nuclear fuel would hold about  $1.11\text{E}9 \text{ GBq}$  ( $30 \text{ MCi}$ )  $^{137}\text{Cs}$ . To put this activity into perspective, the Chernobyl accident, discussed in detail below, released approximately  $8.5\text{E}7 \text{ GBq}$  ( $2.3 \text{ MCi}$ ) of  $^{137}\text{Cs}$  into the atmosphere.

One alternative to long-term storage in SFPs, and ultimately disposal in a repository, is fuel reprocessing. Principally, fuel reprocessing (or recycling) is used to recover unused uranium and plutonium in the spent fuel for use in future fuel elements (i.e. closing the fuel cycle). Other applications, most notably past nuclear weapons production, utilize the reprocessed fuel as well. It is estimated that approximately 30% of the natural uranium otherwise required for fuel elements will be saved by utilizing reprocessed fuel (WNA, 2005b.). A secondary reason is to reduce the volume of material that requires disposal. With the removal of long-lived isotopes such as  $^{235}\text{U}$ ,  $^{238}\text{U}$  and  $^{239}\text{Pu}$ , the level of radioactivity will be significantly reduced after the fission products decay.

Fuel reprocessing has occurred since the 1940s. In the U.S., no commercial reprocessing plants are now in operation. Although a total of three have been built at West Valley, N.Y., Morris, IL., and Barnwell, S.C., only the West Valley plant was ever put into

operation. France, India, and Russia however, have all maintained active reprocessing plants to support their nuclear power programs.

Today, all commercial reprocessing plants use the PUREX process (WNA, 2005b.). The PUREX process is based on the fact that uranium and plutonium can exist in a number of valence (oxidation) states. Because of differences in their oxidation and reduction potentials, it is possible to oxidize or reduce one of these elements without disturbing the other (Lamarsh, 2001).

Figure 2-12 illustrates a simplified flow diagram of a PUREX reprocessing plant. In this process, the fuel rods are first cut into short lengths in the mechanical head-end portion of the plant. These pieces are then heated to remove tritium, krypton-85, and other fission product gases trapped within the fuel. The fuel is then dissolved in a concentrated solution of boiling nitric acid ( $\text{HNO}_3$ ), passes through a filter to remove undissolved components and enters the middle of the first extraction column. In this column, uranium and plutonium are extracted via an organic solvent and flow up the column. At the same time, nitric acid scrubs the solvent of any fission products and is removed at the bottom of the column. The organic solution passes to a second column where plutonium is reduced and separated from the uranium. The uranium is moved into a third column where it is stripped from the solution via  $\text{HNO}_3$  and moved to a recovery plant for purification and reuse. Each can be further purified by processing through additional extraction columns or in the case of plutonium, passing through ion exchange resins (Lamarsh, 2001).

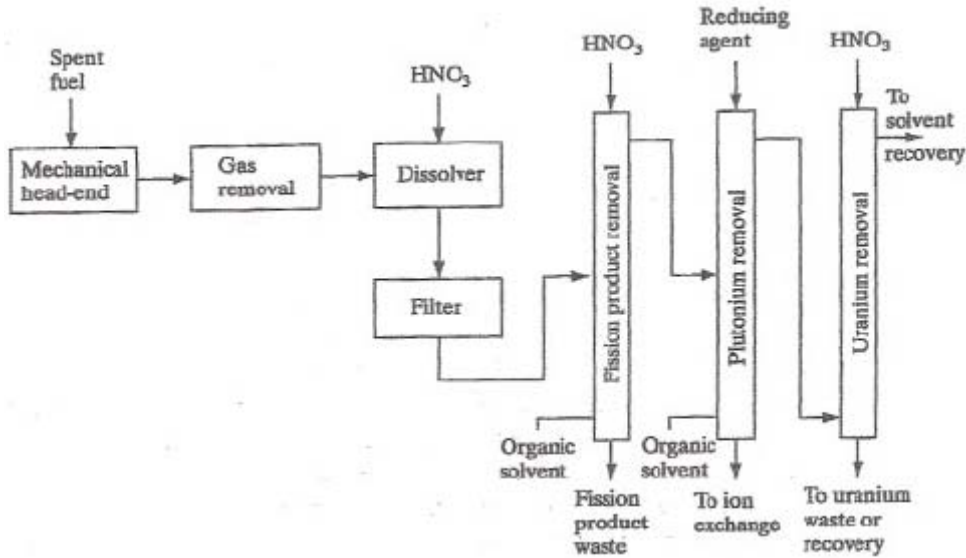


Figure 2-12: PUREX reprocessing plant (Lamarsh, 2001).

### Probability of a Spent Fuel Attack

It is generally accepted that the possibility of a serious accident or a successful terrorist attack at a nuclear power reactor, which could release large quantities of radioactive fission products to the environment, is remote. In the United States, reactor sites are some of the most guarded facilities in the country. Reactors are also designed with multiple barriers which all must fail in order for a large fission product release. In essence, the reactor fuel core must melt, the primary reactor components must be breached, and containment structures must be open to the environment. Additionally, safety systems such as reactor core flooding, containment building cooling and pressure suppression systems must all be inoperable to cause a release. With these multiple layers of safety, it would take a tremendous effort to cause a large release of fission products from the reactor vessel itself.

The TMI accident in 1979 demonstrates the requirement that many or all of the safety barriers must fail in order for a large fission product release to the environment. On March 28 in TMI Unit 2, the main feedwater pumps stopped, caused by either a mechanical or

electrical failure, preventing the steam generators from removing heat from the reactor core. When this occurred, the turbine and reactor automatically shut down causing a pressure increase in the core. In order to decrease the rising pressure, a relief valve automatically opened at the top of the pressure vessel. After sufficient pressure decrease occurred, the valve should have closed but did not. Additionally, signals at the operator station failed to show that the valve was still open. As a result, cooling water poured out through the valve causing the core to overheat. Conflicting information led operators to believe the level of water in the core to be sufficient when in fact, a loss-of-coolant event was initiating. Because adequate cooling was not available, the nuclear fuel overheated to the point where the zirconium cladding ruptured and the fuel began to melt. By the evening of March 28, the core appeared to be adequately cooled and the reactor stable.

Over the next few days, the presence of a large hydrogen bubble in the dome of the pressure vessel created concerns of an explosion or rupture, in turn leading to a breach of containment. Due to efforts to reduce the size of the bubble and a lack of oxygen, this did not occur.

After the TMI accident, small quantities of radioactive gases were measured off-site but no other radioactive materials were released from the containment facility as many previously feared would occur. Estimates are that the average dose to about 2 million people in the area was only about 0.01 mSv (1 mrem) (NRC, 2005).

The TMI event demonstrated the design safety of the nuclear reactor containment facility. Although some of the built-in safety features failed, causing the reactor core to melt, the overlapping safety measures ensured a major release of fission products to the environment did not occur.

Because of the safety features afforded to reactor vessels, most experts agree that the focus of concerns should be directed toward the SFP. The probability of an accidental or intentional event resulting in a substantial release of fission products however, has generated considerable controversy over the past few years.

In 2001, the NRC published NUREG 1738 in which the agency documented a study of SFP accident risk at decommissioned nuclear power plants. In this study, the agency confirmed that the most severe accident potential is associated with the loss of water from the pool. Depending on a number of factors (i.e. density of fuel configurations, time since spent fuel discharge from the reactor, and fuel burn up), the authors concluded that the decay heat may be sufficient enough for the fuel cladding to heat up, swell, and burst after loss of pool water. NUREG 1738 states, “The breach in the clad releases radioactive gases present in the gap between the fuel and clad (i.e. a gap release). If the fuel continues to heat up, the zirconium clad will reach the point of rapid oxidation in air. This reaction of zirconium and air, or zirconium and steam, is exothermic. The energy released from the radiation, combined with the fuel’s decay energy, can cause the reaction to become self-sustaining and ignite the zirconium. The increase in heat from the oxidation reaction can also raise the temperature in adjacent fuel assemblies and propagate the oxidation reaction. The zirconium fire would result in a significant release of the spent fuel fission products that would be dispersed from the site in the thermal plume from the zirconium fire” (NRC, 2001).

The NRC identified nine initiating event categories in the assessment of SFP risk:

1. Loss of offsite power from plant-centered and grid-related events
2. Loss of offsite power from events initiated by severe weather
3. Internal fire

4. Loss of pool cooling
5. Loss of coolant inventory
6. Seismic event
7. Cask drop
8. Aircraft impact
9. Tornado missile

The results of this study indicated that the risks at SFP were low because of the very low likelihood of a zirconium fire even though the consequences from a zirconium fire could be serious. Of the nine initiating events analyzed, only large earthquakes and cask drop events were found to be important to risk, neither of which would likely be caused by terrorist activities.

In 2003, Alvarez, et al. performed a similar analysis to investigate alternatives to densely-packed storage in SFPs. Due to the severe consequences of such a release and the inability to predict the actions of terrorists, the authors surmise the existing risk to be very real and proposed actions to minimize it. In the study, they propose physical change to SFP storage arrangements, among other things, that would correct the most obvious vulnerabilities of pools to loss of coolant and fire. The most costly of their proposals, shifting fuel to dry cask storage about five years after discharge from a reactor, would cost an estimated \$3.5 - \$7 billion for dry storage of approximately 35,000 tons of older spent fuel that would otherwise be stored in pools in 2010. For comparison, they determined property losses from the deposition downwind of the  $^{137}\text{Cs}$  released by a SFP fire would likely be hundreds of billions of dollars.



Recognizing the importance of this issue, the U.S. Congress asked the National Academies in Fiscal Year 2004 to provide independent scientific and technical advice on the safety and security of commercial spent nuclear fuel storage in the U.S. Specific charges to the National Academies committee set up for this task included analyzing potential safety and security risks of spent fuel currently stored in SFPs, potential advantages of storing fuel in dry casks and risks of terrorist attacks or theft of these materials. Congress requested a classified report addressing these charges within 6 months. The National Academies committee fulfilled this request in July 2004. In 2006, a public version of the classified report was released for public review, representing the latest views on the safety and security of commercial SFPs.

In their study, the National Academies committee reaffirmed the need for SFPs to store recently discharged fuel and that successful attacks by terrorists, though difficult, are possible. Furthermore, they indicated additional analyses are needed to more fully understand the vulnerabilities and consequences of a propagating zirconium cladding fire.

Determination of risk and severity of consequences for such an event remains a topic of debate. Within the past few years, the NRC has maintained that the likelihood of an accident (or terrorist event) leading to the critical loss of water in a SFP is very low (less than one in 100,000 per pool per year). Previously in NUREG 1738, the NRC estimated a probability for an accidental spent fuel fire as  $0.6 - 2.4 \times 10^{-6}$  per pool per year. In their analysis, Alvarez, et. al., multiplied the accident probability from NUREG 1738 by the existing 103 SFP to calculate the probability of occurrence to be 0.2 – 0.7 percent in 30 years. To estimate the increased risk due to terrorist events, they performed their analysis using the upper limit of 0.7 derived for an accident scenario. Although not reviewed for this

study, Sandia National Laboratory has recently completed a classified study relating to the probability of a successful attack at a SFP.

Similarly to the NRC and Alvarez group, the National Academies committee realized the difficulty in addressing the charge concerning risk of terrorist attacks on SFPs. They concluded that it could not address its charge using quantitative and comparative risk assessments. The committee decided instead to examine a range of possible terrorist attack scenarios in terms of their potential for damaging SFPs and dry storage casks and their potential for radioactive material releases (NAS, 2006). This allowed the committee to make qualitative judgments about the vulnerability of SFPs and the potential measures that could be taken to mitigate them.

The NRC has continually rejected the severe implications of the Alvarez report and has asserted that the possibility of a terrorist attack on a nuclear reactor complex is speculative and simply too far removed from the natural or expected consequences of agency action. Not all countries agree with the NRC stance however. France, for example, has installed anti-aircraft missiles around its SFP at its reprocessing facilities (INESAP, 2005) and German officials require dry storage casks to be stored inside a shielded building (Alvarez et al., 2003).

Many other agencies and groups have taken either side of this ongoing debate. Proponents of the nuclear industry and the NRC still maintain that the probability of such an event is extremely remote and that critics have “overestimated the likely consequence of a spent fuel fire and underestimated the ability of plant operators to cool the spent fuel in a damaged pool” (CRS, 2005). As stated previously, the latest National Academies report

stating a successful attack is possible lends credence to the counter arguments of such a probability.

The National Academies committee considered air attacks using large civilian aircraft or smaller aircraft laden with explosives, ground attacks by well-armed and well-trained individuals, attacks involving combined air and ground attacks, and thefts of spent fuel for use in a RDD.

Despite the improved security measures involving commercial air travel, the committee feels that attacks with civilian aircraft remain a credible threat. Assaults by large aircraft would impart tremendous energy impulses into targeted facilities. Additionally, the general destruction and fires created would complicate efforts to reduce the consequences of a successful attack. From the information presented during their study, the committee feels the U.S. government should implement security measures to prevent air attacks.

Ground attack scenarios investigated in this report include direct assaults by armed groups and assaults having both air and ground components. Nuclear plants are required by the NRC to maintain a professional guard force at each plant to defend against a Commission-developed design basis threat. For this study, the NRC did not provide a formal briefing to the National Academies committee for a radiological sabotage scenario. Because of this, the National Academies committee did not have enough information to judge whether the security measures taken at nuclear power plants are sufficient to defend against direct assault attacks. For attack scenarios that combine ground and air components (i.e. infiltration by ground troops followed by attacks from the air), the National Academies committee felt that some scenarios were feasible. For security reasons however, these scenarios are only discussed in the classified report.

The National Academies committee reports that theft of large quantity of spent fuel for use in a RDD is unlikely. Spent fuel would require heavy shielding to handle and heavy equipment to remove despite the controls in place to deter and detect thefts. Although theft and removal of individual fuel rods may be easier, the amount of material would be relatively small and might not be an attractive target.

The nuclear industry and the NRC have asserted that the robust construction and stringent security requirements at nuclear power plants make them less vulnerable to terrorist attack than softer targets such as chemical plants and refineries. Briefings from the Department of Homeland Security however suggested that al-Qaida initially included unidentified nuclear plants among the list of September 11, 2001 targets but eliminated them when the number of planned attacks were scaled back (NAS, 2006).

In this report, the consequences of these attacks are described as either “maximum credible releases” or “best-estimate releases.” Maximum credible releases describe the largest releases of radioactive material following an successful terrorist attack. The estimated releases described in NUREG-1738 and Alvarez et al. are considered by the committee as maximum credible releases. Best-estimate releases describe the median estimates of release and are used by the committee to describe the latest NRC analyses reviewed in preparation of their report. The difference between these scenarios are modeled and analyzed in this study.

In summary, the committee judged in their report that the plausibility of an attack on a SFP, coupled with the public fear associated with radiation in general, makes this an issue in which the possibility cannot be dismissed. Both sides of the argument have generated compelling arguments for their particular stance. Regardless of the position one favors in

this debate however, the severe consequences of such an event and the complex planning already demonstrated by well-funded terrorists make an attack on a SFP an event that should be fully investigated and understood.

### Radionuclides of Concern in Spent Fuel Accidents

As discussed previously, fission produces a very large number of fission products, ranging from atomic number 30 (zinc) to 65 (terbium) and from atomic mass number 72 to 161. Splitting of the nucleus into two equal fragments however is not the most probably mode observed. In fact, asymmetric modes are much more favorable. Maximum fission product yields for both  $^{235}\text{U}$  and  $^{239}\text{Pu}$  are depicted in Figure 2-13.

For  $^{235}\text{U}$ , the maximum fission product yields occur around atomic mass numbers 95 and 138. The  $^{239}\text{Pu}$  curve has a similar shape but the maximum yields are slightly different than  $^{235}\text{U}$ .

Table 2-1 below lists the major fission products formed, along with half-lives and yield percentages, following the fissioning of  $^{235}\text{U}$  and  $^{239}\text{Pu}$ .

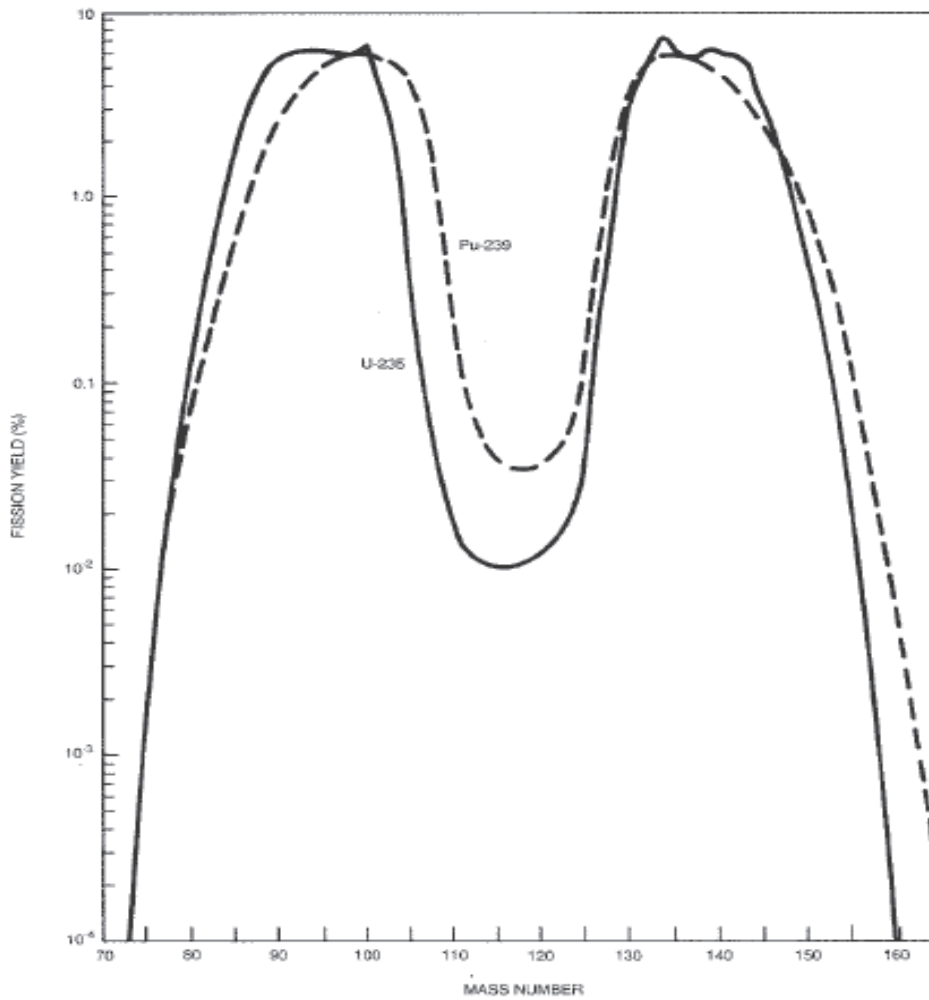


Figure 2-13: Fission product curve (NAS, 1996)

Table 2-1: Fission products formed in nuclear reactor core (NAS, 1996).

Nuclide	Half-life	Fission Yield (%)	
		<sup>235</sup> U	<sup>239</sup> Pu
<sup>84</sup> Br	31.80 m	0.967	0.444
<sup>85m</sup> Kr	4.48 h	1.300	0.565
<sup>85</sup> Kr	10.72 y	0.285	0.128
<sup>87</sup> Kr	1.37 h	2.520	0.990
<sup>88</sup> Kr	2.84 h	3.550	1.320
<sup>89</sup> Kr	3.15 m	4.600	1.440
<sup>90</sup> Kr	32.30 s	4.860	1.400
<sup>88</sup> Rb	17.70 m	3.570	1.360
<sup>89</sup> Rb	15.40 m	4.770	1.680
<sup>90</sup> Rb	2.60 m	4.500	1.390
<sup>90m</sup> Rb	4.30 m	1.240	0.680
<sup>91</sup> Rb	58.00 s	5.670	2.160
<sup>89</sup> Sr	50.50 d	4.780	1.690
<sup>90</sup> Sr	29.10 y	5.910	2.110
<sup>91</sup> Sr	9.51 h	5.930	2.490
<sup>92</sup> Sr	2.71 h	5.910	3.040
<sup>93</sup> Sr	7.40 m	6.370	3.920
<sup>90</sup> Y	2.67 d	5.920	2.110
<sup>91</sup> Y	58.50 d	5.930	2.490
<sup>92</sup> Y	3.54 h	5.980	3.060
<sup>93</sup> Y	10.20 h	6.370	3.920
<sup>95</sup> Zr	64.00 d	6.490	4.890
<sup>97</sup> Zr	16.80 h	5.930	5.320
<sup>95</sup> Nb	34.97 d	6.490	4.890
<sup>97</sup> Nb	1.23 h	5.950	5.370
<sup>99</sup> Mo	2.79 d	6.120	6.160
<sup>101</sup> Mo	14.60 m	5.180	5.940
<sup>98m</sup> Tc	6.02 h	5.380	5.420
<sup>101</sup> Tc	14.20 m	5.180	5.950
<sup>104</sup> Tc	18.00 m	1.920	5.960

Table 2-1 (cont.): Fission products formed in nuclear reactor core (NAS, 1996).

Nuclide	Half-life	Fission Yield (%)	
		<sup>235</sup> U	<sup>239</sup> Pu
<sup>103</sup> Ru	39.27 d	3.040	6.950
<sup>105</sup> Ru	4.44 h	0.972	5.360
<sup>106</sup> Ru	1.02 y	0.403	4.280
<sup>105</sup> Rh	35.40 h	0.972	5.360
<sup>125</sup> Sb	2.76 y	0.029	0.115
<sup>129m</sup> Te	33.60 d	0.127	0.270
<sup>132</sup> Te	3.26 d	4.280	5.230
<sup>131</sup> I	8.04 d	2.880	3.850
<sup>132</sup> I	2.28 h	6.320	5.390
<sup>133</sup> I	20.80 h	6.690	6.930
<sup>134</sup> I	52.60 m	7.710	7.270
<sup>135</sup> I	6.57 h	6.300	6.450
<sup>136</sup> I	1.39 m	2.970	1.740
<sup>133</sup> Xe	5.24 d	6.700	6.980
<sup>133m</sup> Xe	2.23 d	0.189	0.232
<sup>135m</sup> Xe	15.30 m	1.000	1.680
<sup>135</sup> Xe	9.10 h	6.540	7.600
<sup>137</sup> Xe	3.82 m	6.060	6.040
<sup>138</sup> Xe	14.20 m	6.420	5.120
<sup>139</sup> Xe	39.70 s	5.040	3.050
<sup>140</sup> Xe	13.70 s	3.620	1.600
<sup>137</sup> Cs	30.17 y	6.220	6.690
<sup>138</sup> Cs	32.20 m	6.640	5.910
<sup>139</sup> Cs	9.30 m	6.280	5.350
<sup>139</sup> Ba	83.70 m	6.350	5.600
<sup>140</sup> Ba	12.75 d	6.270	5.540
<sup>141</sup> Ba	18.30 m	5.790	5.230
<sup>142</sup> Ba	10.70 m	5.730	4.600
<sup>140</sup> La	40.27 h	6.280	5.550
<sup>141</sup> La	3.90 h	5.810	5.310
<sup>142</sup> La	92.50 m	5.830	4.910
<sup>141</sup> Ce	32.50 d	5.800	5.260
<sup>143</sup> Ce	33.00 h	5.940	4.430
<sup>144</sup> Ce	284.60 d	5.470	3.740
<sup>147</sup> Nd	10.99 d	2.250	2.040



Besides  $^{137}\text{Cs}$ , long-lived, and biologically-significant, radioisotopes of potential concern in spent fuel include:  $^{90}\text{Sr}$ ,  $^{99}\text{Tc}$ ,  $^{129}\text{I}$ ,  $^{237}\text{Np}$ ,  $^{239}\text{Np}$ ,  $^{238}\text{Pu}$ ,  $^{239}\text{Pu}$ ,  $^{241}\text{Pu}$ ,  $^{241}\text{Am}$ , and  $^{242}\text{Cu}$  (ORNL, 1994).

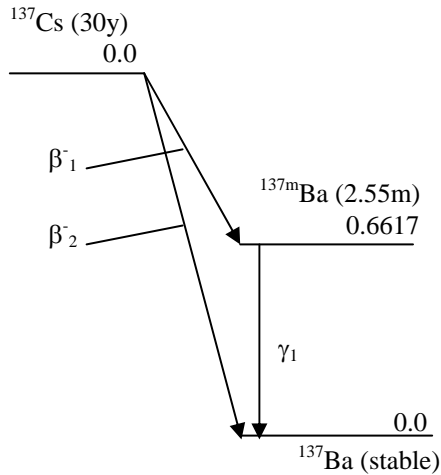
Although all radioactive materials listed above would be considered at an incident involving a release at a SFP, depending on the age of the spent fuel involved, this research will specifically study the two most prevalent radionuclides which contribute to downwind contamination and ultimately human exposure:  $^{137}\text{Cs}$  and  $^{90}\text{Sr}$ . As discussed below,  $^{131}\text{I}$  was a major contributor to dose at Chernobyl but is not considered in this study because of its short half-life.

#### Cesium-137

$^{137}\text{Cs}$  is considered one of the most important fission products because of its relatively high yield (about 6 atoms per hundred fissions, regardless of the type of fission involved), long physical half-life (30 years), and its well documented mobility in biological systems (NCRP, 1977).  $^{137}\text{Cs}$  also accounts for about half of the fission product activity in 10-year-old fuel (Alvarez, 2003). As depicted in the radioactive decay scheme in Figure 2-14,  $^{137}\text{Cs}$  decays to  $^{137\text{m}}\text{Ba}$  and then to stable  $^{137}\text{Ba}$  via internal conversion, or directly to  $^{137}\text{Ba}$  (RADAR, 2006).

Prior to 1986, the principal source of  $^{137}\text{Cs}$  released to the environment had been from atmospheric testing of nuclear weapons. Nuclear devices with a total fission yield equivalent to 194 megatons of TNT have been exploded and have produced approximately 1.26E9 GBq (34 MCi) (National, 1971). Most of this  $^{137}\text{Cs}$  released into the environment was injected into the stratosphere and resulted in a relatively uniform worldwide deposition. In 1986

however, the Chernobyl accident resulted in the single greatest release of  $^{137}\text{Cs}$  in history and is discussed in depth below.



Radiation	Particles/ Transition	Energy/ Particle (MeV)
$\beta^-_1$	0.9440	0.1743
$\beta^-_2$	0.0560	0.4163
$\gamma_1$	0.9011	0.6617

Figure 2-14:  $^{137}\text{Cs}$  decay scheme (RADAR, 2006)

Cesium is generally one of the less mobile radioactive metals in the environment. It preferentially adheres quite well to soil and is generally not a major contaminant in groundwater but exhibits appreciable reconcentration in both terrestrial and aquatic ecosystems. In terrestrial vegetation,  $^{137}\text{Cs}$  originates from both direct deposition on plant surfaces and accumulation from the soil in which the plants grow. Generally, direct foliar absorption is the predominant mode of plant contamination when the deposition rate is relatively high and is transferred throughout the food chain. In freshwater environments

however, the total accumulation of  $^{137}\text{Cs}$  in the system may be relatively more important than the deposition rate (NCRP, 1977).

When taken into the body either by inhalation or ingestion, cesium behaves similarly to potassium and is distributed uniformly throughout the body. The primary source of internally deposited cesium is gastrointestinal absorption from food and water. The absorbed cesium tends to concentrate in the muscles because of their large mass. With biological half-lives of 2 and 110 days (Argonne, 2005a.),  $^{137}\text{Cs}$ , like potassium, is excreted from the body fairly quickly. While in the body, cesium delivers a radiation dose to body tissues from both beta radiation from  $^{137}\text{Cs}$  decay and gamma radiation from  $^{137\text{m}}\text{Ba}$  decay (see Figure 2-14) with the main health concern an increased likelihood for inducing cancer.

To determine the rate and concentrations in which  $^{137}\text{Cs}$  is transferred through the food chain, Gustafson, et al., performed a study illustrating the average annual  $^{137}\text{Cs}$  deposition measured in the midwestern U.S. for the years 1960 through 1970 due to  $^{137}\text{Cs}$  fallout. This, and the average daily intake ( $\text{pCi } ^{137}\text{Cs}/\text{g } ^{40}\text{K}$ ) by adults and infants in the Chicago area for the same period, is plotted in Figure 2-15.

For determination of the annual daily intake, the standard adult diet used consisted of 16 components: bread, eggs, fresh leaf vegetables, fresh root vegetables, milk, poultry, fresh fish, flour, macaroni, meat, dried beans, fresh fruit, potatoes, canned fruit, canned fruit juices, and canned vegetables. Combined into five major categories (milk, grain products, meat, fruits, and vegetables), these foods account for more than 90% of the adult  $^{137}\text{Cs}$  intake for the study. The average annual content was based on four quarterly samplings per year.

The infant diet consisted of evaporated and formula milk, cereals, canned baby fruits, meats, and vegetables. For this diet, 70-90% of the infant  $^{137}\text{Cs}$  intake was found to come from milk at a ratio of  $^{137}\text{Cs}$  to  $^{40}\text{K}$  similar to those for the adult case listed in Figure 2-15.

Illustrated in Figure 2-15 is a one-year delay between maximum deposition rate and the occurrence of a maximum level of  $^{137}\text{Cs}$  in the adult diet. The authors postulate that this trend was mainly due to variable time lags in production and marketing, with the result that some foodstuffs contaminated by the relatively heavy deposition in 1958-59 were still available for consumption in 1961. A similar delay accounts for the slower decrease after 1964. Even though the increase and subsequent decrease in  $^{137}\text{Cs}$  content is delayed, it is apparent that the concentration in the adult diet coincides with the rate of deposition.

Maximum deposition rates were reached in 1963, one year after maximum atmospheric testing. The majority of all atmospheric tests concluded in 1963 with the signing of the atmospheric test ban. This is evident in this study as deposition rates steadily begin to fall in 1964. Slight increases in deposition are seen during 1968-1970 due to continued atmospheric testing by France and China.

The authors continued  $^{137}\text{Cs}$  measurements after the test ban in an attempt to identify the importance of root uptake and/or recycling of the radionuclide in the diet, as well as carry-over of  $^{137}\text{Cs}$  in grains. As evident in Figure 2-15, one or more of these parameters are the probable cause of the continued dietary average of 0.222 – 0.296 Bq (6.0 – 8.0 pCi)  $^{137}\text{Cs}/\text{g}$   $^{40}\text{K}$  measured after 1968.

Although many subsequent studies of  $^{137}\text{Cs}$  behavior in the environment have been performed, to date this study by Gustafson, et al. is relevant in that it shows how pathway

analysis contributes to the understanding of human exposure. Pathway analysis will be used extensively in this study to help illustrate the effects of an incident at a spent fuel pool.

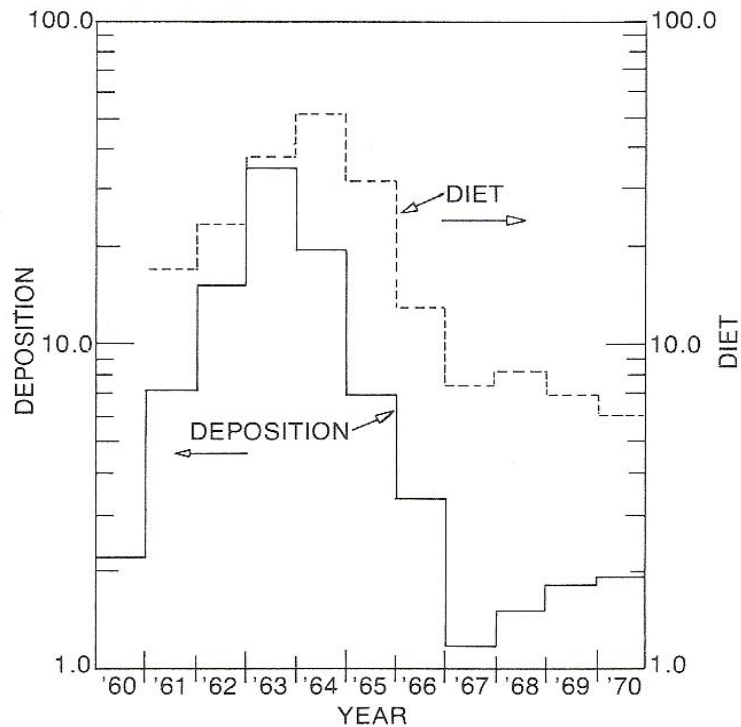


Figure 2-15: Annual average <sup>137</sup>Cs deposition in the midwestern U.S. and average annual <sup>137</sup>Cs level in the Chicago adult diet (NCRP, 1977).

In studies following the Chernobyl accident, the reindeer-herding groups of central Norway have been found to have some of the highest <sup>137</sup>Cs exposure levels of any monitored group. Whole-body contents and dietary habits have been investigated regularly in this population since 1987 due to the vulnerability of the lichen-reindeer-human food chain to cesium deposition. In 2000, Mehli et al published a study investigating the impact of Chernobyl fallout to this population. In 1986, activity concentrations up to 105 kBq kg<sup>-1</sup> (2.84 μCi kg<sup>-1</sup>) were measured in reindeer meat from this area. Studies showed that reindeer herders in the central parts of the country were the most exposed population group. The highest whole-body contents of cesium in the group were found in the spring of 1988 with

concentrations of  $220 \text{ Bq kg}^{-1}$  ( $5.95 \text{ nCi kg}^{-1}$ ) and  $580 \text{ Bq kg}^{-1}$  ( $15.68 \text{ nCi kg}^{-1}$ ) for women and men, respectively (see Figure 2-16 below). Consumption of reindeer meat at this time was estimated to contribute up to 90% of the total intake of cesium.

Following the accident in 1986, Norwegian authorities recommended that the individual effective dose should not exceed 5 mSv (500 mrem) in the first year after the accident and 1 mSv in the following years. With a dose conversion factor of  $2.5 \mu\text{Sv y}^{-1}$  per  $\text{Bq kg}^{-1}$ , adapted from the 1988 United Nations Scientific Committee on the Effects of Atomic Radiation report to the General Assembly, 1 mSv (100 mrem) committed dose results from a whole body cesium concentration of  $400 \text{ Bq kg}^{-1}$  ( $10.81 \text{ nCi kg}^{-1}$ ) (Mehli et al, 2000).

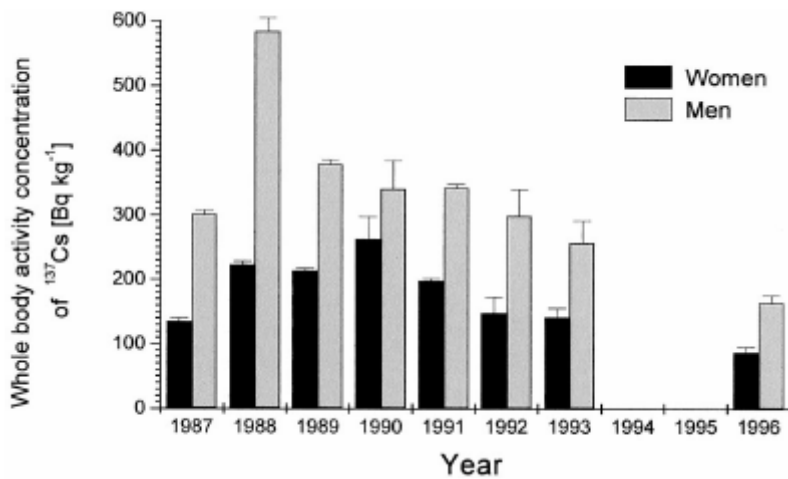


Figure 2-16: Average whole body <sup>137</sup>Cs activity in Norwegian reindeer herders (Mehli et al., 2000).

In their study, the authors focused on total household consumption of reindeer meat and wild foods like freshwater fish, game, berries, and mushrooms, as well as changes in diet due to fallout. In total, 110 persons (44 women and 66 men) from 63 of the 102 households participated in the whole-body measurements and dietary surveys. Their results showed the mean whole body dose in 1996 had reduced to  $88 \pm 7 \text{ Bq kg}^{-1}$  ( $2.38 \pm 0.19 \text{ nCi kg}^{-1}$ ) for

women and  $164 \pm 11 \text{ Bq kg}^{-1}$  ( $4.43 \pm 0.30 \text{ nCi kg}^{-1}$ ) for men (see Figure 2-16). Utilizing the same dose conversion factor as above, these values correspond to annual doses of approximately  $0.22 \text{ mSv y}^{-1}$  ( $22 \text{ mrem y}^{-1}$ ) for women and  $0.41 \text{ mSv y}^{-1}$  ( $41 \text{ mrem y}^{-1}$ ) for men - well below the recommended maximum acceptable dose of  $1 \text{ mSv y}^{-1}$  ( $100 \text{ mrem y}^{-1}$ ) for exposure to the general public.

All participants in the study still maintained a considerable intake of reindeer meat, with median annual intakes estimated to be 50 kg for women and 53 kg for men. About 30% reported consumption of less reindeer meat and freshwater fish in 1995-1996 but about 50% had resumed higher meat and fish consumptions due to less concern for cesium contamination in selected foods. It is also reported in this study that although the median intakes were similar, women generally consumed reindeer meat with lesser contamination than that consumed by men. This accounts for the differences in whole body dose observed in the study.

Common countermeasures employed for reducing the intake of cesium into the diet involved selection of reindeer from lesser-contaminated grazing areas to live-monitoring of animals prior to consumption to use of clean fodder prior to slaughter. The majority of households participating in the survey believed that use of countermeasures gave them the possibility of influencing possible health effects.

In addition to reduced intake by some and application of countermeasures, the authors felt the reduction in whole body  $^{137}\text{Cs}$  activity was also due in part to physical decay and lower transfer of cesium contamination to reindeer.

These studies are included to demonstrate how cesium migrates through the food chain and ultimately into the human body. As this study illustrates below, external exposure

to  $^{137}\text{Cs}$  provides the largest contribution to human dose. Although not insignificant, this internal dose component does contribute a fraction to the expected overall dose. Preventing (or limiting) uptake of  $^{137}\text{Cs}$  must be a major goal in any large-scale response to an incident at a SFP. For persons who uptake significant amounts of  $^{137}\text{Cs}$ , remedial measures exist to prevent retention of this radionuclide and ultimately reduce the body burden.

Ferric hexacyanoferrate,  $\text{Fe}_4[\text{Fe}(\text{CN})_6]_3$ , the decorporation agent commonly referred to as “insoluble Prussian Blue (PB),” is utilized for personnel with internal contamination of medically-significant amounts of cesium and thallium. In the U.S., the Oak Ridge Institute for Science and Education is the sole distributor of PB. PB has a very high affinity for cesium and thallium and enhances excretion of these isotopes from the body by means of ion exchange. These ions are ordinarily excreted into the intestine, reabsorbed from the gut into the bile, and then excreted again into the gastrointestinal (GI) tract. Orally administered PB readily binds to these isotopes in the gut, thus interrupting its re-absorption from the GI tract and thereby increases fecal excretion (REAC/TS, 2002).

To date, the use of PB for cesium decorporation has been verified by a variety of studies. Initially, PB was found to dramatically reduce the internal cesium on animals in laboratory studies and by human volunteers. In one case, two adult male subjects ingested 37 kBq (1  $\mu\text{Ci}$ ) of carrier-free  $^{137}\text{Cs}$ . Each subject experienced normal biological half-lives of 110-115 days over 6 months’ time after ingestion. Ten months after ingestion however, each subject took several daily oral doses of PB. In both cases, the biological half-life was reduced to about 40 days, with no detectable change in the potassium content in the body (NCRP, 1977).



The most dramatic accident in which PB was administered occurred in Goiania, Brazil in September of 1987. Approximately 250 persons received external or internal cesium-137 contamination as a result of a radiological accident after two scavengers dismantled a teletherapy unit at an abandoned cancer treatment facility in search for valuable recyclable materials. After failing to pry open the lead container containing over 5.18E4 GBq (1400 Ci) of  $^{137}\text{Cs}$  (Argonne, 2005c.), the scavengers sold it to a junkyard owner. In the days that followed, the junkyard owner opened the container to reveal the luminous blue powder which family and friends were exposed to in numerous ways, including external exposure, direct ingestion, and application to the surfaces of their bodies. The resulting medical symptoms experienced by those in contact with the powder were not initially recognized as being due to radiation exposure. One of the irradiated individuals connected the illnesses with the container and took it to the local Public Health Department where a physicist identified the radioactive material and took measures to assess the extent of contamination and evacuate two areas. Shortly thereafter, additional physicists and physicians were dispatched to Goiania where upon arrival found that a stadium had been designated as a triage area. During triage, 20 patients were determined to need hospital treatment. Of these patients, 4 died due to hemorrhagic and septic complications associated with acute radiation exposure (IAEA, 1988). In all, 46 patients between the ages of 4 and 38 years were treated with PB for up to 150 days. Adult doses of PB generally ranged from 1 to 10 grams daily while four adults received 20 grams daily in divided doses. Children were given 1 to 1.5 grams daily in 2 to 3 divided doses. In this accident, PB was found to significantly expedite cesium decorporation in all cases. Other than gastritis, constipation

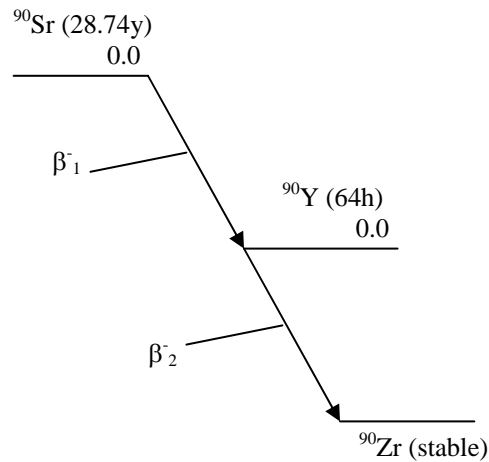
and other relatively minor gastrointestinal symptoms in a few patients, no significant adverse effects of increased PB administration were observed (REAC/TS, 2002).

## Strontium-90

$^{90}\text{Sr}$  is also considered one of the most important fission products in spent fuel. Similar to  $^{137}\text{Cs}$ , it has a high yield (3-4 atoms per 100 fissions) and relatively long half-life (~29 years) (NCRP, 1991). Unlike  $^{137}\text{Cs}$  however,  $^{90}\text{Sr}$  is relatively mobile in the environment and can move down with percolating water to underlying layers of soil and into groundwater even though it preferentially adheres to soil particles (Argonne, 2005b.). As it undergoes radioactive decay,  $^{90}\text{Sr}$  emits a fairly low energy beta particle in decay to yttrium-90 ( $^{90}\text{Y}$ ). With a much shorter half-life of approximately 64 hours,  $^{90}\text{Y}$  also undergoes beta decay but releases a much more energetic beta particle and becomes stable  $^{90}\text{Zr}$  (RADAR, 2006). Figure 2-17 illustrates the significant decay properties of  $^{90}\text{Sr}$  and  $^{90}\text{Y}$  (NOTE: the decay scheme is simplified to omit any transition that does not contribute more than 0.1% to the total energy per transition). It is important to note that the  $^{90}\text{Y}$  contributions to dose will be greater than the  $^{90}\text{Sr}$  contribution individually due to the higher beta energy and is assumed to be reflected in all  $^{90}\text{Sr}$  dose conversion factors as reported in EPA Federal Guidance Report 11.

Strontium can be taken into the body by eating contaminated food, drinking contaminated water, or breathing contaminated air. In the body, strontium behaves similarly to calcium. Approximately 20% to 30% of all intake is absorbed from the gastrointestinal tract. This quantity of strontium is distributed in three ways: a) deposition in the bone volume; b) distributed in an exchangeable pool that is considered to be comprised of the

plasma, extracellular fluid, soft tissue, and bone surfaces; or c) removed from the body by urinary or fecal excretion (NCRP, 1991).



Radiation	Particles/ Transition	Energy/ Particle (MeV)
$\beta_1$	1.0000	0.1958
$\beta_2$	0.9999	0.9337

Figure 2-17:  $^{90}\text{Sr}$  decay scheme (RADAR, 2006)

Published by the ICRP in 1972, and reproduced in summary in NCRP Report 84 in 1985, a quantitative metabolic model (referred to as the “ICRP Model” herein) was developed to calculate radiation dose to various parts of the bone tissue for the alkaline earth metals (calcium, radium, strontium and barium). The ICRP Model is based on accumulated knowledge of the mechanisms of skeletal distribution and metabolism of fallout  $^{90}\text{Sr}$  in humans and radionuclide retention as a result of animal experiments at a variety of research laboratories (NCRP, 1991). Although beyond the scope of this report, the specific findings of these studies provide important background to the conclusions presented in this study and are discussed in depth in NCRP Report No. 110.

Since its development, the ICRP Model has been subsequently extended and modified as knowledge of alkaline earth metals behavior has increased. Animal experiments indicate that bone sarcoma, hematopoietic dyscrasia and neoplasia, and tumors of soft tissue near bone may be important endpoints in the exposure of humans to high doses of  $^{90}\text{Sr}$ . The incidence of bone sarcoma and other malignant diseases have only been seen at average skeletal doses of the highest dose levels (i.e. tens of Gy). Research results indicate a curvilinear dose-response relationship similar to the experience with the nonlinear dose-response relationship curve seen in radium dial painters. Comparison with radium-226 ( $^{226}\text{Ra}$ ) effects in humans using the relative effectiveness ratios of  $^{90}\text{Sr}/^{226}\text{Ra}$  developed from animal studies for predicted bone sarcoma induction in humans and with external radiation experience for leukemia induction in humans has yielded the following estimates: 1) 1 bone sarcoma per  $10^4$  person Gy; and 2) 3 leukemias per  $10^4$  person Gy for populations exposed to radiostrontium below 10 Gy (NCRP, 1991).

As discussed in the next section,  $^{137}\text{Cs}$  and  $^{90}\text{Sr}$  still remain the radionuclides of concern in the environment many years after the Chernobyl accident.

### Chernobyl Accident

On 26 April 1986, the single greatest release of man-made radioactive materials in history occurred at the Chernobyl nuclear power plant in the former Soviet Union (present day Ukraine), approximately 80 miles north of Kiev. This accident revealed that the RBMK reactors in the Soviet Union (i.e. Chernobyl-4 reactor, Figure 2-18) suffered from an extraordinary mixture of bad design, bad regulation and bad operation. Table 2-2 lists various design, management and regulatory problems that contributed to this accident.

Due to a dramatic power surge, the reactor fuel elements ruptured and the resultant explosive force of steam lifted off the 2000-ton cover plate (Shlyakhter and Wilson, 1992) of the reactor, releasing fission products to the atmosphere. A second explosion expelled fragments of burning fuel and graphite from the core and allowed air to rush in, causing the graphite moderator to burst into flames. The graphite burned for nine days and caused the main release of radioactivity into the environment. The total estimated activity released after the Chernobyl accident was  $2 \times 10^{10}$  GBq, of which approximately  $3 \times 10^9$  GBq came from short-lived  $^{131}\text{I}$ ,  $4 \times 10^8$  GBq came from  $^{134}\text{Cs}$  and  $^{137}\text{Cs}$ , and  $7 \times 10^9$  GBq came from noble gases (Gonzalez, 2005). Based on the latest assessments by the NEA, Table 2-3 updates the estimated radionuclide release for select isotopes (NEA, 2002). It is also estimated that at least 5% of the remaining radioactive material in the core was released in the accident (WNA, 2005).

Both professional and non-professional personnel participated in the response to the accident. During the first few months after the accident, approximately 200,000 workers, later called “liquidators,” worked in the region when radiation exposures were highest. In all, over 600,000 liquidators were registered as involved in stabilization and clean-up activities, including clean up around the reactor, construction of the sarcophagus, decontamination, building of roads, and destruction and burial of contaminated buildings, forests, and equipment.

Table 2-2: Causes of the Chernobyl Accident (Adapted from Shlyakhter and Wilson, 1992).

<b>Design Failures</b>
Positive void coefficient that left more neutrons available for chain reactions.
Control rod design which added reactivity for a few seconds.
Ability of plant operators to override safety features.
Emergency cooling system designed to only protect against a break in one coolant pipe at a time.
<b>Management Shortcomings</b>
Failure of plant personnel to study other reactor accidents.
Failure to communicate the existence of other accidents to engineers and operators.
Failure to inform engineers and operators about the design weaknesses of the reactor.
Operating with only seven control rods in the core.
Carrying out a test under unstable conditions.
Refusal to listen to criticism regarding procedures.
<b>Regulatory Problems</b>
Failure to demand a clear set of operating rules.
Failure to ensure that unusual procedures be discussed and checked in advance.
Failure to perform a full safety analysis.

Table 2-3: Current estimate of Chernobyl radionuclide release (Source: NEA, 2002).

Radionuclide	Core Activity on 26 Apr 1986 (GBq)	Total Release (GBq)	% Release
<sup>131</sup> I	3.20E+09	1.76E+09	55%
<sup>134</sup> Cs	1.80E+08	5.40E+07	30%
<sup>137</sup> Cs	2.80E+08	8.50E+07	30%
<sup>89</sup> Sr	2.30E+09	1.15E+08	5%
<sup>90</sup> Sr	2.00E+08	1.00E+07	5%
<sup>33</sup> Xe	6.50E+09	6.50E+09	100%
<sup>103</sup> Ru	4.80E+09	1.68E+08	4%
<sup>106</sup> Ru	2.10E+09	7.30E+07	3%
<sup>238</sup> Pu	1.00E+06	3.50E+04	4%
<sup>239</sup> Pu	8.50E+05	3.00E+04	4%
<sup>240</sup> Pu	1.20E+06	4.20E+04	4%
<sup>241</sup> Pu	1.70E+08	6.00E+06	4%

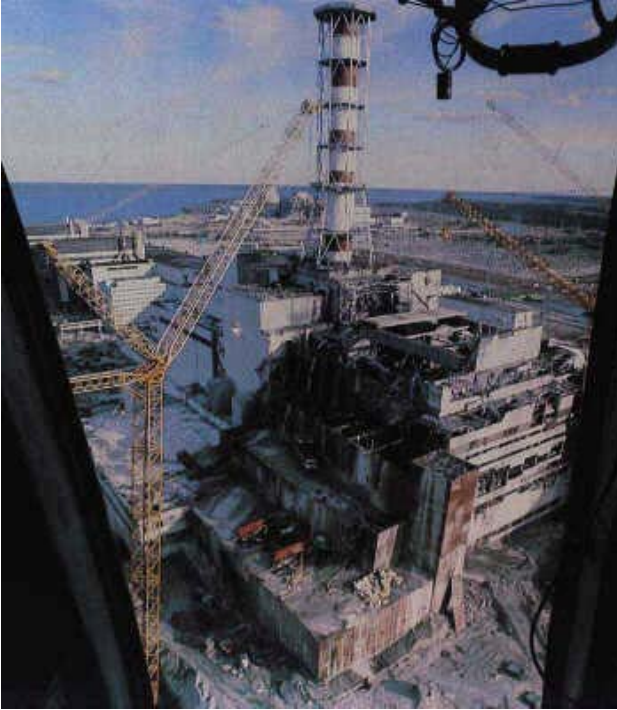


Figure 2-18: Chernobyl-4 Reactor (InfoUkes, 1997).

### Environmental Effects

The release of radioactive material into the atmosphere consisted of gases, aerosols and finely fragmented fuel. During the first 10 days of the accident when important releases of radioactivity occurred, meteorological conditions changed frequently, causing significant variations in release direction and dispersion parameters. The composition and characteristics of the radioactive material in the plume changed during its passage due to wet and dry deposition, decay, chemical transformations and alterations in particle size. The larger particles, particularly fuel particles, were deposited close to the reactor. Smaller particles were more widely dispersed by the wind and deposited primarily by rainfall.

Three main areas of contamination, which were defined as those with  $^{137}\text{Cs}$  deposition density greater than  $37 \text{ kBq m}^{-2}$  ( $1 \text{ Ci km}^{-2}$ ), are in Belarus, Russia, and Ukraine. The three areas have been designated the Central, Homyel'-Mabilyow-Bryansk, and Kaluga-

Tula-Orel areas. The Central area (see Figure 2-19) is within ~ 100 km of the reactor, predominantly to the west and northwest of the reactor, in Ukraine. The Homyl'-Mabilyow-Bryansk area (see Figure 2-19) is centered 200 km to the north-northeast in Belarus and Russia. The Kaluga-Tula-Orel area (not pictured in Figure 2-19) is located ~ 500 km to the northeast in Russia.



Figure 2-19: Radioactive contamination in areas around Chernobyl reactor (Wikipedia, 2005).

Beyond these areas in the former Soviet Union, many areas in northern and eastern Europe experienced  $^{137}\text{Cs}$  deposition in the range of  $37 - 200 \text{ kBq m}^{-2}$  as well and represent about one-third of the contamination found in the three areas discussed previously (Gonzalez,



2005). Deposition of radioactive materials of significantly less activity was fairly evenly distributed throughout all of the Northern Hemisphere.

### Human Exposure Effects

The accident caused the deaths of 31 power plant employees and firemen within a few days or weeks, 28 of which were due to radiation exposure. Acute radiation sickness was confirmed for 134 liquidators; 41 receiving whole-body doses from external irradiation of less than 2.1 Gy and 93 receiving higher doses and had more severe acute radiation sickness. Of these 93 liquidators receiving doses higher than 2.1 Gy, 50 were between 2.2 and 4.1 Gy, 22 were between 4.2 and 6.4 Gy, and 21 were between 6.5 and 16 Gy (Gonzalez, 2005). The skin doses from beta exposures, evaluated for eight patients with acute radiation sickness, were in the range of 400-500 Gy. Average doses for the liquidators were about 100 mSv (UNSCEAR, 2000a).

Acute radiation effects can occur if personnel receive high doses of radiation over a short time. Table 2-4 lists the acute radiation effects, or “syndromes,” along with their respective thresholds and characteristics.

Table 2-4: Acute Radiation Syndromes (Hall, 2000).

<b>Syndrome</b>	<b>Range of Dose (Gy)</b>	<b>Characteristics</b>
Hematopoietic	3-8	radiation damage to blood forming system
Gastrointestinal	> 10	radiation damage to epithelial lining of gastrointestinal system
Cerebrovascular	>100	neurologic and cardiovascular breakdown occurs

With whole-body doses received between 3-8 Gy, or 3-8 Sv for external exposures to gamma radiation, effects of the hematopoietic syndrome occur. At these doses, mitotically active precursor cells are sterilized by the radiation, and subsequent supply of mature red blood cells, white blood cells and platelets are subsequently diminished. The full effect of this action is delayed until the mature circulating cells begin to die off and the supply of new cells from the depleted precursor population is inadequate to replace them. After this delay (i.e. latency period), the depression of blood elements leads to an onset of chills, fatigue, petechial hemorrhages in the skin and ulcerations of the mouth. Granulocyte depression leads to infections and fever, while platelet depression results in bleeding, impairment of immune mechanisms and possibly anemia caused by hemorrhage. Death occurs in this syndrome unless the bone marrow has begun to regenerate in time. Infection is an important cause of death but may be controlled by antibiotic therapy (Hall, 2000).

A common term used to determine the rate of death is the “LD<sub>50</sub>.” Defined as the dose that causes a mortality rate of 50% in an experimental group within a specified period of time, the estimated dose to cause this occurrence in humans is between 3 and 4 Gy (300 and 400 rad) for young adults without medical intervention. Humans develop signs of hematological damage and recover from it much more slowly than most other mammals. The peak incidence of human deaths from hematological damage occurs at about 30 days after exposure but continues for up to 60 days. Therefore, the LD<sub>50</sub> for humans is expressed as LD<sub>50/60</sub> (Hall, 2000).

At whole body doses greater than 10 Gy (1000 rad), but less than 100 Gy (10,000 rad), death usually occurs between 3 and 10 days due primarily to the depopulation of the epithelial lining of the gastrointestinal tract. In the gastrointestinal tract, stem cells confined

to crypts provide a continuous supply of new cells which move up the villi, differentiate, and become functioning cells. The cells at the top of the villi are continuously sloughed off slowly and replaced by the new cells. At doses of this magnitude, a large portion of the stem cells are sterilized without much affect on the differentiated or functioning cells. As these cells are sloughed off, there are no replacement cells produced to take their place. Consequently, the villi begin to shorten and shrink, and eventually the surface lining of the intestine is completely flat. Prolonged diarrhea, extending for several days, is usually an indicator of doses > 10 Gy (1000 rad). After a few days, a person will show signs of dehydration, loss of weight, emaciation and complete exhaustion with death occurring within a few days (Hall, 2000).

A whole body dose of 100 Gy (10,000 rad) or more results in serious damage to all organ systems. Because the level of exposure is so great, cerebrovascular damage causes death quicker than the time required to express damage to the hematopoietic or gastrointestinal systems. The exact and immediate cause of death is not fully understood. It has been suggested that the increase in the fluid content of the brain, due to leakage from small vessels, results in a buildup of pressure within the confines of the skull and results in central nervous system shutdown. After severe nausea and vomiting occurs, usually in a matter of minutes, manifestations of disorientation, loss of coordination of muscular movements, respiratory distress, diarrhea, convulsive seizures and coma occur prior to death (Hall, 2000).

For exposures to the public,  $^{131}\text{I}$  and  $^{137}\text{Cs}$  were the only significant radionuclides contributing to dose in human populations.  $^{131}\text{I}$ , being the main contributor to thyroid doses, was received mainly by internal exposures within a few weeks after the accident. External

exposures from  $^{137}\text{Cs}$  have been the main contributor to dose for all organs and tissues other than the thyroid. To a lesser degree, consumption of foods contaminated with  $^{90}\text{Sr}$  contributed to internal exposures mainly to bone and bone marrow.

For the 116,000 persons evacuated from the most contaminated regions, the average dose was determined to be 30 mSv (3 rem) (UNSCEAR, 2000a.). For those who continued to reside in contaminated areas, a dose of 10 mSv (1 rem) was determined during the first decade after the accident with maximum values of the doses possibly an order of magnitude higher. Outside the three countries primarily affected, doses were estimated to reach a maximum of 1 mSv (0.1 rem) in the first year and progressively decreasing doses in subsequent years. The estimated lifetime dose was determined to be 2-5 times greater (UNSCEAR, 2000a.). These doses are well below the annual dose from natural background of 2.4 mSv (0.24 rem) (UNSCEAR, 2000b.) and are, therefore, of little radiological significance.

In their 2000 report to the General Assembly, the UNSCEAR reported that about 1,800 cases of thyroid cancer have developed in children exposed at the time of the accident. Apart from this, there is no evidence of a major public health impact attributable to radiation exposure as of 2000. Furthermore, they found that there is “no scientific evidence of increases in overall cancer incidence or mortality or in non-malignant disorders that could be related to radiation exposure. The risk of leukemia, one of the main concerns owing to its short latency time, does not appear to be elevated, not even among the recovery operation workers. Although those most highly exposed individuals are at an increased risk of radiation-associated effects, the great majority of the population is not likely to experience serious health consequences” (UNSCEAR, 2000a.).

Under the auspices of the United Nations Chernobyl Forum's Expert Group "Health," three WHO committees convened to provide an updated assessment of the UNSCEAR human health consequences utilizing extensive epidemiological studies and other data available after the UNSCEAR report. The WHO determined the epidemiological studies relating to thyroid disease and solid cancers in the exposed population available after the UNSCEAR 2000 report support the conclusions made above of no increases in cancer induction. For increased risk of leukemia, the WHO found neither strong evidence for nor against the association between *in utero* exposure and Chernobyl fallout. Likewise, even though an increase in leukemia rates among children was seen after 1996, there was no evidence that these excesses were more pronounced in areas of contamination. For adults in exposed general populations, no convincing evidence was found for increased incidence of leukemia. Recent studies of Russian liquidators exposed to greater than 150 mGy (15 rad) suggest a possible two-fold increase in non-chronic lymphocytic leukemia. At this time, the WHO states there is "clearly a need to clarify the existing observations...indicating a possible relationship." In summary, except for the possible increase in leukemia of liquidators, the WHO and UNSCEAR findings appear to agree with one another (WHO, 2005a.).

In September 2005, the Chernobyl Forum released, "Chernobyl: The True Scale of the Accident," a three-volume, 600 page report to assess the 20-year impact of the Chernobyl accident. The Forum, made up of 8 UN specialized agencies, compiled the latest research to help settle the outstanding questions about how much death, disease and economic fallout really resulted from the accident.

Many important findings included in this report confirm the information previously presented. Others are presented to provide a clear understanding of the true scale of the accident consequences and also to suggest ways for the countries affected to address major economic and social problems. Some of these findings include (WHO, 2005b.):

1. Approximately 1000 on-site reactor staff and emergency workers were heavily exposed to high-level radiation on the first day of the accident. Among the 200,000 or more workers exposed within the first year, an estimated 2200 radiation-induced deaths can be expected during their lifetime.

2. An estimated 100,000 people live in areas previously considered areas of “strict control”. This report suggests the definitions of these zones be revisited and relaxed in light of the new findings.

3. About 4000 cases of thyroid cancer have resulted and at least 9 children have died. As reported previously, the survival rate among these victims has been approximately 99%.

4. Most emergency workers and people living in contaminated areas received relatively low doses as comparable to natural background levels.

5. Poverty, “lifestyle” diseases and mental health problems pose a far greater threat to local communities than radiation exposure.

6. Relocation of residential populations proved to be a deeply traumatic experience for the more than 350,000 people affected.

7. Structural elements of the sarcophagus have degraded and pose a risk of collapse that would release large quantities of radioactive dust.

8. A comprehensive plan to dispose of tons of high-level waste must still be developed.

9. Ambitious rehabilitation and social benefit programs, started by the former Soviet Union and continued by Belarus, Russia and Ukraine, need reformulation due to changes in radiation controls, poor targeting and funding shortages.

In agreement with the UNSCEAR 2000 report, this report found no evidence for any increased incidence of leukemia and cancer above the 4000 cases of thyroid cancer previously discussed. Dr. Michael Repacholi, manager of WHO's Radiation Program, states, "the health effects of the accident were potentially horrific, but when you add them up using validated conclusions from good science, the public health effects were not nearly as substantial as had at first been feared" (WHO, 2005b.).

It is estimated that a total of up to 4,000 of the approximately 600,000 people (200,000 emergency workers, 116,000 evacuees and 270,000 residents of the most contaminated areas) affected by the higher radiation exposure could eventually die. As about one quarter of them will eventually die from spontaneous cancer not caused by radiation exposure from the Chernobyl accident, the increase of about 3% will be difficult to observe (WHO, 2005b.).

#### Exclusion Zone

During the four months after the accident, approximately 116,000 members of the public were evacuated from their homes in the region around the reactor. A "exclusion zone" was established (Figure 2-20) within 30 km of the reactor, in modern Ukraine and Belarus, to prohibit public access to the highest dose rates and contamination levels. The exclusion zone covers an area of 2044 km<sup>2</sup> and encompasses 2 towns (Pripyat and Chernobyl) and 74 villages (UIAR, 2001).

Today, the exclusion zone is governed by a special Ukrainian State Department, the Administration of the Exclusion Zone and of the Zone of Obligatory Resettlement (UIAR, 2001). Under authority from this department, the UIAR performed an extensive characterization of the exclusion zone beginning in 1997 and released the data in 2001. UIAR's work included extensive soil sampling and measurements to develop the most detailed contamination maps of the exclusion zone to date. The characterization methods and results are included in this study to help validate the dispersion modeling results obtained from HPAC.



Figure 2-20: Chernobyl Exclusion Zone (Mycio).



## Dispersion Modeling

Dispersion models are used in conjunction with an event of this nature to determine if the surrounding population will be exposed to the radioactive materials released to the environment. The degree of exposure will be a function of the mixing of radioactive materials in the horizontal or vertical axis of the plume, how close the receptor is to the centerline of the plume and how long the receptor is in the plume.

Dispersion (or diffusion) is a random process which ultimately dilutes the radionuclides in the plume. The radioactive particles tend to move in different directions at different rates and are strongly influenced by wind direction and wind speed. Dispersion is primarily governed by turbulence. Three types of turbulence that act to disperse a plume are mechanical turbulence (i.e. air flowing over rough features), shear turbulence (i.e. differences in wind speed between the plume and ambient atmosphere) and buoyancy turbulence (i.e. atmospheric stability). Over time, the dispersion process will create a Gaussian distribution in both the horizontal and vertical directions (see Figure 2-21).

“Plume rise” is one of the most important parameters in determining the dispersion of radionuclides following a release. As the name implies, it is a measure of the plume rise into the atmosphere (above the stack height) during a release and is important in determining the direction of dispersion and behavior of the particles in the plume. Plume rise is directly proportional to the vertical ejection velocity and the temperature of the plume while inversely proportional to wind speed and buoyancy turbulence. Increases in vertical ejection velocity forces the plume higher into the air but also causes an increase in dilution to occur. Plumes will continue to rise if the temperature of the plume is greater than ambient temperature. Light winds allow a plume to stay intact as it rises while stronger winds tend to bend the

plume and quickly mix it with the ambient air. Plume rise varies depending on the source. For example, spills from pressurized containers may have an ejection velocity but not necessarily in the vertical direction, fires have no ejection velocity but are very buoyant and dense gases act as liquids and tend to move downhill regardless of wind.

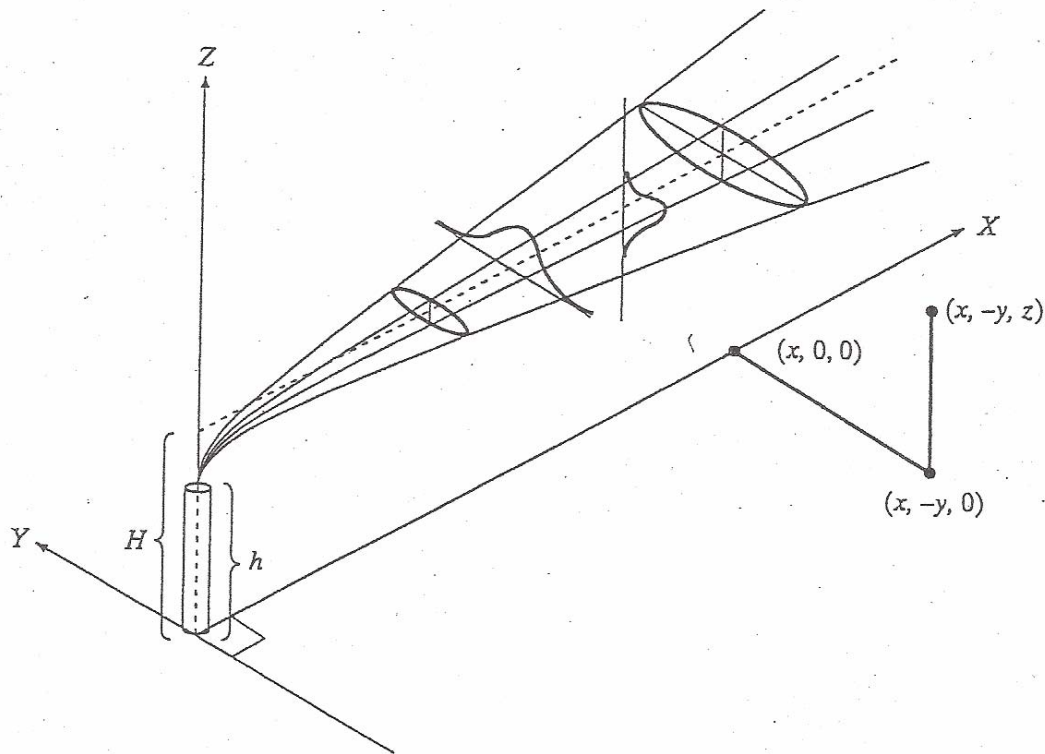


Figure 2-21: Plume dispersion showing Gaussian distributions in horizontal and vertical directions (Turner, 1970).

The downwind shape of the plume is dependent on the adiabatic lapse rate and the environmental lapse rate. The adiabatic lapse rate is defined as the rate of temperature change that occurs in the atmosphere as a function of elevation. The environmental lapse rate refers to the change of temperature with altitude for the stationary atmosphere and can

vary during the day. Six traditional plume shapes include: fanning plumes, lofting plumes, looping plumes, coning plumes, fumigating plumes and trapping plumes.

Fanning plumes form under very stable conditions. These plumes, dispersed at the stack height, tend to be narrow in the vertical direction due to confinements in both upward and downward directions but disperse greatly in the horizontal directions. When viewed from above, they have a characteristic fan shape.

Lofting plumes form when there is a stable layer beneath an unstable layer. Downward dispersion is inhibited by the stable layer, but the unstable layer above allows the plume to loft upwards. Resultant plumes have a flat bottom and a rising top.

Looping plumes form within unstable surface layers, with super-adiabatic lapse rates from the ground up to the plume height. A super-adiabatic lapse rate occurs when the temperature decreases with height at a rate of greater than  $10^{\circ}\text{C km}^{-1}$ . These plumes rise and sink rapidly as they pass through thermal layers and tend to have high ground level concentrations occurring close to the stack.

Coning plumes occur when there is a deep, nearly neutral lapse rate extending from the surface upward past the plume height (i.e. the environmental lapse rate is equal to the adiabatic lapse rate). Neutral conditions allow the plume to spread evenly in both vertical and horizontal directions, resulting in a cone shape.

Fumigating plumes occur when an inversion layer above the plume inhibits upward dispersion but unstable conditions below allow rapid downward mixing. This rapid mixing usually results in sudden increases in pollutant concentrations at ground levels.

Trapping plumes are formed when released in an unstable layer situated between stable layers above and below. The stable, or inversion, layers trap the plume at a particular height by acting as a barrier which prevents atmospheric mixing in the vertical directions.

To determine concentrations at downwind locations, “Gaussian Plume Dispersion Models” and “Puff Models” are commonly utilized. Gaussian Plume Dispersion Models assume constant meteorological conditions and produce straight line trajectories to determine downwind concentrations. Utilized in conjunction with the Pasquill-Gifford Stability Categories, horizontal and vertical concentration profiles at downwind points are assumed to be normally distributed about the plume center line along the downwind direction. Lateral and vertical dispersion coefficients describe the standard deviations of the corresponding distribution at each location downwind from the source. Puff models use puffs to represent instantaneous sources or simulation of emissions over a period of time. Each puff is treated as a separate entity by the model and is transported at a speed and direction determined at its center of mass. Puff models incorporate changes in wind speed, direction, and stability by utilizing gridded weather data over the area of release (NWS, 2005).

To simulate incidents at SFP in the U.S., the HPAC software tool suite is utilized. Primarily developed by the Titan Corporation for the DTRA, HPAC simulates the transport/dispersion of hazardous materials throughout the atmosphere and has become the DoD primary CBRNE operational modeling and simulation tool suite. Originally developed to meet the needs of the military, HPAC has evolved into peacetime applications by providing estimates of effects on the physical environment and the resultant effects on the exposed population for a variety of incidents (HPAC, 2004).

HPAC is an integrated package of software modules and legacy codes. Source term modules estimate the amount, rate, form, and physical configuration of hazard material releases. Existing source term capabilities from HPAC 4.03 included CBRNE incidents involving: chemical/biological facilities; nuclear facilities; chemical/biological weapons; nuclear weapons accidents; nuclear weapons use; enemy missile intercept; and radiological weapon incident. The latest source term capabilities added to HPAC 4.04 include: explosive incidents, predicting hazards from toxic materials in a three dimensional urban environment, releases of toxic materials inside buildings and the venting to the outside for subsequent transport, release of toxic materials from industrial facility incidents and release of toxic chemicals from road, rail and water transport vehicle accidents.

Hazardous materials are transported and dispersed into the atmosphere using Titan's SCIPUFF model. SCIPUFF is a puff dispersion model that uses a collection of Gaussian puffs to predict three-dimensional, time-dependent pollutant concentrations. In addition to the average concentration value, SCIPUFF predicts the statistical variance in the concentrations resulting from the random fluctuations of the wind (Wikipedia, 2006a.). SCIPUFF was initially developed under Electric Power Research Institute sponsorship in the mid-1980's. The DNA, predecessor of DTRA, adopted the model and applied it to nuclear dust cloud transport problems in the late-1980's and early-1990's. SCIPUFF was ported to Microsoft Windows for DNA starting in 1993. Later, it was joined with elements of the NRC Radiological Assessment for Consequence Analysis, commonly referred to as RASCAL, model and a climatology database, to provide an end-to-end capability to analyze potential radiological releases from nuclear reactor facilities. Under DoD counterproliferation

sponsorship, this combined end-to-end capability was integrated with the ability to analyze chemical and biological hazards to form HPAC (HPAC, 2004).

The release environment is specified using high-resolution weather, terrain, and land cover data. This allows HPAC to address the impact of spatially and temporally varying weather and the effects of local terrain features on transport/dispersion patterns. Two datasets are available to cover two scenarios: surface climatology and upper air climatology. Surface climatology is utilized for near-surface, short duration releases and is based on 20 years of observation data from 500 sites worldwide. Most sites are near major cities or nuclear facilities. Upper air climatology is utilized for worldwide coverage following long duration releases and are based on a 2.5 x 2.5 degree gridded model up to 16 km in altitude. Historical, real-time and forecast weather can be utilized for many areas of the world. HPAC has built-in logic to select the appropriate datasets based on the criteria listed above.

All HPAC results are probabilistic as total uncertainty is estimated based on turbulence model uncertainty, weather data uncertainty, and event location uncertainty. Resolution and accuracy to a radius of 1 km can be achieved and be overlaid onto high-resolution maps.

### Radiation Exposure Modeling

RESRAD was developed by Argonne National Laboratory for the DOE. Unlike HPAC which determines a dose to a general area, RESRAD is used primarily to calculate site-specific residual radioactive material guidelines as well as radiation dose and excess lifetime cancer risks to chronically exposed on-site residents by completing pathway analyses of the hazards.

RESRAD (version 6.3 used in this analysis) is the forerunner of a family of codes for more specific evaluations of environmental pollutants. These codes (see Table 2-5) were generally developed on the basis of the fundamental algorithms used in RESRAD (Yu, 2001).

Table 2-5: RESRAD family of codes (Yu, 2001).

<b>CODE</b>	<b>DESCRIPTION</b>
RESRAD-BUILD	Calculates doses to persons inside structures from radioactive materials on or in the walls, ceiling, or floors.
RESRAD-CHEM	Performs environmental transport and risk analyses of hazardous chemicals similar to those performed by RESRAD.
RESRAD-BASELINE	Calculates doses and risks from radionuclide and chemical concentrations measured in environmental media.
RESRAD-OFFSITE	Couples an atmospheric dispersion model and a groundwater transport model with RESRAD, thereby permitting calculation of doses to persons beyond the boundary of a site.
RESRAD-RECYCLE	Calculates doses to workers and members of the general public from the recycle of materials containing traces of radioactive materials.
RESRAD-ECORISK	Calculates risks to ecological receptors from exposure to hazardous chemicals.

The latest code to be introduced, RESRAD-BIOTA, provides a complete spectrum of biota dose evaluation capabilities. From methods for general screening to comprehensive receptor-specific dose estimations, RESRAD-BIOTA has become one of the more prominent models endorsed by the ICRP for assessing the impact of ionizing radiation to non-human populations.

RESRAD has become popular because of its adaptability to specific exposure situations. Default dose conversion factors for ingestion and inhalation are derived from the EPA's Federal Guidance Report No. 13. User-specific factors also can be specified in lieu of

the default parameters for most bioaccumulation and transfer factors and for ingestion and inhalation dose factors.

As illustrated in Figure 2-22, nine environmental pathways are considered in RESRAD: direct exposure, inhalation of dust particles and radon, and ingestion of foods, meat, milk, aquatic foods, water, and soil.

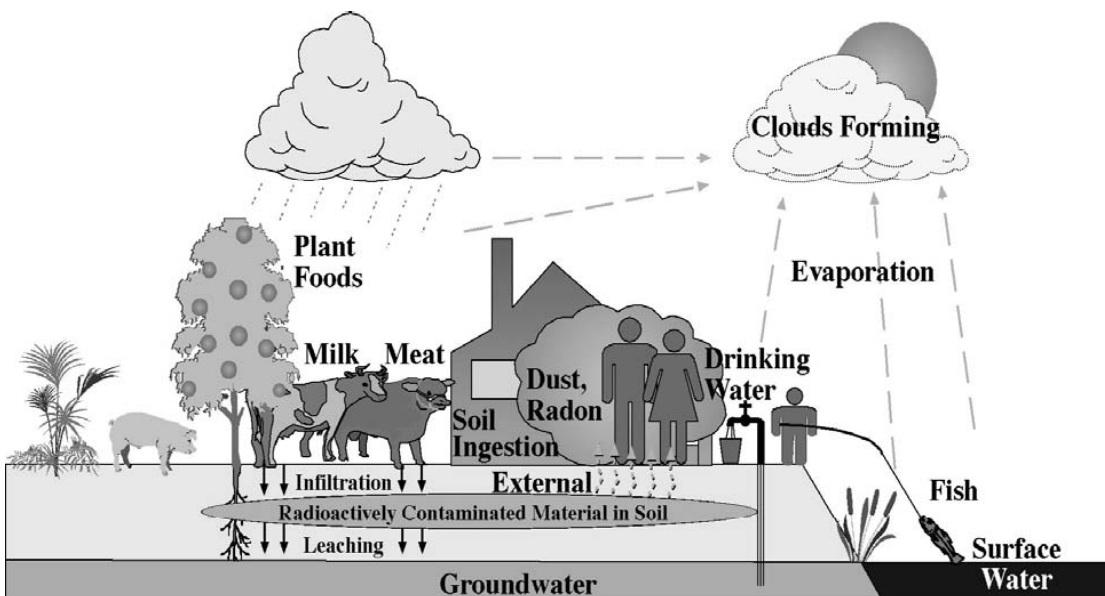


Figure 2-22: RESRAD environmental pathways (Yu, 2001).

A schematical representation of the major pathways used to derive the site-specific guidelines is illustrated in Figure 2-23. Minor pathways (i.e. external radiation from contaminated water) for on-site exposures are not taken into account in deriving soil guidelines because the dose contribution is expected to be insignificant.

As illustrated in Figure 2-23, the pathway analysis for deriving guidelines from a dose limit has four parts: source analysis, environmental transport analysis, dose/exposure analysis and scenario analysis.



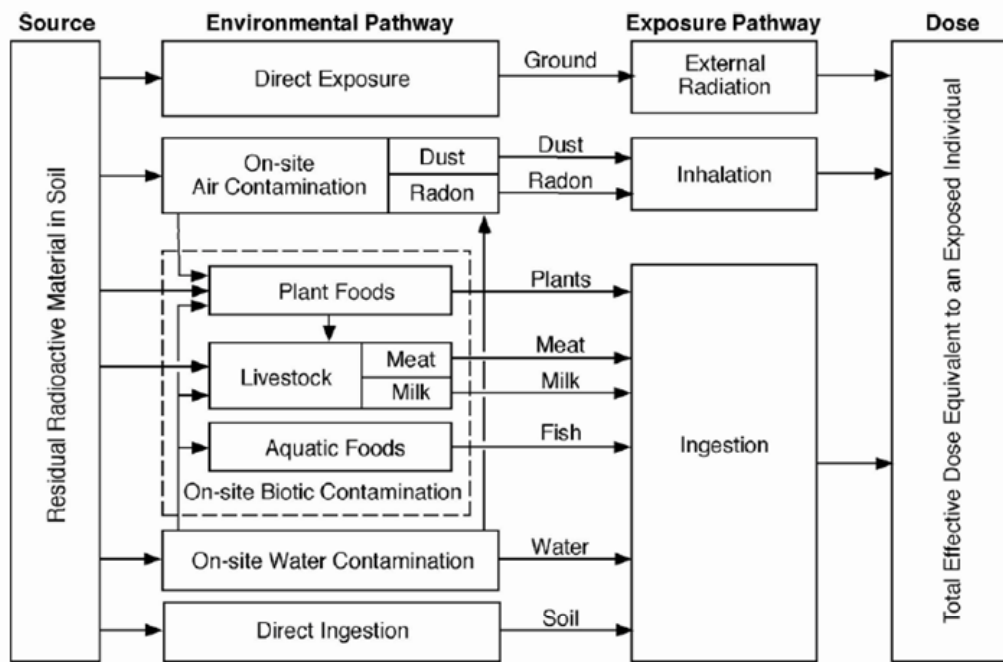


Figure 2-23: RESRAD pathway model (Yu, 2001).

Source analysis addresses the problem of deriving the source terms that determine the rate at which residual radioactivity is released into the environment. The geometry of the contaminated zone, the concentrations of the radionuclides present, the ingrowth and decay rates of the radionuclides, and the removal rate by erosion and leaching determine this release rate.

Environmental transport analysis addresses the problems of both identifying environmental pathways by which radionuclides can migrate from a source to a human exposure location and determining the migration rate along these pathways.

Exposure/dose analysis addresses the problem of the derivation of DCFs for the radiation dose that will be incurred by exposure to ionizing radiation.

RESRAD output can be displayed in the form of five textual reports and a multitude of graphical options. Textual reports include: summary (input parameters, dose summary, etc.), detailed (source factors, pathway summary, etc.), concentration (concentrations in all media), risk (risk slope factors, excess cancer risks, etc.), and progeny (dose contributions from progeny). Graphical outputs include: dosage contributions of selected nuclides, radionuclide concentrations in various media, ratios of individual radionuclides dose contribution per concentration, soil guidelines, and excess cancer risk.

### Determination of Environmental Cleanup Goals

The NRC developed the LTR to govern decommissioning activities at NRC-regulated sites. Under the CERCLA, the EPA could invoke more restrictive regulations. At times, these sometimes-conflicting regulations have caused confusion as to which criteria drive the remediation or decommissioning process.

A difference in the culture and regulatory history of these agencies has led to the adoption of different approaches to managing issues involving radioactive materials. While the NRC uses an annual dose criterion to determine acceptable levels of residual contamination, the EPA uses a lifetime cancer risk criterion. It is sometimes unclear if the remediation criteria in the LTR provide a level of protection of public health and the environment that is consistent with criteria established by EPA under CERCLA.

Potentially complicating this process even further is the recent ICRP proposal for assessing the impact of ionizing radiation to non-human populations. The existing recommendations, published in 1990 as ICRP Publication 60, do not specifically address protection of non-human species from ionizing radiation. The ICRP set up a Task Group in

2000 to consider a broader framework for radiation protection of the environment rather than just humans. This decision was developed to fill a conceptual gap in radiological protection and to clarify how the proposed framework can contribute to the attainment of society's goals of environmental protection (ICRP, 2003). The ICRP does not intend to set regulatory standards for protecting the environment. Instead, the Commissions intent is to recommend a framework that can be used as a practical tool to provide high-level advice and guidance to help regulators and operators demonstrate compliance with existing legislation. At this point, the impacts of these new ICRP recommendations to NRC- or EPA-regulated sites are not fully understood. Although not specifically addressed in this study, the ICRP proposals are included here for completeness.

#### Regulations Pertaining To Remediation

As previously stated, the NRC and the EPA each utilize unique sets of regulations when performing remediation and decommissioning activities at radioactively contaminated sites. The NRC uses what is commonly referred to as a "top-down" approach. This approach uses a radiation specific protection approach, based on dose, which focuses on human health protection. Conversely, the EPA uses what is termed a "bottom-up" approach. This approach uses a radiation protection program, based on risk, which protects both human health and environmental resources. Although the intent of each is to return a site that is safe from the harmful effects of ionizing radiation, the differing manner in which this is done can lead to confusion and frustration on the part of the site managers.

## NRC Regulations

NRC regulations are set forth in 10 CFR Part 20, Subpart E. This regulation governs all NRC-regulated facilities with the exception of thorium mills and uranium recovery facilities (governed by 10 CFR Part 40, Appendix A). Subpart E specifies two radiation criterion, one to permit the unrestricted use of a contaminated site after license termination and the other to permit the restricted use of a contaminated site after license termination.

Under Subpart E, a site is acceptable for unrestricted use if (NCRP, 2004):

1. The annual TEDE of the average member of a critical group does not exceed 0.25 mSv (25 mrem); and
2. The concentration of radioactive materials is reduced to levels that are consistent with ALARA.

When an NRC licensee can demonstrate that compliance with the annual dose criterion of 0.25 mSv (25 mrem) for unrestricted use is not reasonably achievable or would result in net harm to the public or the environment, a site can be considered acceptable for license termination under restricted conditions if:

1. The licensee ensures legally enforceable institutional controls are in place that provides reasonable assurance that the annual TEDE will not exceed 0.25 mSv (25 mrem); and
2. The residual radiation levels are reduced so that there is a reasonable assurance that the annual TEDE would remain ALARA if institutional controls ever failed.

Furthermore, the NRC stipulates that these levels, although considered ALARA, must be below 1 mSv (100 mrem). At times, the NRC will allow this threshold to be 5 mSv (500 mrem) when the licensee demonstrates that further reductions to comply with the 1 mSv (100

mrem) criterion are not technically achievable, would be prohibitively expensive, or would result in net harm to the public or environment.

## EPA Regulations

EPA regulations for decommissioning of radioactive sites were developed under CERCLA. The principle regulation implementing this is the National Oil and Hazardous Substances Pollution Contingency Plan, or NCP, in 40 CFR Part 300 (NCRP, 2004). Unlike the NRC guidelines above which set compliance limits, CERCLA only defines a process for determining acceptable remediation actions for a site and specifies goals for the remediation.

CERCLA states that remediation goals at a site shall be protective of human health and the environment. These goals should be developed taking into account (EPA, 1990):

1. ARARs established under other federal or state environmental laws;
2. For known or suspected carcinogens, an upper bound on lifetime cancer risk of between  $10^{-6}$  and  $10^{-4}$  from all substances and all exposure pathways combined at specific sites; and
3. For noncarcinogens, including uranium, a hazard index of one or less. A hazard index of less than or equal to one means it is unlikely for even sensitive populations to experience adverse health effects. A hazard index greater than one means there is a possibility for non-cancerous effects on humans.

An emphasis on the use of ARARs in establishing protective remediation goals reflects the purpose of CERCLA, which is to address environmental contamination that is not adequately regulated under other laws. For example, federal and state drinking water standards established under the SDWA are specified as ARARs for remediation of

groundwater or surface waters that are current or potential sources of drinking water. Thus, compliance with regulations established under other laws would not normally result in a need for remediation under CERCLA.

The EPA emphasizes the use of risk, rather than dose, in establishing remediation levels. This allows the EPA to relate lifetime cancer risks to concentrations of radionuclides in environmental media and resulting exposures using cancer risk coefficients developed in Federal Guidance Report No. 13 and ICRP Publication 72. These risk coefficients have been incorporated in EPA's HEAST and gives risks of cancer incidence per unit concentration of radionuclides in environmental media (HEAST, 2001).

#### Other Regulations

Although outside the scope of this study, it must be recognized that states can play an important role in regulating remediation of sites licensed under NRC and are potentially subject to remediation under CERCLA. If states are Agreement States, they may adopt the NRC's LTR as written or impose more stringent dose limits. States also engage in regulatory oversight, approve work plans, perform independent sampling and analysis, and promote public participation in remediation decisions.

#### Approaches to Remediation

As stated previously, the NRC uses criterion based on dose, widely considered the "dose approach" or "top-down" approach, for determining remediation or decommissioning efforts while the EPA criterion is based on risk, or commonly called the "risk approach" or "bottom-up" approach.

By definition, the dose assigned by the “dose approach” is calculated by multiplying a dose conversion factor by the TEDE. This approach is based on an annual exposure to radiation and follows the ICRP effective dose equivalent approach. Given that radiation exposures are justified, two basic elements are established in this approach: (1) a limit is placed on radiation dose to individuals from all controllable sources, corresponding to a maximum allowable risk for any routine exposure situation; and (2) a reduction of all controllable exposures ALARA (NCRP, 2004). Figure 2-24a further illustrates the elements of the dose approach.

Dose conversion factors were established by the ICRP in Publication 30 (ICRP, 1979) and are expressed as dose per unit exposure. Revised dose conversion factors were published in Publication 72 (ICRP, 1996), but until recently, have been used sparingly at some sites as the new factors place more emphasis on the ingestion pathway, rather than the inhalation pathway, and are more applicable to the general public. Each radionuclide has a unique dose conversion factor depending on the type of radiation emitted, relative strength of radiation, target organs and tissues and cancer induction rates.

The “Risk Approach” is calculated directly by assigning a unit of risk (i.e. probability of an individual developing cancer) for every unit of exposure (or cancer slope factor) and multiplying it by the total exposure. Expression of the risk factor varies depending on its application. For example, for an intake of a particular radionuclide, it will be expressed as the probability of adverse effect for that radionuclide/pCi intake. As with the NRC approach, the risk approach is also based on two basic elements, assuming radiation exposures are justified. This approach establishes (1) a goal for acceptable risk; and (2) allowance for an

increase in risks above the goal, based primarily on considerations of technical feasibility and cost (NCRP, 2004). Figure 2-24b. further illustrates the elements of the risk approach.

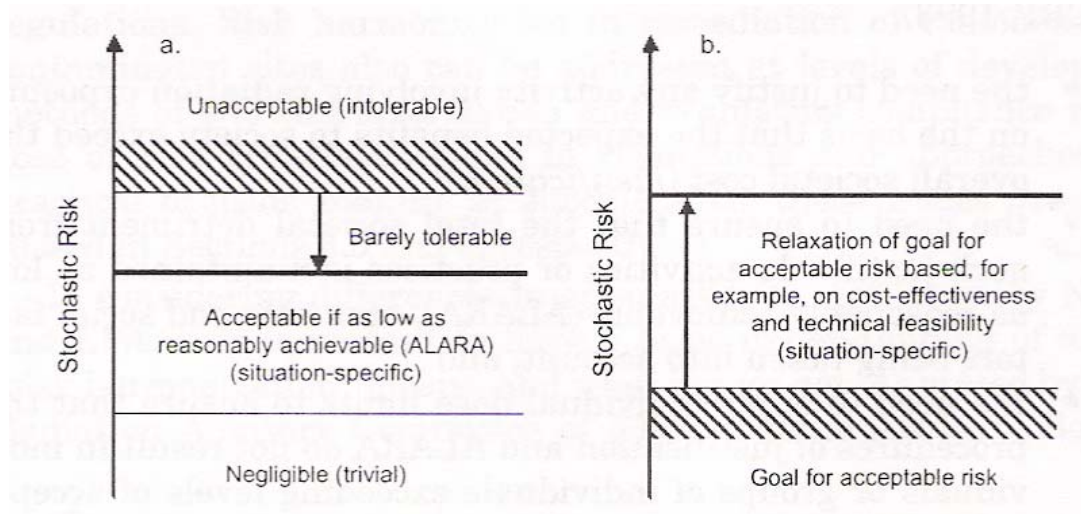


Figure 2-24: Depiction of (a) radiation paradigm and (b) chemical paradigm for cancer risk management (NCRP, 2004).

Slope factors are best estimates of the lifetime excess total cancer risk per unit intake or exposure. Slope factors are similar to dose conversion factors but instead of assigning a unit of dose for every unit of exposure (i.e. Sv pCi<sup>-1</sup>), a unit of risk is assigned for every unit of exposure (i.e. probability of adverse effect pCi<sup>-1</sup>). Current slope factors are based on updated and improved radiation risk coefficients in Federal Guidance Report No. 13 and ICRP Publication 72 and are published in HEAST (HEAST, 2001). The EPA has generated inhalation and ingestion slope factors for most radionuclides and can be obtained at <http://www.epa.gov/radiation/heast/>.

Also, dose values can be converted into risk, and vice versa, using conversion factors. A conversion factor of  $7.0 \times 10^{-2} \text{ Sv}^{-1}$  is commonly utilized and agrees with a lifetime cancer



incidence risk of  $3.0 \times 10^{-4}$  from receiving  $0.15 \text{ mSv y}^{-1}$  ( $15 \text{ mrem y}^{-1}$ ) over 30 years.

Therefore, risk is calculated by using the following equation:

$$\text{Risk} = \text{total dose (Sv)} \times \text{conversion factor } (7.0 \times 10^{-2} \text{ Sv}^{-1})$$

#### NRC/EPA Memorandum of Understanding

In recognition of their mutual commitment to protect the public health and safety and the environment, the NRC and the EPA entered into a Memorandum of Understanding (MOU) in the fall of 2002. This understanding was established to create the basic framework for the relationship of the agencies in the decommissioning and decontamination of NRC-licensed sites in order to facilitate decision-making and not to establish any new requirements or rights on parties not subject to the agreement. (EPA/NRC, 2002)

Under the MOU, the EPA would continue to defer to the NRC for decision-making in the decommissioning of NRC-licensed sites except in the following circumstances:

1. The NRC determines there is radioactive groundwater contamination in excess of EPA's Maximum Contamination Limits (MCLs).
2. The NRC contemplates either restricted release or the use of alternate criteria for license termination.
3. The radioactive contamination at the time of license termination exceeds the corresponding levels in Table 1 of the MOU (Table 2-6 below).

Table 2-6: Consultation Triggers for Residential and Commercial/Industrial Soil Contamination (Adapted from EPA/NRC, 2002).

Radionuclide	Residential Soil Concentration	Industrial/Commercial Soil Concentration
<sup>3</sup> H	228 pCi/g	423 pCi/g
<sup>14</sup> C	46 pCi/g	123,000 pCi/g
<sup>22</sup> Na	9 pCi/g	14 pCi/g
<sup>35</sup> S	19,600 pCi/g	32,200,000 pCi/g
<sup>36</sup> Cl	6 pCi/g	10,700 pCi/g
<sup>45</sup> Ca	13,500 pCi/g	3,740,000 pCi/g
<sup>46</sup> Sc	105 pCi/g	169 pCi/g
<sup>54</sup> Mn	69 pCi/g	112 pCi/g
<sup>55</sup> Fe	269,000 pCi/g	2,210,000 pCi/g
<sup>57</sup> Co	873 pCi/g	1,420 pCi/g
<sup>60</sup> Co	4 pCi/g	6 pCi/g
<sup>59</sup> Ni	20,800 pCi/g	1,230,000 pCi/g
<sup>63</sup> Ni	9,480 pCi/g	555,000 pCi/g
<sup>90</sup> Sr + Decay	23 pCi/g	1,070 pCi/g
<sup>94</sup> Nb	2 pCi/g	3 pCi/g
<sup>99</sup> Tc	25 pCi/g	89,400 pCi/g
<sup>129</sup> I	60 pCi/g	1,080 pCi/g
<sup>134</sup> Cs	16 pCi/g	26 pCi/g
<sup>137</sup> Cs + Decay	6 pCi/g	11 pCi/g
<sup>152</sup> Eu	4 pCi/g	7 pCi/g
<sup>154</sup> Eu	5 pCi/g	8 pCi/g
<sup>192</sup> Ir	336 pCi/g	544 pCi/g
<sup>210</sup> Pb + Decay	15 pCi/g	123 pCi/g
<sup>226</sup> Ra	5 pCi/g	5 pCi/g
<sup>227</sup> Ac + Decay	10 pCi/g	21 pCi/g
<sup>228</sup> Th + Decay	15 pCi/g	25 pCi/g
<sup>232</sup> Th	5 pCi/g	5 pCi/g
<sup>234</sup> U	401 pCi/g	3,310 pCi/g
<sup>235</sup> U + Decay	20 pCi/g	39 pCi/g
<sup>238</sup> U + Decay	74 pCi/g	179 pCi/g
total uranium	47 mg/kg	1230 mg/kg
<sup>238</sup> Pu	297 pCi/g	1,640 pCi/g
<sup>239</sup> Pu	259 pCi/g	1,430 pCi/g
<sup>241</sup> Pu	40,600 pCi/g	172,000 pCi/g
<sup>241</sup> Am	187 pCi/g	568 pCi/g
<sup>242</sup> Cm	32,200 pCi/g	344,000 pCi/g
<sup>243</sup> Cm	35 pCi/g	67 pCi/g

## CHAPTER III

### METHODS AND MATERIALS

#### Chernobyl Exclusion Zone Characterization

The UIAR characterization of the Chernobyl exclusion zone was performed through a combination of *in situ* monitoring and soil sampling for  $^{137}\text{Cs}$  and  $^{90}\text{Sr}$ . The zone was divided into 10,000  $\text{m}^2$  sampling sites. Prior to soil sampling at each site, the gamma exposure rate ( $\mu\text{R h}^{-1}$ ) was measured at several positions utilizing certified dosimeters, DRG-01T, at a height of 1 m (UIAR, 2001).

To determine terrestrial density ( $\text{kBq m}^{-2}$ ) of cesium contamination in the soil, four parallel sub-samples were taken from each sample: one sub-sample of  $1000 \text{ cm}^3$  and three sub-samples of  $100 \text{ cm}^3$  each. The specific activities of  $^{134}\text{Cs}$  and  $^{137}\text{Cs}$  were measured by gamma spectroscopy in each sub-sample. If the relative deviation of the values of  $^{137}\text{Cs}$  specific activity, calculated by  $(C_{\text{max}} - C_{\text{min}}) / (C_{\text{max}} + C_{\text{min}})$ , exceeded 0.15, sub-samples had been mixed together again and then homogenized in order to satisfy the above criteria. When the criterion was reached, one  $100 \text{ cm}^3$  sub-sample was selected for measurements of  $^{90}\text{Sr}$  specific activity.

Terrestrial density of cesium soil contamination ( $\text{kBq m}^{-2}$ ) was calculated as:

$$A_s = (M * \sum_i C_i m_i) / (S * \sum_i m_i)$$

where **M** = mass of complex sample (kg)

**S** = sampling area ( $\text{m}^2$ )

**m<sub>i</sub>** = mass of i-th sub-sample measured (kg)

Relative uncertainties of determination of these values (95% confidence level), expressed in percentages, include the measurement uncertainties and uncertainties caused by deviation of activities measured in parallel sub-samples (UIAR, 2001).

Preparation of soil samples for  $^{90}\text{Sr}$  analyses are first incinerated for 4 hours. After injection of a tracer element,  $^{85}\text{Sr}$ , the samples were treated with a 6 molar  $\text{HNO}_3$  solution during 2 hours of permanent mixing and heating. After filtration, hydroxides of high-valence metals (Fe, Al, Ti, Mn, Th, & U) are extracted by adding ammonia without carbon into the solution. Then, after acidification, the solution was left for 3 weeks in order to for  $^{90}\text{Sr}$  and  $^{90}\text{Y}$  to come into secular equilibrium. After this period, a stable isotope of yttrium is added into solution and extracted by ammonia without carbon. Obtained precipitate was incinerated to  $\text{Y}_2\text{O}_3$  and analyzed after decay of radium progenies (UIAR, 2001).

Gamma spectroscopy measurements of the samples were carried out on a low-background, high-resolution gamma spectrometer (GEM-30185) with passive shielding. Beta measurements were made on a low-background beta-radiometer (Canberra-2400). All equipment and associated calibration samples were properly certified (UIAR, 2001).

### Site Selection

A successful incident at a predominantly urban SFP site will result in many more direct human health effects than an incident at a predominantly rural SFP site due to higher population densities. Conversely, a successful incident at a rural SFP site would more directly affect a substantial amount of agricultural production. Every decision made after an incident, from initial response actions to long term recovery, will be driven

by the varying parameters at the specific sites. Although it is not possible to create a specific health physics evaluation that would encompass both rural and urban SFP sites adequately, a thorough understanding of both scenarios will help identify the important pathways that significantly contribute to human dose for each and provide guidance for response.

For this study, successful SFP incidents at both rural and urban sites were evaluated. In order to select a SFP for each analysis, the population within a 30-km radius of each U.S. commercial power reactor sites was generated (based on 2002 population data) to determine the potential population levels. For purposes of this study, populations under 50,000 are considered predominantly rural while populations over 500,000 are considered predominantly urban.

### Dispersion Modeling

To estimate the radiological dispersion in a hypothetical scenario such as the one developed in this study, HPAC utilizes a spent fuel release computation based on air dropped munitions. Specifically, this computation infers a situation in which one or more air dropped munitions impact a SFP, resulting in a “zircalloy” fire where radiological materials are dispersed. A secondary option available for dispersion of spent fuel involves a fuel cladding failure. By HPAC definition, a zircalloy fire occurs in a SFP when the fuel cladding material ignites as a result of the very high temperatures obtained after a loss of coolant occurs. A “fuel cladding failure” involves a breach of the cladding material either from mechanical damage or damage caused during the fuel irradiation. HPAC only includes three fuel batches (i.e. 1 batch equals 1/3 of a reactor core) in the

zircalloy scenario with the remaining spent fuel assumed to be in a fuel cladding failure condition. This is due to the fact that after approximately 5 years in a SFP, the fresh fuel from the reactor will decay enough to reduce the likelihood of zircalloy ignition by decay heat.

The “historical weather option” in HPAC was utilized for this study. The historical weather option incorporates the observed weather conditions for the 15<sup>th</sup> or 16<sup>th</sup> of the chosen month in 1990 for a typical day observation and 20-year averaged monthly statistics data for summary observations. With the historical weather option, weather parameters for each scenario are obtained from the nearest observation point of the accident location where weather data is measured. The rural and urban scenarios evaluated in this study were determined by performing one individual scenario for each calendar month. Utilizing identical accident parameters, 12 individual scenarios were performed to identify the average and worst-case radionuclide deposition around the SFP, as well as determining the predominant dispersion direction of the resulting plume. Upon evaluating the 12 individual scenarios, the month which represents the worst-case and/or representative conditions is selected as the scenario for evaluation of radiation exposure via RESRAD modeling.

For the dispersion analysis, the settings of the appropriate HPAC accident parameters are selected to represent either worst-case and/or realistic conditions. For example, the parameter “sprays” represents the availability of water sprays to cool the fuel elements in the absence of coolant in the pool. To create worst-case conditions, this parameter is set to represent the absence of sprays. Conversely, the “exhaust area” parameter selected represents the open area of a typical SFP as depicted in Figure 2-11

and thus represents a realistic parameter setting. Table 3-1 provides a complete list and brief description of the HPAC parameters utilized in this study. These parameters descriptions are included to demonstrate how HPAC calculates dispersion of radionuclides based on the previous discussion (i.e. plume rise).

Table 3-1: HPAC parameter descriptions.

Parameter	Description
Batches	Represents the number of fuel batches in the fuel at the time of the accident. Each batch is assumed to be one third of the reactor core.
Sprays	Settings: <b>on</b> or <b>off</b> . Containment sprays are designed to remove airborne fission products and to condense steam to prevent over-pressurization following an accident.
Release Path	Settings: <b>filtered</b> or <b>unfiltered</b> . Aerosol and particulate fission products released may encounter filter systems that can be very effective at reducing the amount of material released into the environment.
Last Batch in Pool	This date represents the most recent date and time of the latest batch placed in the SFP and is used to calculate the decay of the spent fuel. HPAC assumes all batches to be two years older than the previous batch.
Leak Rate	This value represents the leak rate for the accident. Leak rates range from 0.5%/hr to 100%/hr.
Release Height	The effective height of the material release (above ground level). HPAC recommends a value of zero be used unless the release is through an isolated stack or vent that is at least two times the height of the facility structure. The release height can also be used to account for an elevated release due to plume rise as an alternative to entering buoyancy parameters.
Temperature above Ambient	Buoyancy parameter that represents the release temperature in excess of ambient (20°C).
Vertical Exhaust Velocity	Buoyancy parameter that represents the vertical velocity of the release material.
Exhaust Area	Buoyancy parameter that represents the area through which the release is being exhausted.

For this hypothetical study, the radionuclides that provide the greatest contributions to contamination are identified through the HPAC source term calculated for each scenario respectively. The resulting radionuclide distribution in ground concentration for each contour is then calculated for input into RESRAD, assuming a soil

density of  $1.5 \text{ g cm}^{-3}$  and a depth of contamination of 0.1 m (i.e. all contamination remains at or near the surface).

### Radiation Exposure Modeling

The parameters that control the rate of radionuclide release into the environment and the severity and duration of human exposure at a given location are determined by patterns of human activity referred to as exposure scenarios. There are four generic exposure scenarios used in RESRAD. The actual scenario of a site will depend on numerous factors, including the location of the site, zoning of the land, physical characteristics, etc. Soil guidelines are usually based on a resident farmer exposure scenario and include all environmental pathways for on-site or near-site exposure. This represents the most conservative scenario as it is expected to result in the highest predicted lifetime dose. Other scenarios, such as the suburban resident, industrial worker, or recreationist, can be taken into account by adjusting the scenario parameters in formulas for calculating the transport of radionuclides through the pathways.

Table 3-2 identifies the pathways considered for the four scenarios (Yu, 2001). For the resident farmer scenario, water used for drinking, household purposes, irrigation, and livestock watering is considered to be from a local well in the contaminated area. For the suburban resident scenario, all drinking water, meat or milk consumption considered results from sources other than the contaminated area. Ingestion of plant foods is considered however. For the industrial worker, no consumption of water or foods from the contaminated area is considered. For the recreationist, no water or food consumption, except for on-site fish or game, is considered in the scenario.



Table 3-2: RESRAD scenario pathways.

Pathway	Resident Farmer	Suburban Resident	Industrial Worker	Recreationist
External gamma exposure	Yes	Yes	Yes	Yes
Inhalation of dust	Yes	Yes	Yes	Yes
Radon inhalation	Yes	Yes	Yes	Yes
Ingestion of plant foods	Yes	Yes	No	No
Ingestion of meat	Yes	No	No	Yes
Ingestion of milk	Yes	No	No	No
Ingestion of fish	Yes	No	No	Yes
Ingestion of soil	Yes	Yes	Yes	Yes
Ingestion of water	Yes	No	No	No

Table 3-3 compares key default parameters used in each of the scenarios. All parameters are user-changeable should site-specific input parameters be determined locally.

Table 3-3 RESRAD default parameters.

Parameter	Unit	Resident Farmer	Suburban Resident	Industrial Worker	Recreationist
Exposure duration	yr	30	30	25	30
Inhalation rate	m <sup>3</sup> /yr	8400	8400	11400	14000
Fraction of time indoors	N/A	0.5	0.5	0.17	N/A
Fraction of time outdoors	N/A	0.25	0.25	0.06	0.006
Contaminated fractions of plant food	N/A	0.5	0.1	Not Used	Not Used
Contaminated fractions of milk	N/A	1	Not Used	Not Used	Not Used
Contaminated fractions of meat	N/A	1	Not Used	Not Used	1
Contaminated fractions of aquatic food	N/A	0.5	Not Used	Not Used	0.5
Soil ingestion	g/yr	36.5	36.5	36.5	36.5
Drinking water intake	L/yr	510	Not Used	Not Used	Not Used

For purposes of this study, the rural scenario will utilize the resident farmer default parameters and the urban scenario will utilize the suburban resident default

parameters. The basic dose limit of  $0.25 \text{ mSv y}^{-1}$  ( $25 \text{ mrem y}^{-1}$ ) was selected for use in this study to conform to the NRC regulations set forth in 10 CFR Part 20, Subpart E.

## CHAPTER IV

### RESULTS

#### Chernobyl Exclusion Zone Characterization

The UIAR results presented in this study represent the first time extensive and representative soil sampling occurred on a regular grid in the exclusion zone. The terrestrial density of  $^{137}\text{Cs}$  contamination determined in the Chernobyl exclusion zone during the UIAR study is shown in Figure 4-1, the terrestrial density of  $^{90}\text{Sr}$  is shown in Figure 4-2 and the ratio of  $^{137}\text{Cs}$  to  $^{90}\text{Sr}$  is illustrated in Figure 4-3.

The estimate of the  $^{137}\text{Cs}$  content in the exclusion zone is approximately 4000 TBq (~ 0.11 MCi), which corresponds to the estimates determined in the years directly after the accident.

At the conclusion of this characterization, greater than 95% of  $^{90}\text{Sr}$  was found to be located in the upper 30 cm of soil at most sites. Only a few sites, less than 0.1% of all sites, had more than 20% of the  $^{90}\text{Sr}$  activity migrating below 30 cm. The total inventory of  $^{90}\text{Sr}$  was found to be about 810 TBq (~ 0.022 MCi), which corresponds to 0.4-0.5% of its inventory in the reactor at the time of the accident. This value suggests the  $^{90}\text{Sr}$  contamination determined previously had been overestimated by a factor of 3-4 times (Kasparov).

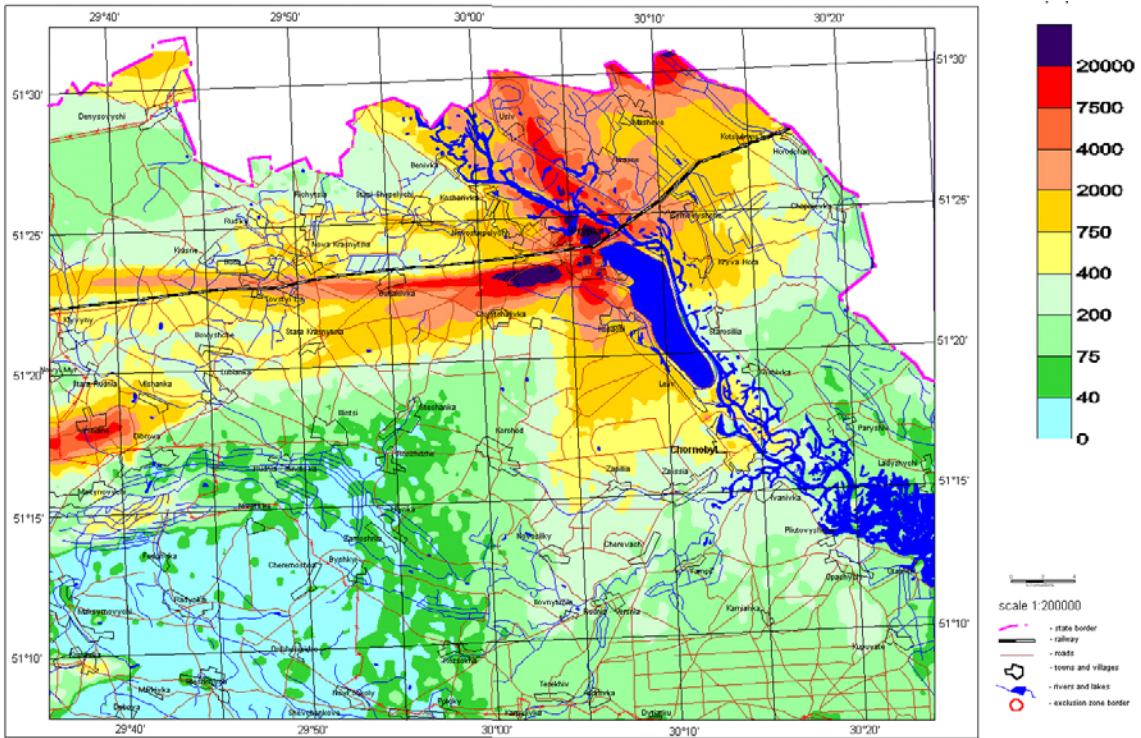


Figure 4-1: Terrestrial density of  $^{137}\text{Cs}$  contamination at Chernobyl ( $\text{kBq m}^{-2}$ ) (UIAR, 2001).

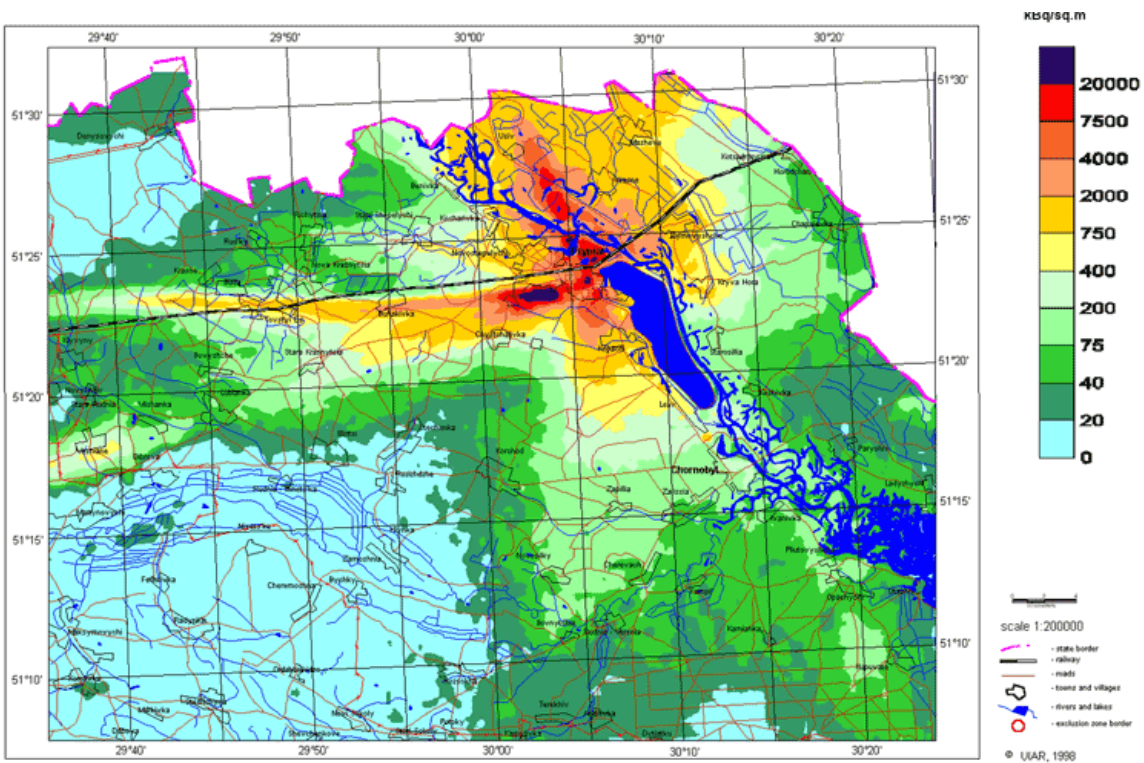


Figure 4-2: Terrestrial density of  $^{90}\text{Sr}$  contamination at Chernobyl ( $\text{kBq m}^{-2}$ ) (UIAR, 2001).

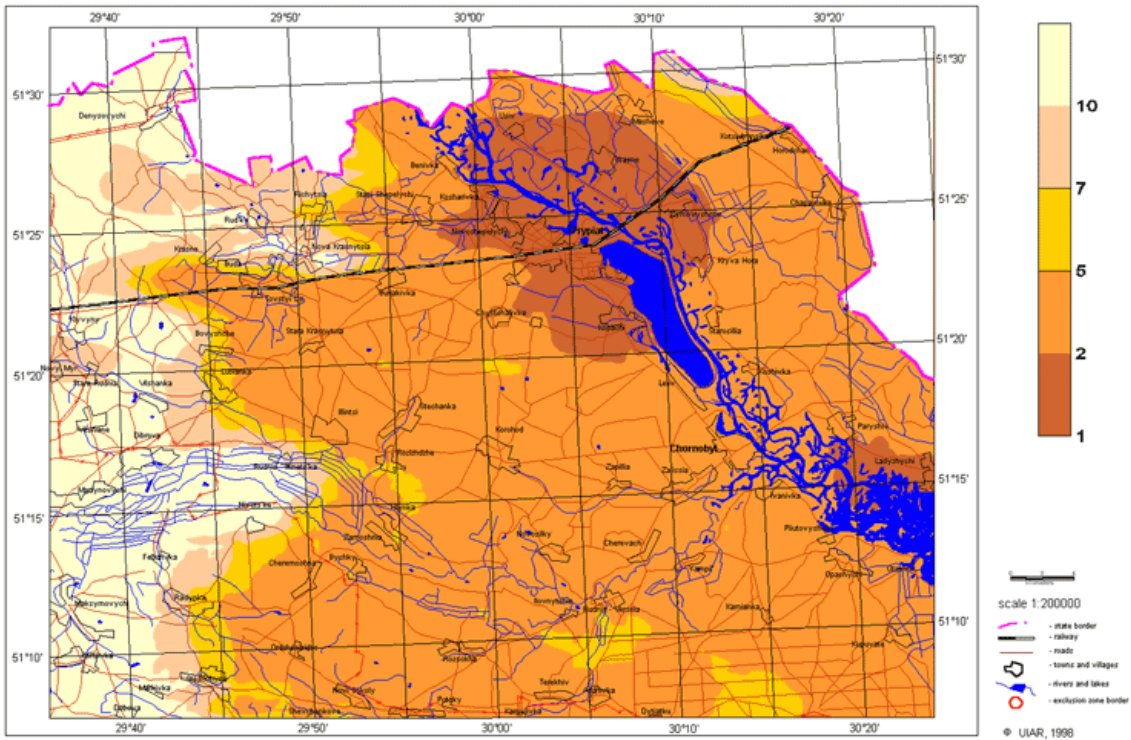


Figure 4-3:  $^{137}\text{Cs}/^{90}\text{Sr}$  activity ( $\text{kBq m}^{-2}$ ) ratio in soil at Chernobyl (UIAR, 2001).

### Site Selection

A map of the 30-km zones around each reactor site is illustrated in Figure 4-4. Based on the criteria discussed previously, the five lowest populations within the 30-km zones are listed in ascending order in Table 4-1. Conversely, the five highest populations are listed in descending order in Table 4-2.

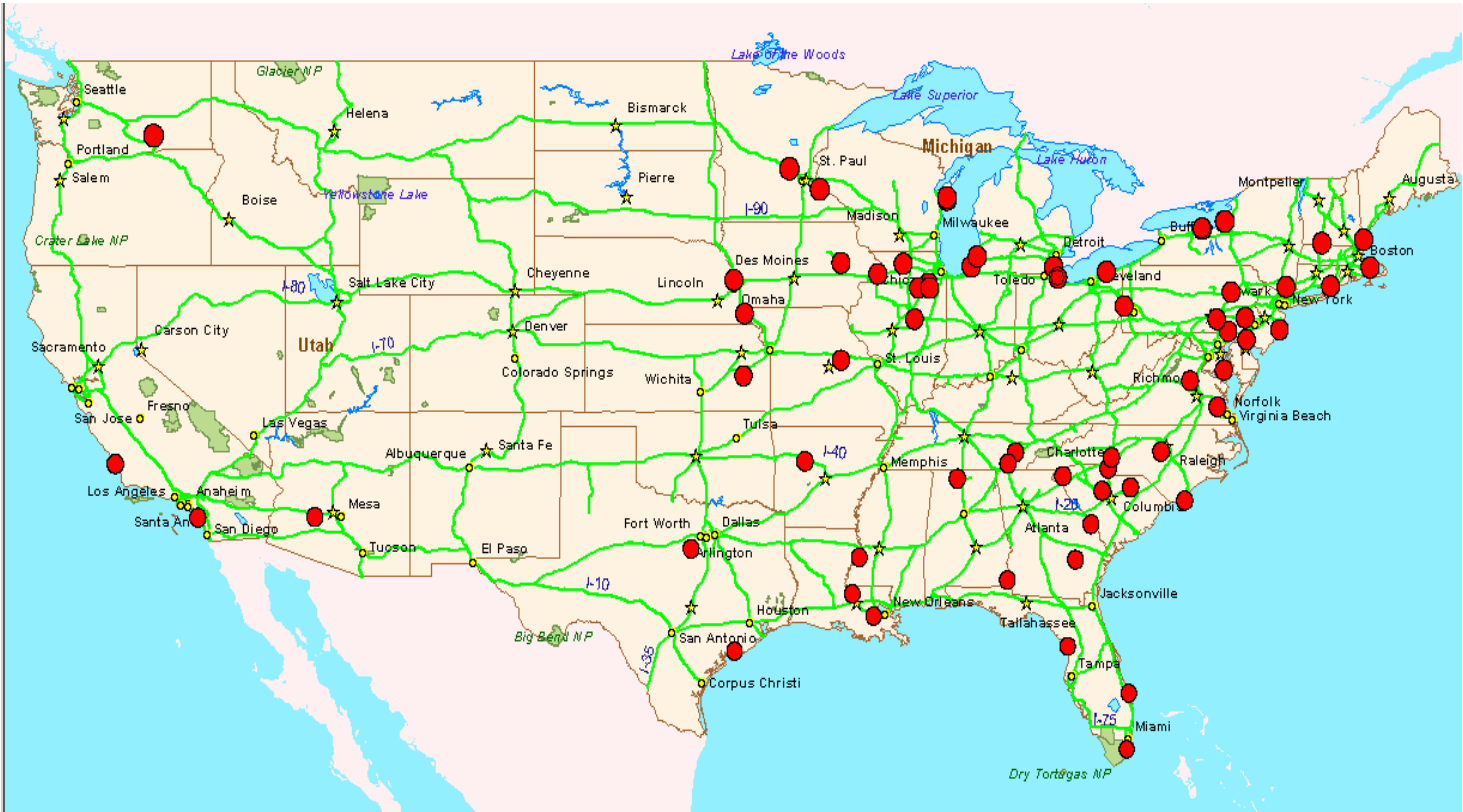


Figure 4-4: 30-km zones around U.S. reactor sites.

Table 4-1: Five smallest populations within 30-km of U.S. reactor sites.

Plant Name	Reactor Type	Location	Pop. at Risk (30 km)	Owner/Operator
Palo Verde	PWR	36 MI W of Phoenix, AZ	11,468	Arizona Public Service Co.
Wolf Creek	PWR	3.5 MI NE of Burlington, KS	14,781	Wolf Creek Nuclear Operating Corp.
Cooper	BWR	23 MI S of Nebraska City, NE	24,648	Nebraska Public Power District
Grand Gulf	BWR	25 MI S of Vicksburg, MS	29,367	Entergy Operations, Inc.
South Texas	PWR	12 MI SSW of Bay City, TX	30,301	STP Nuclear Operating Co.

Table 4-2: Five largest populations within 30-km of U.S. reactor sites.

Plant Name	Reactor Type	Location	Pop. at Risk (30 km)	Owner/Operator
Indian Point	PWR	24 MI N of New York City, NY	1,507,029	Entergy Nuclear IP2 LLC
Limerick	BWR	21 MI NW of Philadelphia, PA	1,098,870	Exelon Generation Co., LLC
Three Mile Island	PWR	10 MI SE of Harrisburg, PA	790,177	AmerGen Energy Co., LLC
McGuire	PWR	17 MI N of Charlotte, NC	759,622	Duke Energy Corp.
Catawba	PWR	6 MI NW of Rock Hill, SC	668,932	Duke Energy Corp.

### Dispersion Modeling

Based on estimated worst-case and/or realistic values as discussed in Chapter 3 above, the HPAC dispersion parameters selected for both rural and urban scenarios are presented in Table 4-3.

Table 4-3: HPAC parameter values utilized in rural and urban scenarios.

Parameter	Scenario Value	Units
Batches	9	N/A
Sprays	Off	N/A
Release Path	Unfiltered	N/A
Last Batch in Pool	1 year prior	N/A
Leak Rate	1	%/hr
Release Height	0	m
Temp above Ambient	900	°C
Vertical Exhaust Velocity	5	m/sec
Exhaust Area	333	m <sup>2</sup>

## Rural Scenario

Based on the criteria discussed previously and the population within the 30-km zone around each reactor site (see Table 4-1), the Wolf Creek power reactor, located approximately 3.5 miles NE of Burlington, Kansas, was the commercial nuclear reactor site chosen to analyze the effects of a rurally located SFP incident. As listed in Table 4-1, the population within 30-km of the Wolf Creek SFP is less than 15,000 and is the second-lowest at-risk population among all the U.S. reactor sites. Despite having a population density larger than the Palo Verde reactor, the Wolf Creek reactor site was selected because of the greater land use for agriculture in the region surrounding this site.

Table 4-4 lists the areas of contamination, generated monthly by HPAC, for the rural scenario utilizing the parameters listed in Table 4-3. These contaminated areas ( $\text{km}^2$ ), resulting from the dispersion of spent fuel, are shown in four activity contours of 37, 3.7, 0.37 and  $0.037 \text{ GBq m}^{-2}$  ( $1.0, 0.1, 0.01$  and  $0.001 \text{ Ci m}^{-2}$ , respectively). The average annual ground deposition for each contour is also presented in Table 4-4.

For this scenario, the radionuclide dispersion from a successful event in April generally represents the worst-case dispersion and was chosen as the incident for conducting RESRAD modeling. As listed in Table 4-4, the contaminated areas in April are greatest in the three highest concentration contours as compared to the other 11 months. In the lowest concentration contour, a May event produces a slightly higher contaminated area but both are generally comparable. Additionally, the area of contamination in all April contours is significantly higher than the mean. Furthermore, greater than 60% of the annual dispersion was found to be released in a direction within  $45^\circ$  of North as illustrated in the April dispersion plot (Figure 4-5). Due to these factors,



the April event is selected because it summarily represents the worst-case HPAC dispersion based on the input parameters selected.

The total activity release calculated by HPAC for this scenario is  $4.81\text{E}+08$  GBq (13 MCi). The major radionuclides that are released and contribute to ground deposition (i.e. greater than 0.02% of the total activity released) are listed in Table 4-5. As this table shows, the percentage of total release is calculated for each radionuclide, along with the estimated ground concentrations within the 3.7, 0.37 and 0.037 GBq m<sup>-2</sup> (0.1, 0.01, and 0.001 Ci m<sup>-2</sup>, respectively) contours, assuming a soil density of 1.5 g/cm<sup>3</sup> and a depth of contamination of 0.1 m. These three activity contours, along with the respective areas of contamination, are utilized in RESRAD to determine dose/risk to the public. Since the 37 GBq m<sup>-2</sup> (1.0 Ci m<sup>-2</sup>) contour is located within the immediate area of the SFP where access to the public would be restricted, it is not included in the RESRAD analysis. For purposes of this study (i.e. both rural and urban scenario), the distribution of radionuclide contamination within each contour is limited to these 7 major nuclides based on the individual percentages of total release.

Although noble gases do not contribute to ground deposition, the total noble gas activity released is included in Table 4-5 as they contribute to the resulting dose rate due to external exposures from airborne concentrations. Figures 4-6 and 4-7 are included to illustrate the total effective dose equivalent (TEDE) levels calculated by HPAC at 2 and 6 days after the SFP incident occurs. The estimated populations affected within the respective contours are also illustrated on each dispersion plot.

Table 4-4: Monthly dispersion results in rural scenario.

Area of Ground Deposition (km <sup>2</sup> )				
Month	37 GBq m <sup>-2</sup> (1 Ci m <sup>-2</sup> ) Contour	3.7 GBq m <sup>-2</sup> (0.1 Ci m <sup>-2</sup> ) Contour	0.37 GBq m <sup>-2</sup> (0.01 Ci m <sup>-2</sup> ) Contour	0.037 GBq m <sup>-2</sup> (0.001 Ci m <sup>-2</sup> ) Contour
January	0.028	0.706	13.983	238.782
February	0.014	0.394	9.476	186.136
March	0.017	0.444	9.342	207.008
April	0.105	2.734	55.368	542.370
May	0.058	1.272	25.519	580.604
June	0.027	0.319	4.208	63.733
July	0.030	0.361	5.748	101.463
August	0.039	0.639	10.382	155.360
September	0.047	1.024	19.806	255.565
October	0.033	0.425	7.051	110.148
November	0.007	0.544	12.241	224.837
December	0.080	1.934	37.954	539.288
<i>Mean</i>	<i>0.040</i>	<i>0.900</i>	<i>17.590</i>	<i>267.108</i>

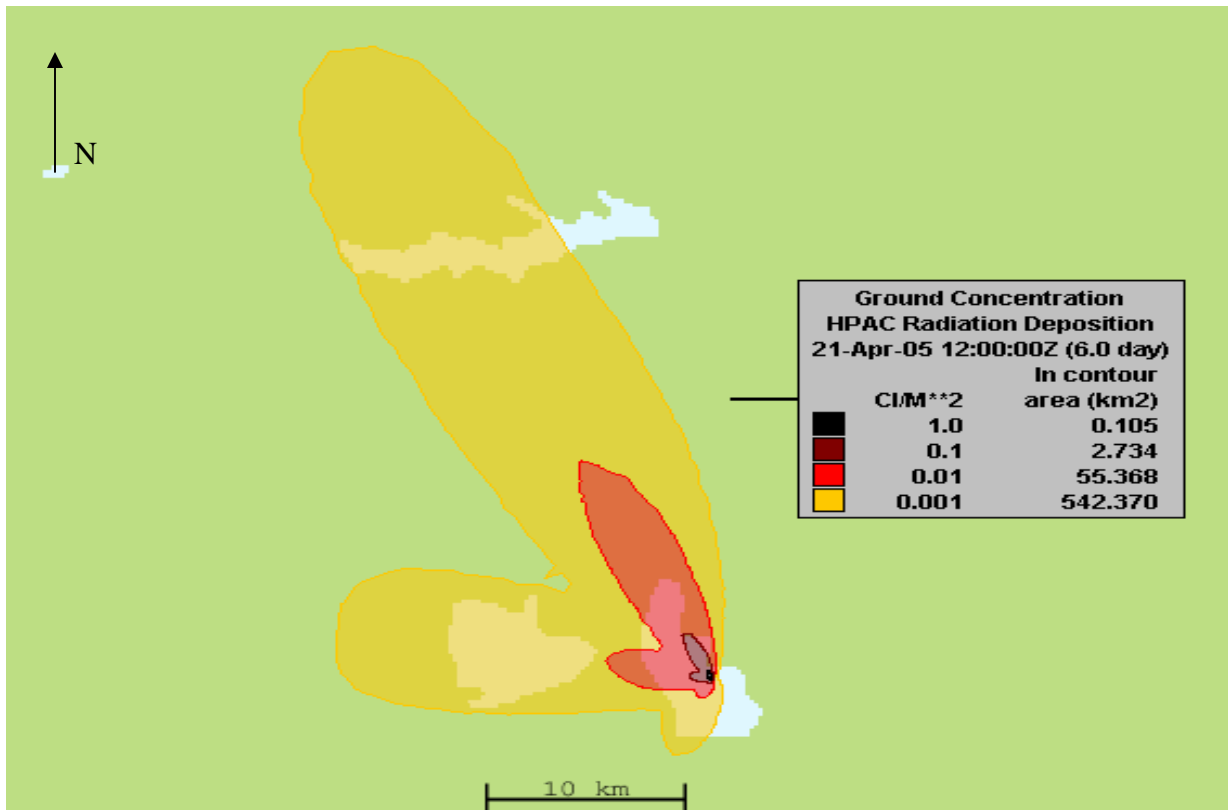


Figure 4-5: HPAC dispersion in rural scenario.

Table 4-5: Radiological dispersion results in rural scenario.

Radionuclides	Nuclide Released (GBq)	Total Activity Released (GBq)	% of release	Radionuclide Concentration 3.7 GBq m <sup>-2</sup> contour (Bq/g)	Radionuclide Concentration 0.37 GBq m <sup>-2</sup> contour (Bq/g)	Radionuclide Concentration 0.037 GBq m <sup>-2</sup> contour (Bq/g)
<sup>144</sup> Ce	4.07E+05	4.81E+08	0.08%	2.09E+01	2.09E+00	2.09E-01
<sup>134</sup> Cs	8.51E+07	4.81E+08	17.69%	4.37E+03	4.37E+02	4.37E+01
<sup>137</sup> Cs	1.59E+08	4.81E+08	33.08%	8.18E+03	8.18E+02	8.18E+01
<sup>147</sup> Pm	1.07E+05	4.81E+08	0.02%	5.51E+00	5.51E-01	5.51E-02
<sup>106</sup> Ru	1.26E+06	4.81E+08	0.26%	6.44E+01	6.44E+00	6.44E-01
<sup>125</sup> Sb	1.07E+06	4.81E+08	0.22%	5.51E+01	5.51E+00	5.51E-01
<sup>90</sup> Sr	7.40E+06	4.81E+08	0.22%	3.81E+02	3.81E+01	3.81E+00
Noble Gases	5.92E+07	4.81E+08	12.31%	N/A	N/A	N/A

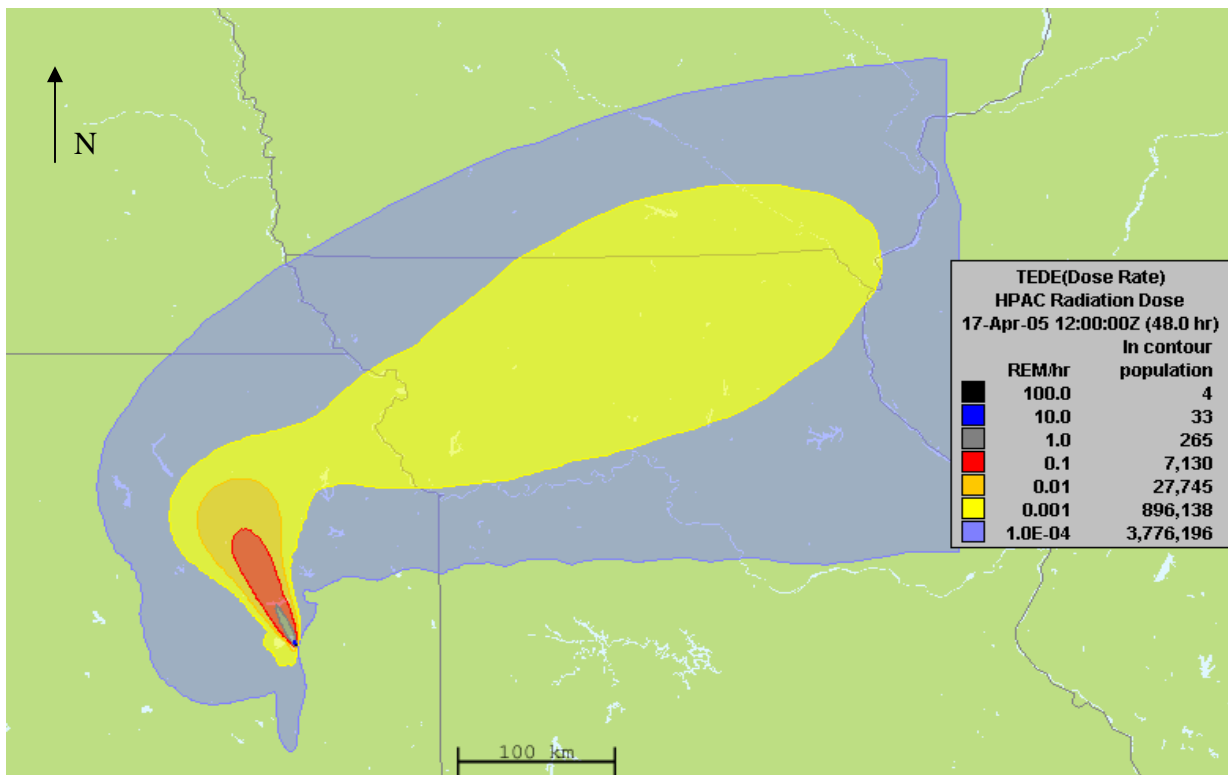


Figure 4-6: Estimates of TEDE at 2 days, rural scenario.

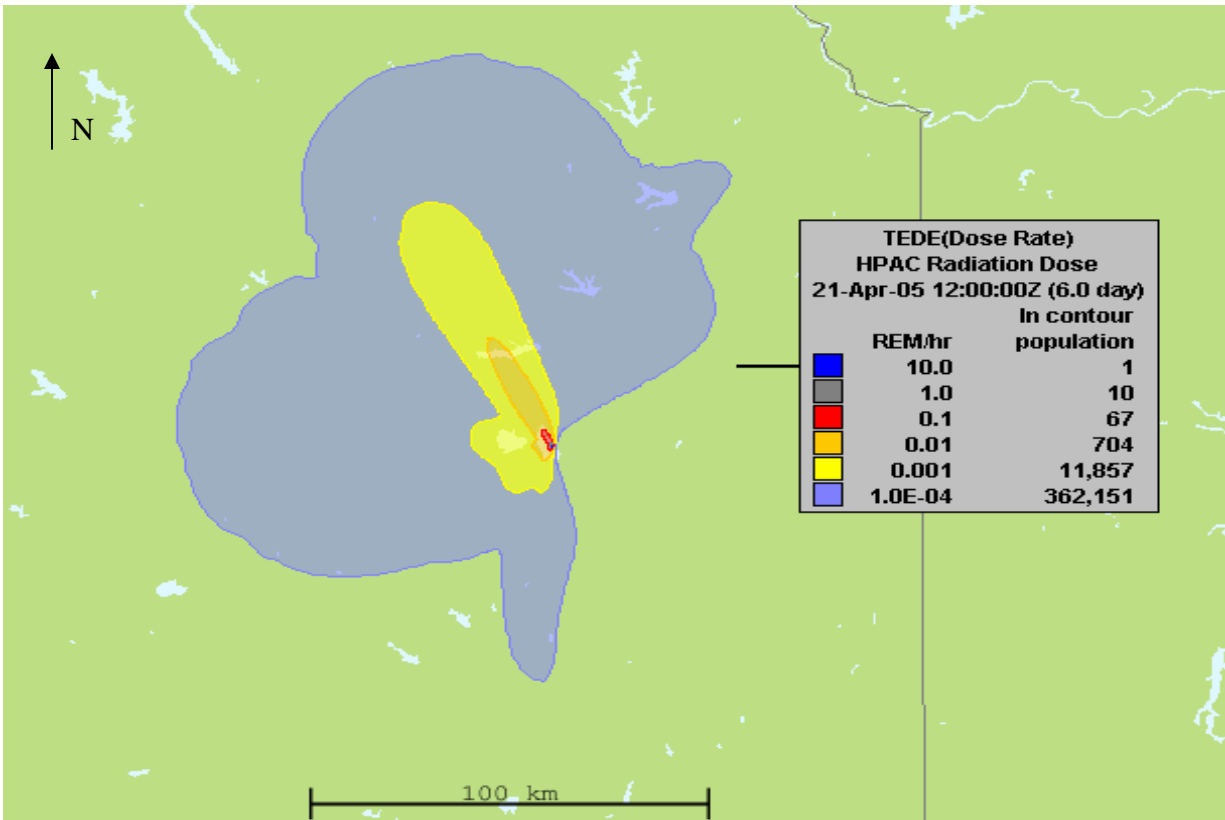


Figure 4-7: Estimates of TEDE at 6 days, rural scenario.

#### Urban Scenario

Based on the population data in Table 4-2, the Indian Point power reactor site was chosen to analyze the effects of a SFP located in a predominantly urban area. At 1,507,029, the population within 30-km of the Indian Point reactor site makes it the largest at-risk population available for this study.

Similarly to the rural scenario, Table 4-6 lists the areas of contamination generated monthly by HPAC for the urban scenario. These contaminated areas ( $\text{km}^2$ ) resulting from the dispersion of spent fuel are shown in the same four activity contours of 37, 3.7, 0.37 and  $0.037 \text{ GBq m}^{-2}$  ( $1.0, 0.1, 0.01$  and  $0.001 \text{ Ci m}^{-2}$ , respectively). The average annual ground deposition for each contour is also presented in Table 4-6.

Evaluation of these results shows that a successful event in January represents the greatest areas of contamination as compared to the other months. Similarly to the rural scenario, the area of contamination in this month is shown to be significantly higher than the mean areas. Further examination of Table 4-6 shows that contamination contours were not generated for several months. In addition, greater than 70% of the annual dispersion was released in a generally North-Eastern direction as illustrated in the January dispersion plot in Figure 4-8.

The total activity release calculated by HPAC for this scenario is  $4.07\text{E}+08$  GBq (11 MCi). The major radionuclides that are released and contribute to ground deposition, identical to the radionuclides in the rural scenario, are listed in Table 4-7. As this table shows, the percentage of total release is calculated for each radionuclide, along with the estimated ground concentrations within the 3.7, 0.37 and 0.037 GBq m<sup>-2</sup> (0.1, 0.01, and 0.001 Ci m<sup>-2</sup>, respectively) contours. Similarly, these three activity contours, along with the respective areas of contamination, are utilized in RESRAD to determine dose/risk to the chronically exposed populations surrounding the urban SFP.

To demonstrate the additional contributions of the noble gases in the urban scenario, Figures 4-9 and 4-10 are included to quantify the total effective dose equivalent (TEDE) levels calculated by HPAC at 2 and 6 days after the SFP incident occurs. The estimated populations affected within the respective contours are also illustrated on each dispersion plot.

Table 4-6: Monthly dispersion results in urban scenario.

Area of Ground Deposition (km <sup>2</sup> )				
Month	37 GBq m <sup>-2</sup> (1 Ci m <sup>-2</sup> ) Contour	3.7 GBq m <sup>-2</sup> (0.1 Ci m <sup>-2</sup> ) Contour	0.37 GBq m <sup>-2</sup> (0.01 Ci m <sup>-2</sup> ) Contour	0.037 GBq m <sup>-2</sup> (0.001 Ci m <sup>-2</sup> ) Contour
January	-	-	8.065	159.734
February	-	-	-	124.940
March	0.005	0.114	1.749	33.945
April	-	-	5.384	134.813
May	0.010	0.143	2.767	43.228
June	0.017	0.375	7.982	162.191
July	0.009	0.073	1.036	17.072
August	0.017	0.318	6.007	120.677
September	0.021	0.394	6.795	186.544
October	-	0.054	2.692	61.609
November	0.012	0.112	1.794	34.383
December	-	-	-	22.850
<i>Mean</i>	<i>0.013</i>	<i>0.251</i>	<i>5.007</i>	<i>95.373</i>

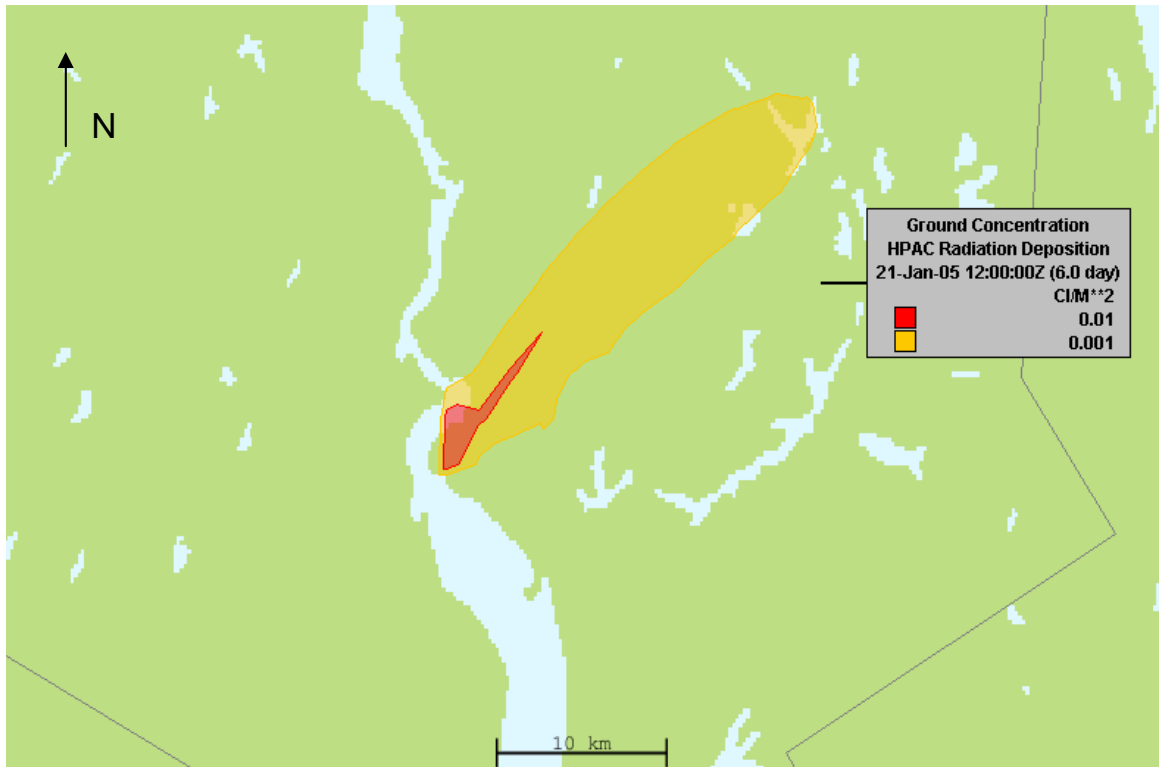


Figure 4-8: HPAC dispersion in urban scenario.

Table 4-7: Radiological dispersion results in urban scenario.

Radionuclides	Nuclide Released (GBq)	Total Activity Released (GBq)	% of release	Radionuclide Concentration 3.7 GBq m <sup>-2</sup> contour (Bq/g)	Radionuclide Concentration 0.37 GBq m <sup>-2</sup> contour (Bq/g)	Radionuclide Concentration 0.037 GBq m <sup>-2</sup> contour (Bq/g)
<sup>144</sup> Ce	3.48E+05	4.07E+08	0.09%	2.11E+01	2.11E+00	2.11E-01
<sup>134</sup> Cs	7.40E+07	4.07E+08	18.18%	4.48E+03	4.48E+02	4.47E+01
<sup>137</sup> Cs	1.37E+08	4.07E+08	33.64%	8.29E+03	8.29E+02	8.29E+01
<sup>147</sup> Pm	9.25E+04	4.07E+08	0.02%	5.62E+00	5.62E-01	5.62E-02
<sup>106</sup> Ru	1.11E+06	4.07E+08	0.27%	6.73E+01	6.73E+00	6.73E-01
<sup>125</sup> Sb	9.25E+05	4.07E+08	0.23%	5.62E+01	5.62E+00	5.62E-01
<sup>90</sup> Sr	6.66E+06	4.07E+08	1.64%	4.03E+02	4.03E+01	4.03E+00
Noble Gases	5.18E+07	4.07E+08	12.73%	N/A	N/A	N/A

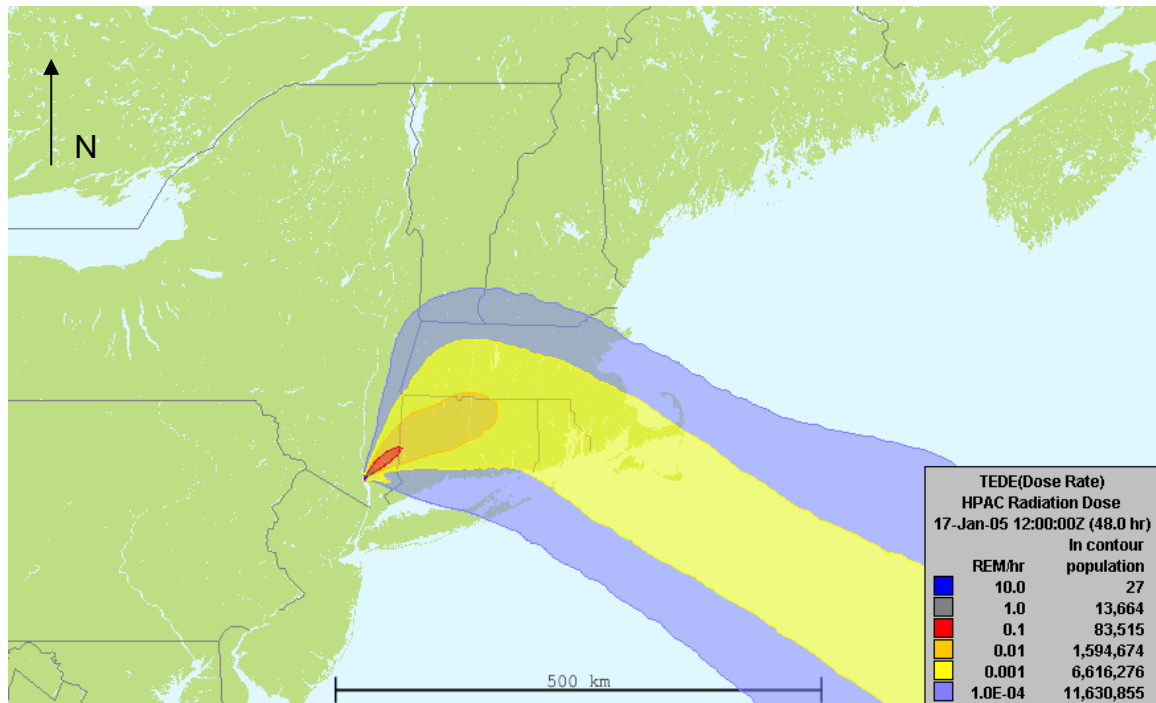


Figure 4-9: Estimates of TEDE at 2 days, urban scenario.

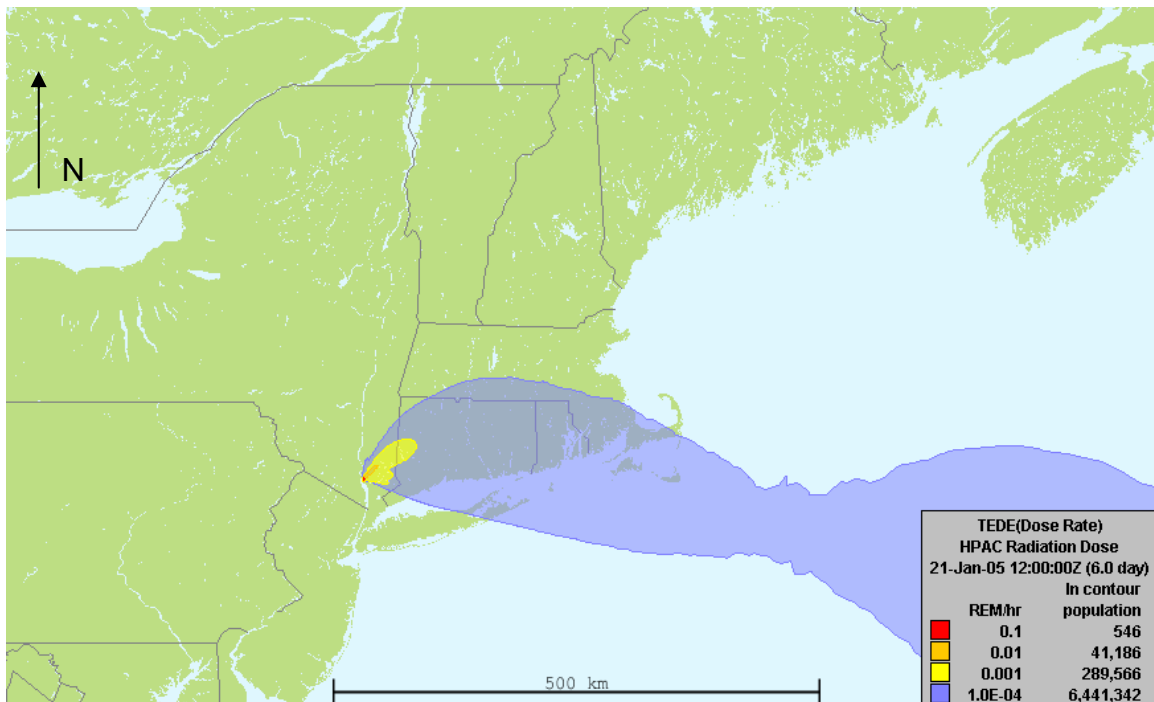


Figure 4-10: Estimates of TEDE at 6 days, urban scenario.

## Radiation Exposure Modeling

Utilizing the RESRAD resident farmer scenario for the rural scenario and the suburban scenario for the urban scenario, along with the default parameters discussed in Chapter 3, the total radionuclide contributions to dose are presented below.

### Rural Scenario

Figure 4-11 illustrates the radionuclide contributions to annual dose of the exposed population in the 2.734 km<sup>2</sup> contour with a concentration of 3.7 GBq m<sup>-2</sup> (0.1 Ci m<sup>-2</sup>). Individual dose components for <sup>134</sup>Cs, <sup>137</sup>Cs, <sup>90</sup>Sr, <sup>106</sup>Ru and <sup>135</sup>Sb by component pathway are illustrated in Figures 4-12 through 4-16, respectively.



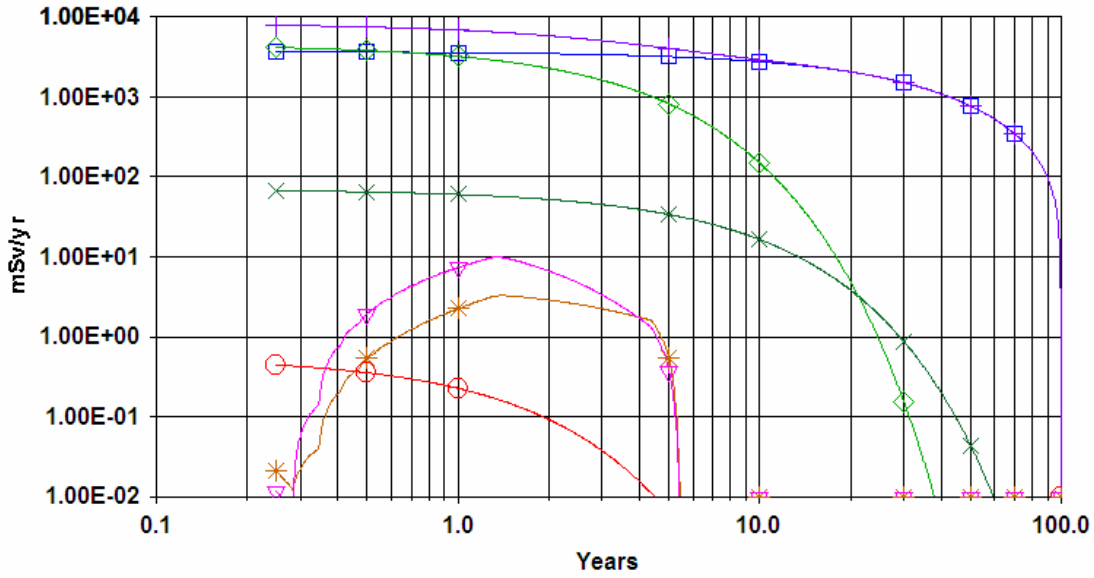


Figure 4-11: Annual dose from radionuclide contamination within 3.7 GBq m<sup>-2</sup> contour, rural scenario.

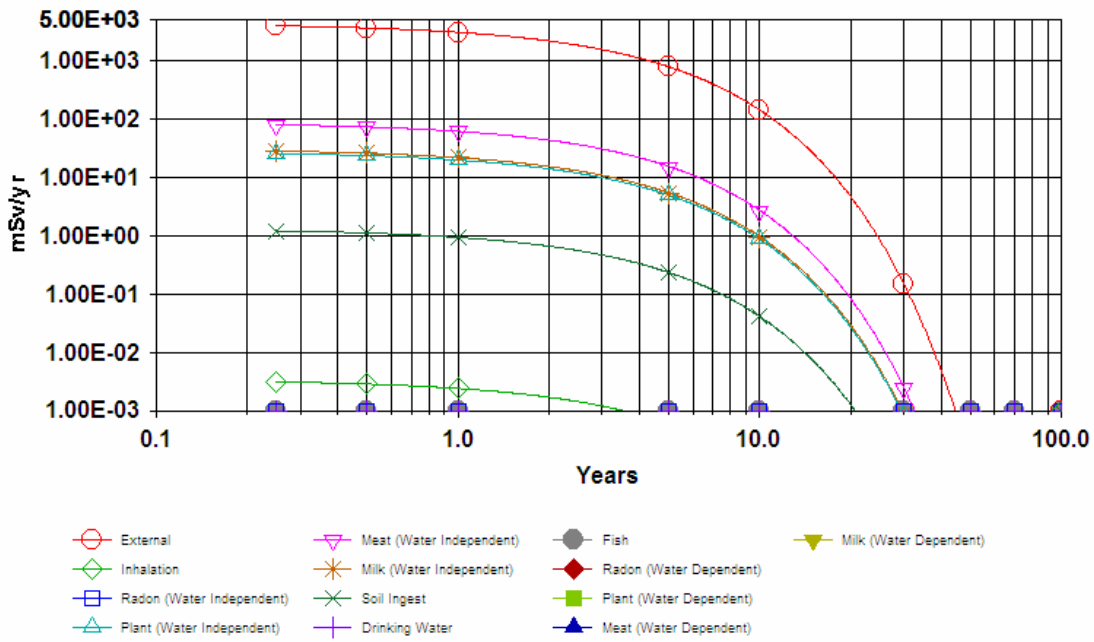


Figure 4-12: <sup>134</sup>Cs dose contribution within 3.7 GBq m<sup>-2</sup> contour, rural scenario.

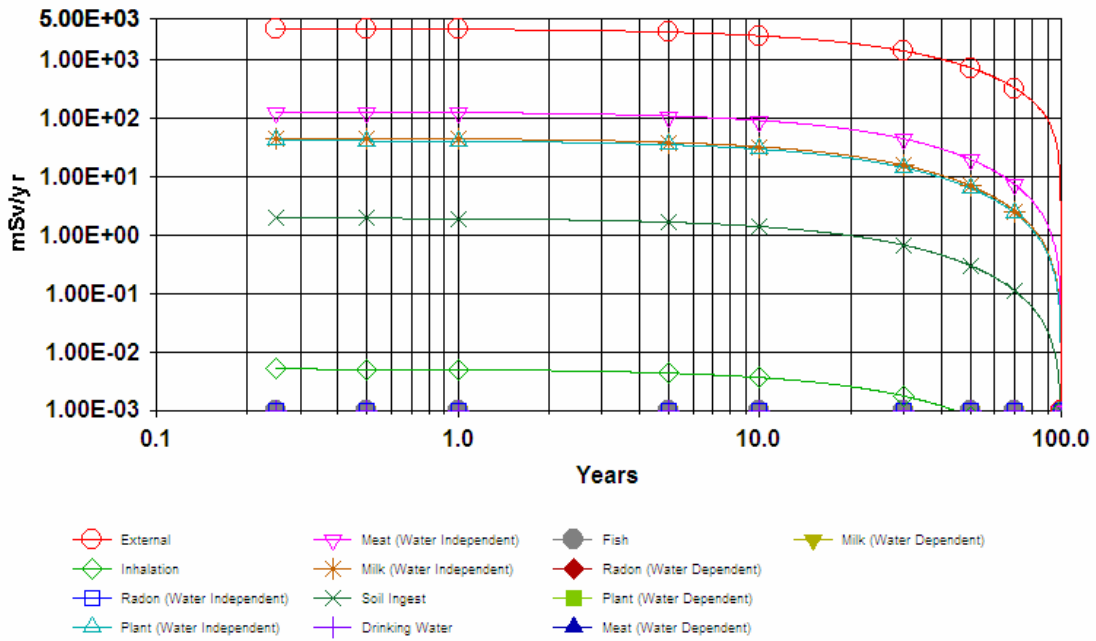


Figure 4-13: <sup>137</sup>Cs dose contribution within 3.7 GBq m<sup>-2</sup> contour, rural scenario.

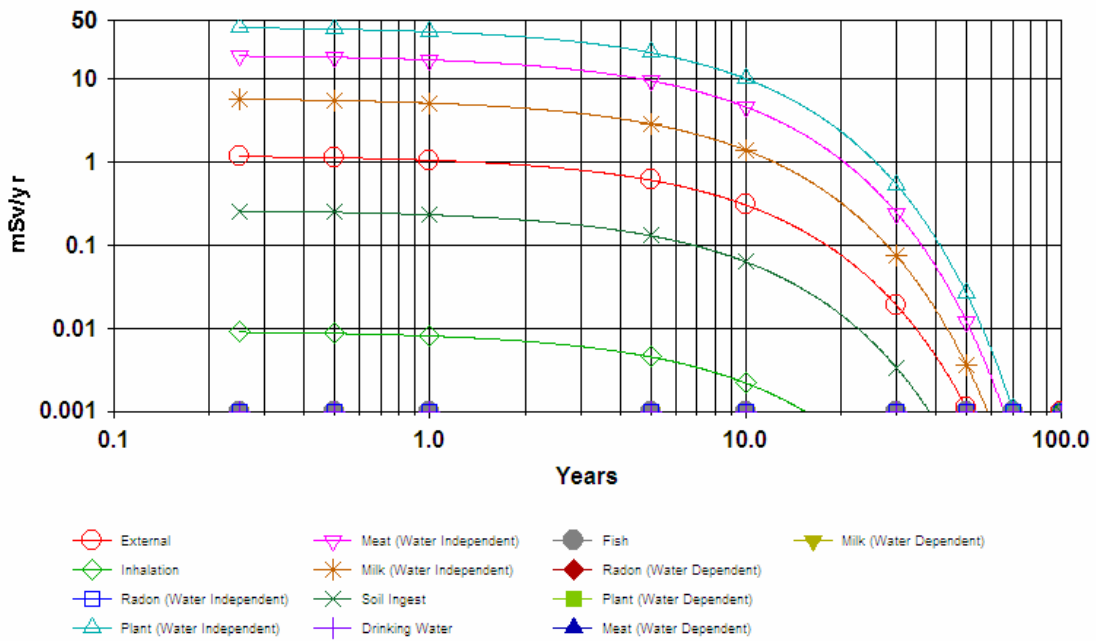


Figure 4-14: <sup>90</sup>Sr dose contribution within 3.7 GBq m<sup>-2</sup> contour, rural scenario.

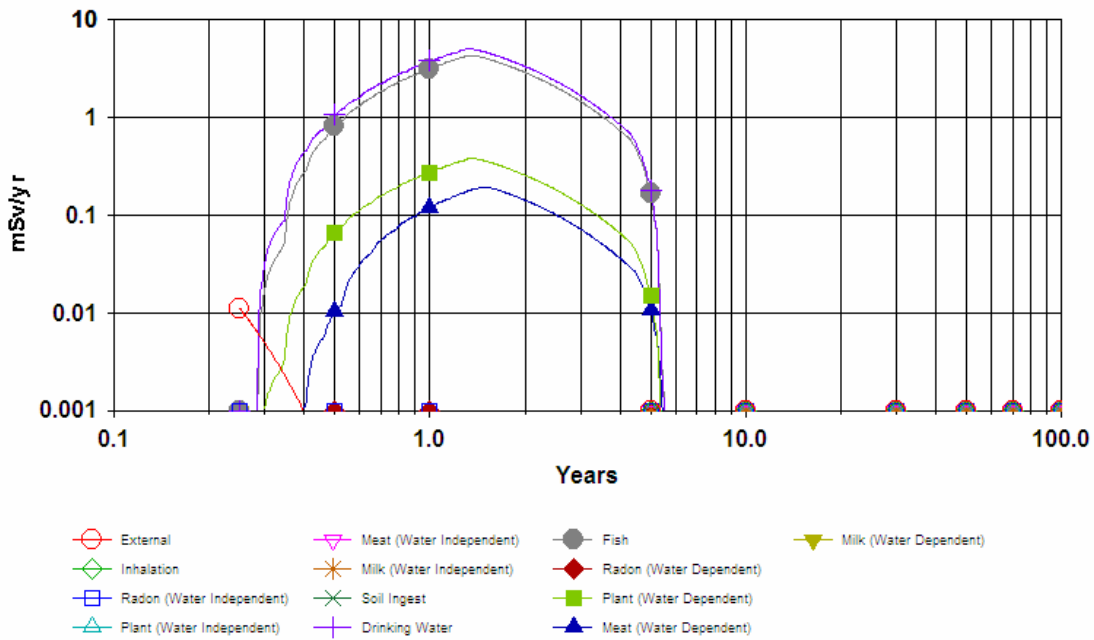


Figure 4-15: <sup>106</sup>Ru dose contribution within 3.7 GBq m<sup>-2</sup> contour, rural scenario.

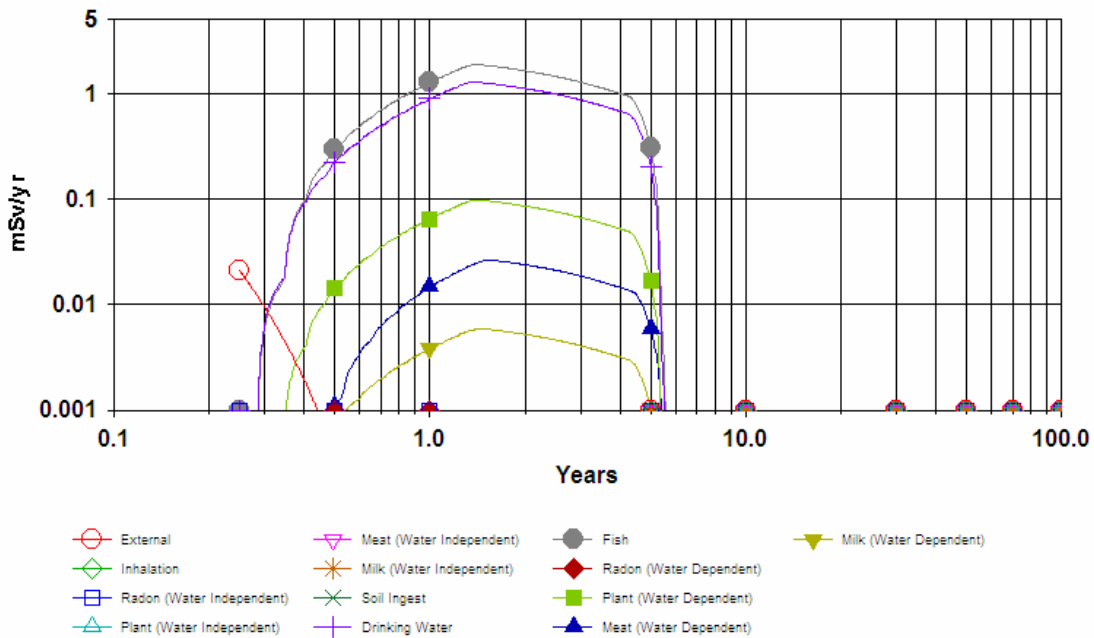


Figure 4-16: <sup>125</sup>Sb dose contribution within 3.7 GBq m<sup>-2</sup> contour, rural scenario.

Figure 4-17 illustrates the radionuclide contributions to annual dose of the exposed population in the 55.37 km<sup>2</sup> contour with a concentration of 0.37 GBq m<sup>-2</sup> (0.01 Ci m<sup>-2</sup>). Individual dose components for <sup>134</sup>Cs, <sup>137</sup>Cs, <sup>90</sup>Sr, <sup>106</sup>Ru and <sup>135</sup>Sb by component pathway are illustrated in Figures 4-18 through 4-22, respectively.

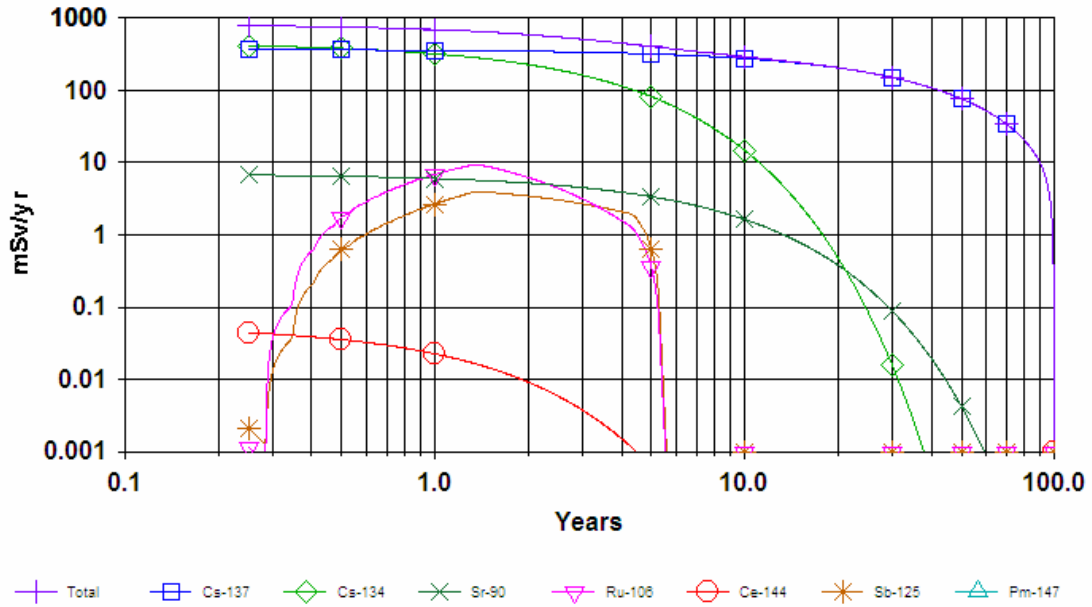


Figure 4-17: Annual dose from radionuclide contamination within 0.37 GBq m<sup>-2</sup> contour, rural scenario.

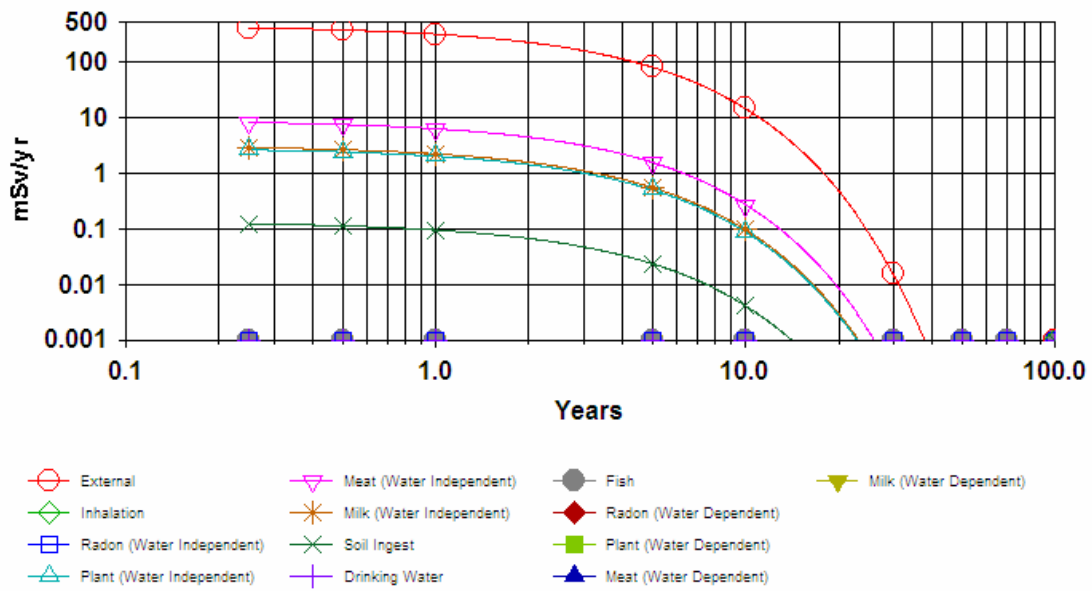


Figure 4-18:  $^{134}\text{Cs}$  dose contribution within  $0.37 \text{ GBq m}^{-2}$  contour, rural scenario.

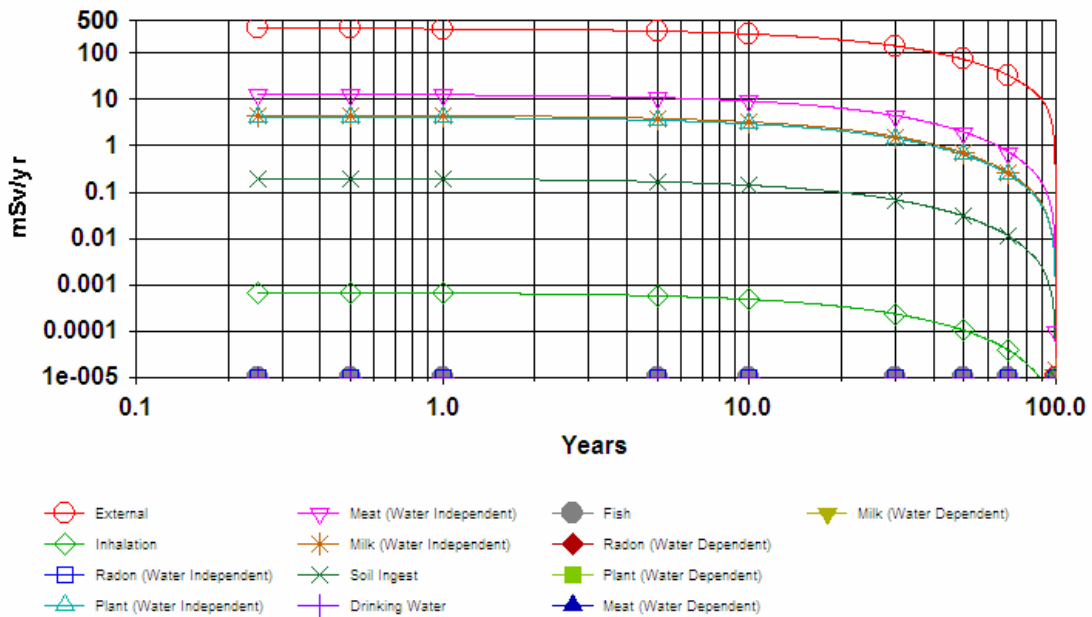


Figure 4-19:  $^{137}\text{Cs}$  dose contribution within  $0.37 \text{ GBq m}^{-2}$  contour, rural scenario.

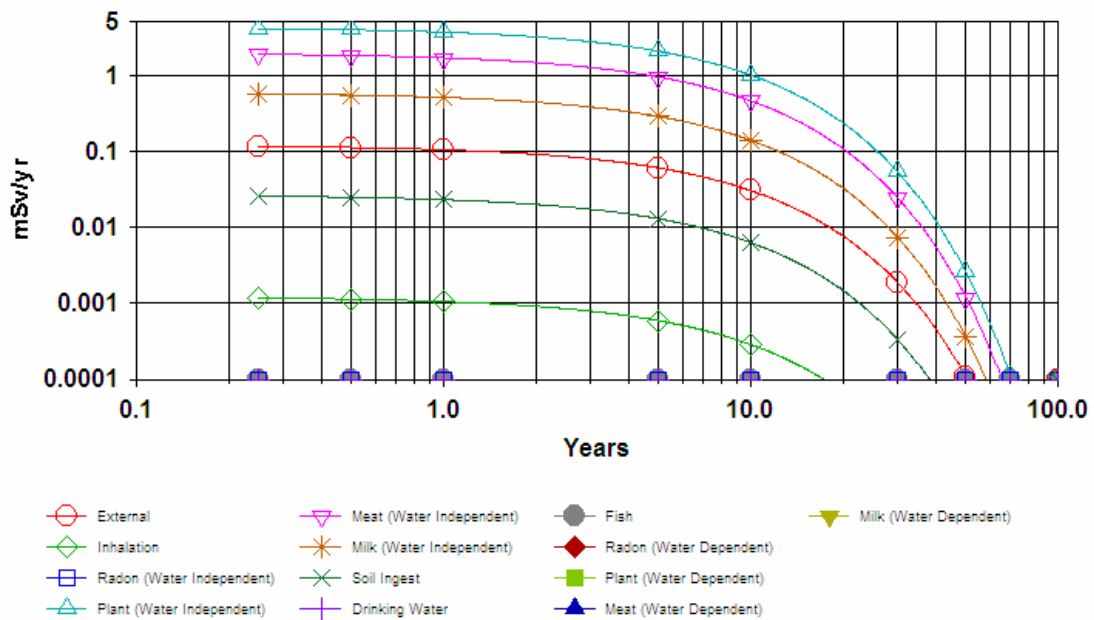


Figure 4-20:  $^{90}\text{Sr}$  dose contribution within  $0.37 \text{ GBq m}^{-2}$  contour, rural scenario.

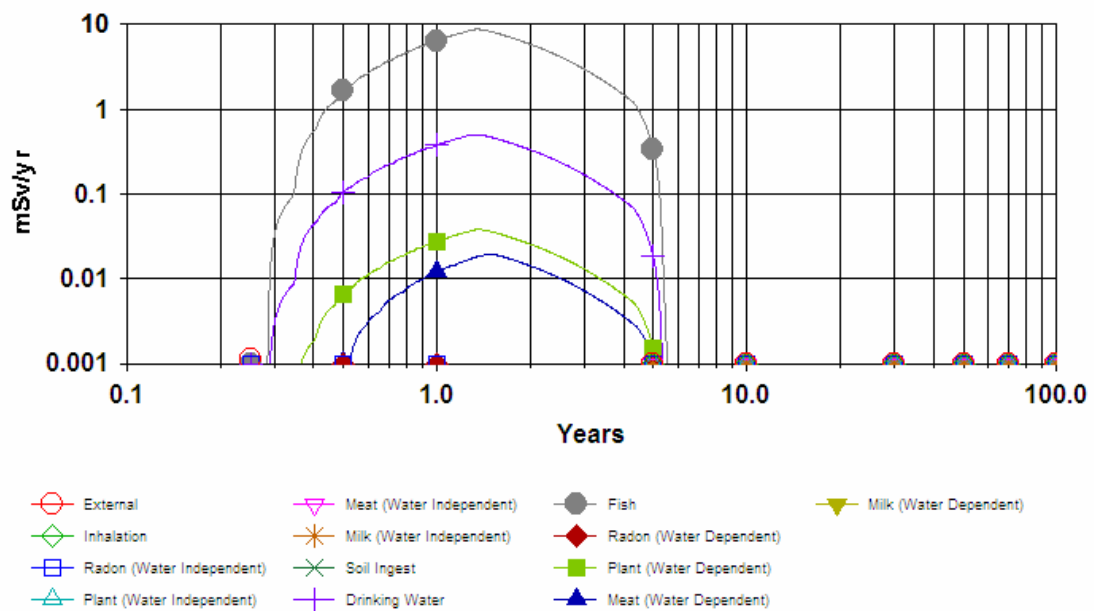


Figure 4-21:  $^{106}\text{Ru}$  dose contribution within  $0.37 \text{ GBq m}^{-2}$  contour, rural scenario.

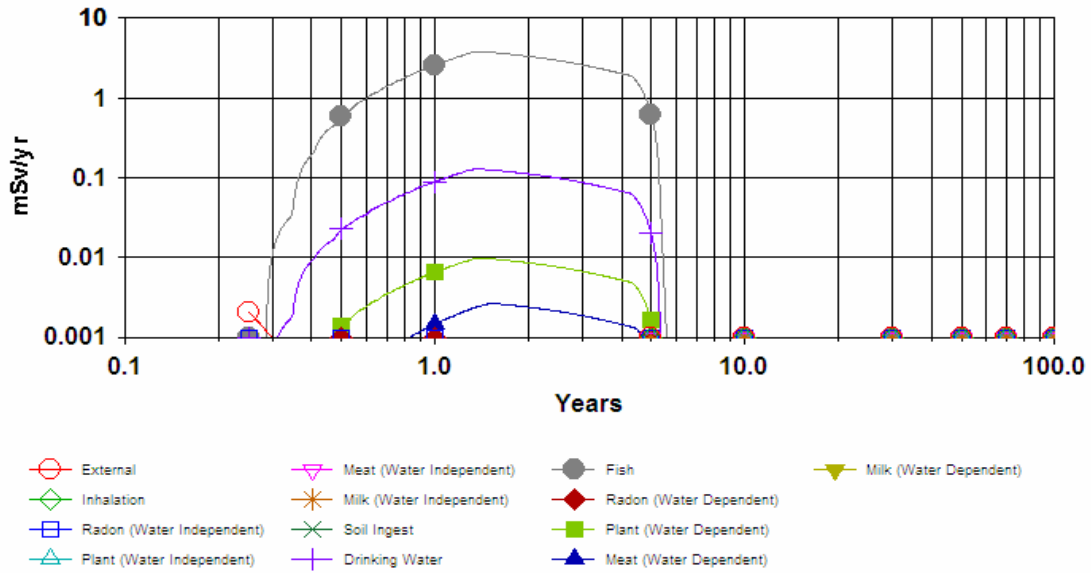


Figure 4-22:  $^{125}\text{Sb}$  dose contribution within  $0.37 \text{ GBq m}^{-2}$  contour, rural scenario.

Figure 4-23 illustrates the radionuclide contributions to annual dose of the exposed population in the  $542.4 \text{ km}^2$  contour with a concentration of  $0.037 \text{ GBq m}^{-2}$  ( $0.001 \text{ Ci m}^{-2}$ ). Individual dose components for  $^{134}\text{Cs}$ ,  $^{137}\text{Cs}$ ,  $^{90}\text{Sr}$ ,  $^{106}\text{Ru}$  and  $^{135}\text{Sb}$  by component pathway are illustrated in Figures 4-24 through 4-28, respectively.

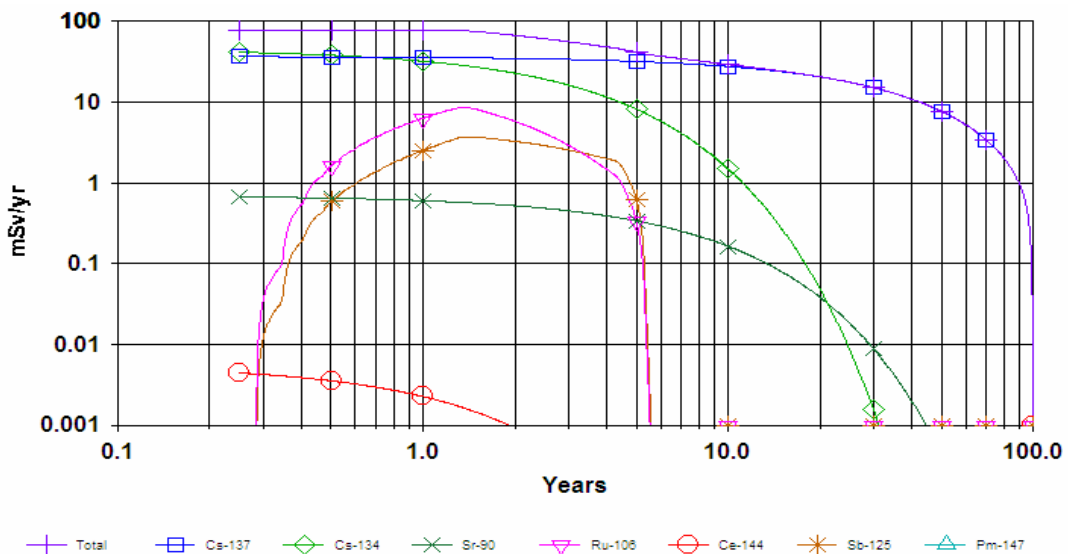


Figure 4-23: Annual dose from radionuclide contamination within  $0.037 \text{ GBq m}^{-2}$  contour, rural scenario.

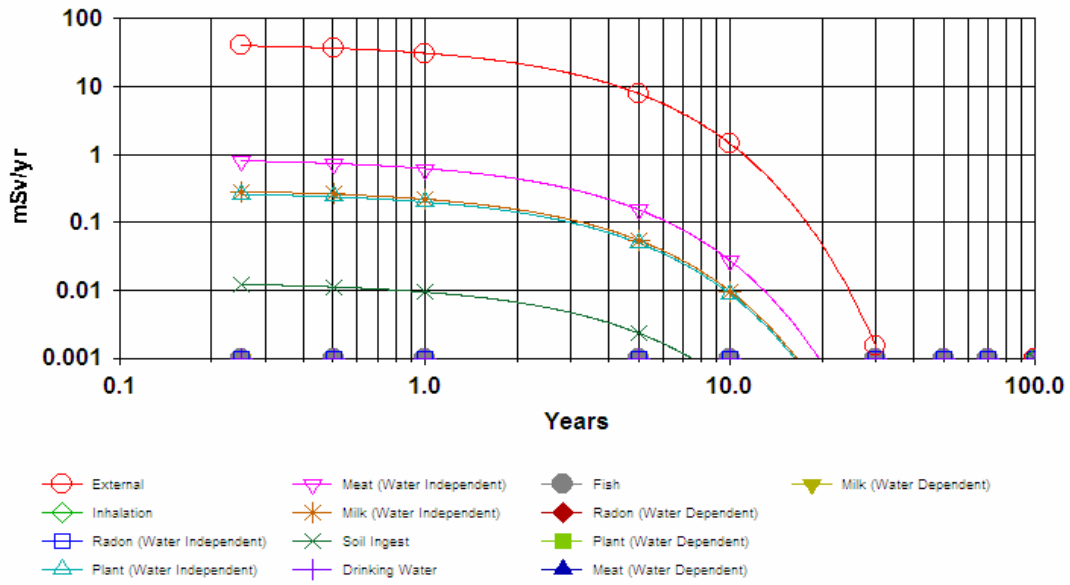


Figure 4-24: <sup>134</sup>Cs dose contribution within 0.037 GBq m<sup>-2</sup> contour, rural scenario.

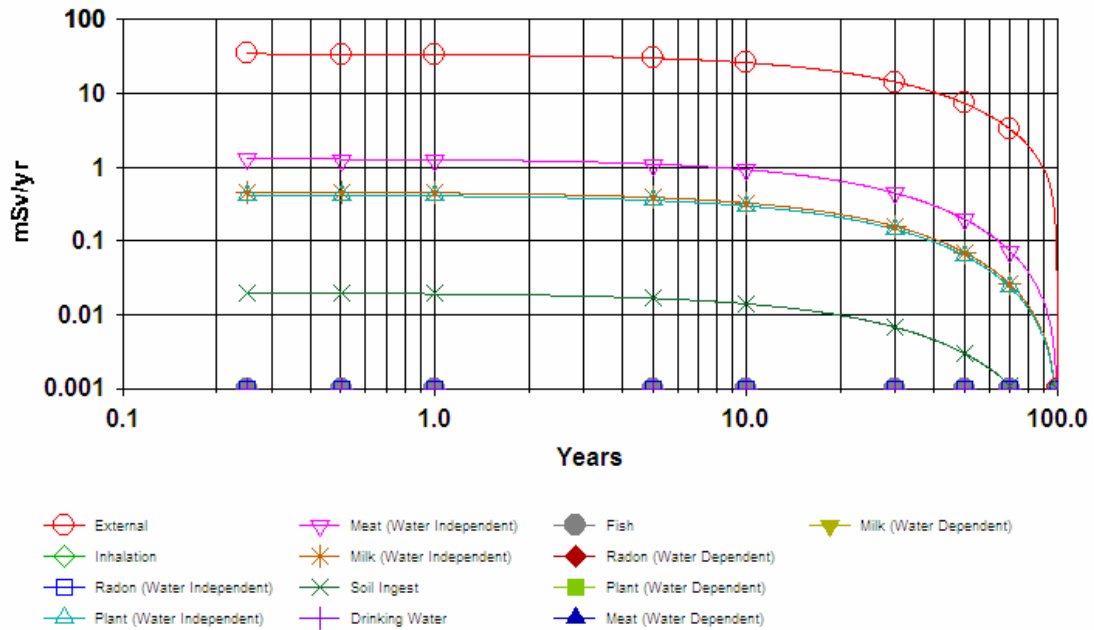


Figure 4-25: <sup>137</sup>Cs dose contribution within 0.037 GBq m<sup>-2</sup> contour, rural scenario.



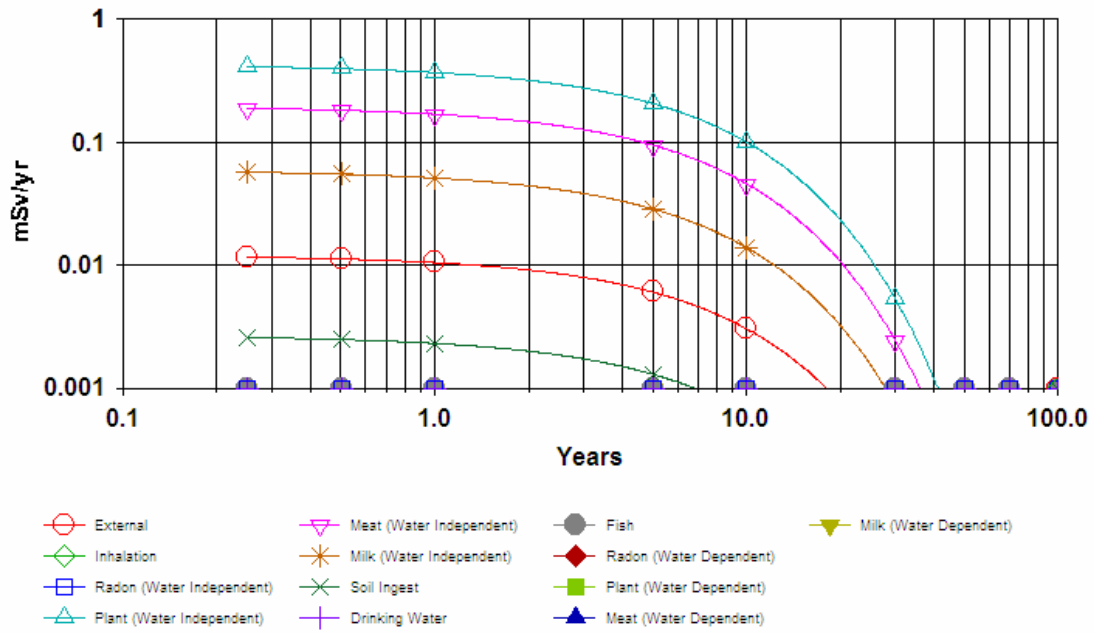


Figure 4-26:  $^{90}\text{Sr}$  dose contribution within  $0.037 \text{ GBq m}^{-2}$  contour, rural scenario.

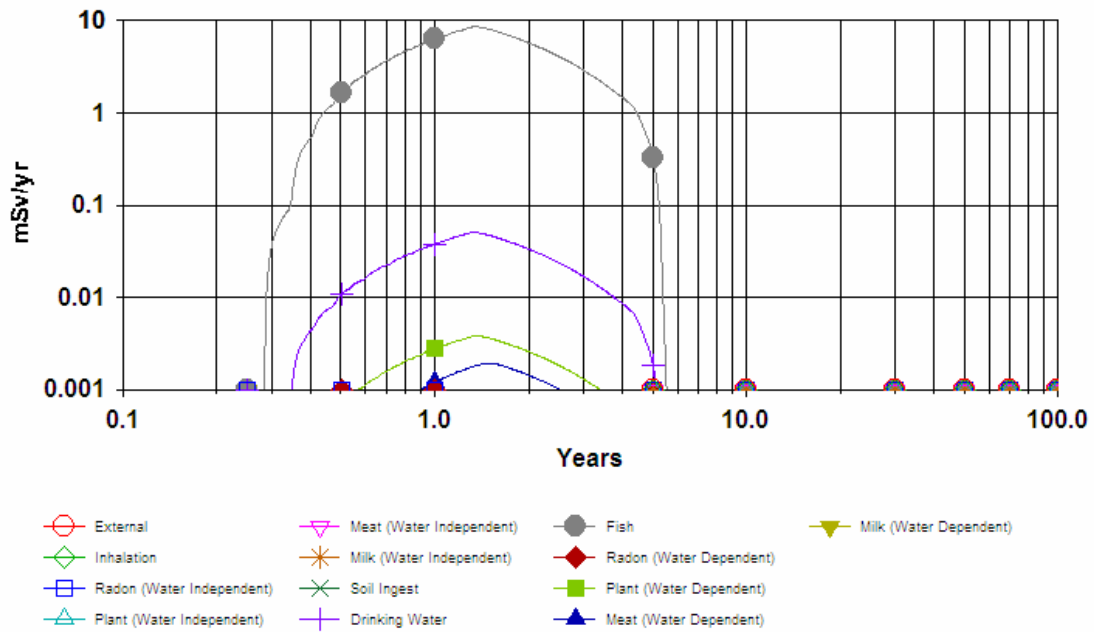


Figure 4-27:  $^{106}\text{Ru}$  dose contribution within  $0.037 \text{ GBq m}^{-2}$  contour, rural scenario.

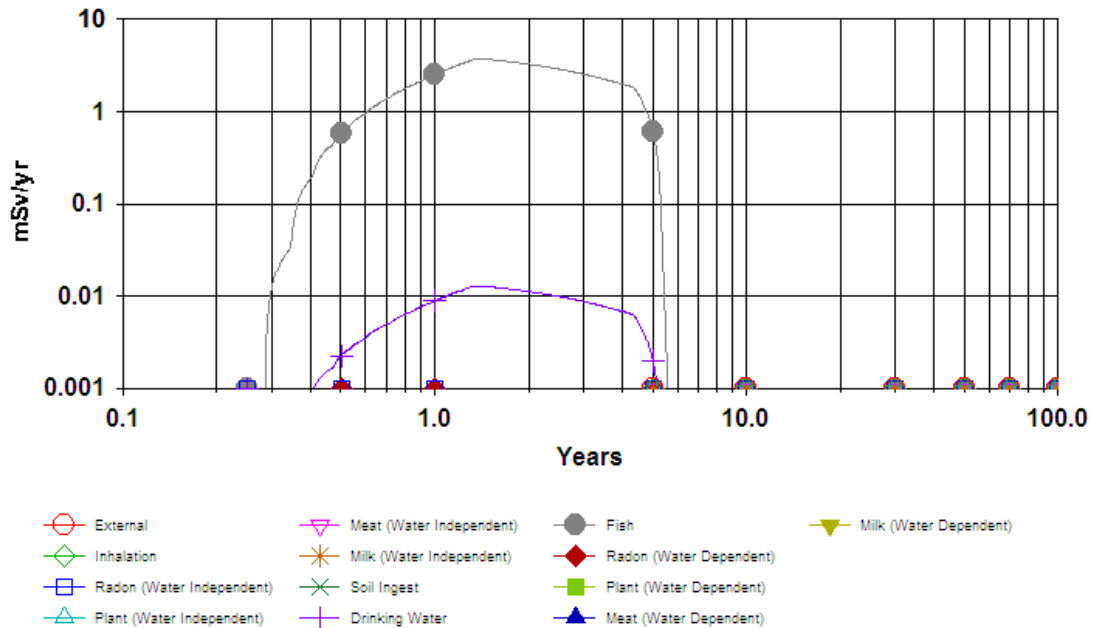


Figure 4-28:  $^{125}\text{Sb}$  dose contribution within  $0.037 \text{ GBq m}^{-2}$  contour, rural scenario.

### Urban Scenario

Figure 4-29 illustrates the radionuclide contributions to annual dose of the exposed population in the  $0.673 \text{ km}^2$  contour with a concentration of  $3.7 \text{ GBq m}^{-2}$  ( $0.1 \text{ Ci m}^{-2}$ ). Individual dose components for  $^{134}\text{Cs}$ ,  $^{137}\text{Cs}$ , and  $^{90}\text{Sr}$  by component pathway are illustrated in Figures 4-30 through 4-32, respectively. NOTE: For the comparatively minor contributions to dose from  $^{106}\text{Ru}$  and  $^{125}\text{Sb}$ , the major pathways to human exposure (i.e. fish and drinking water) as determined in the rural scenario are easily controllable in an urban environment and are thus excluded from in depth analysis in this section of the study.

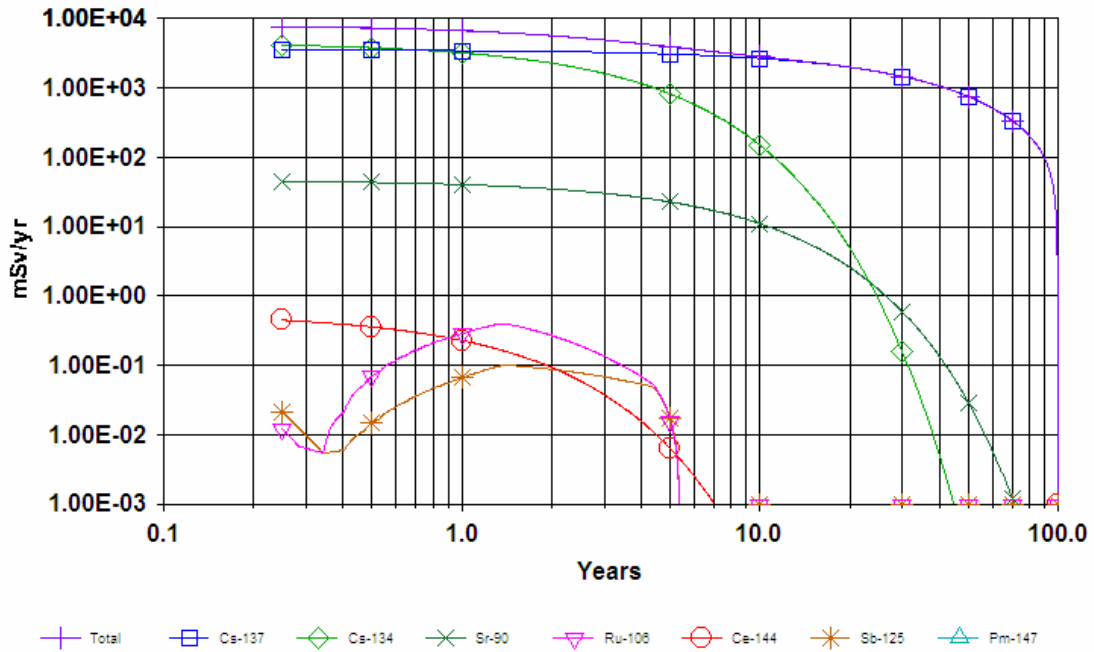


Figure 4-29: Annual dose from radionuclide contamination within 3.7 GBq m<sup>-2</sup> contour, urban scenario.

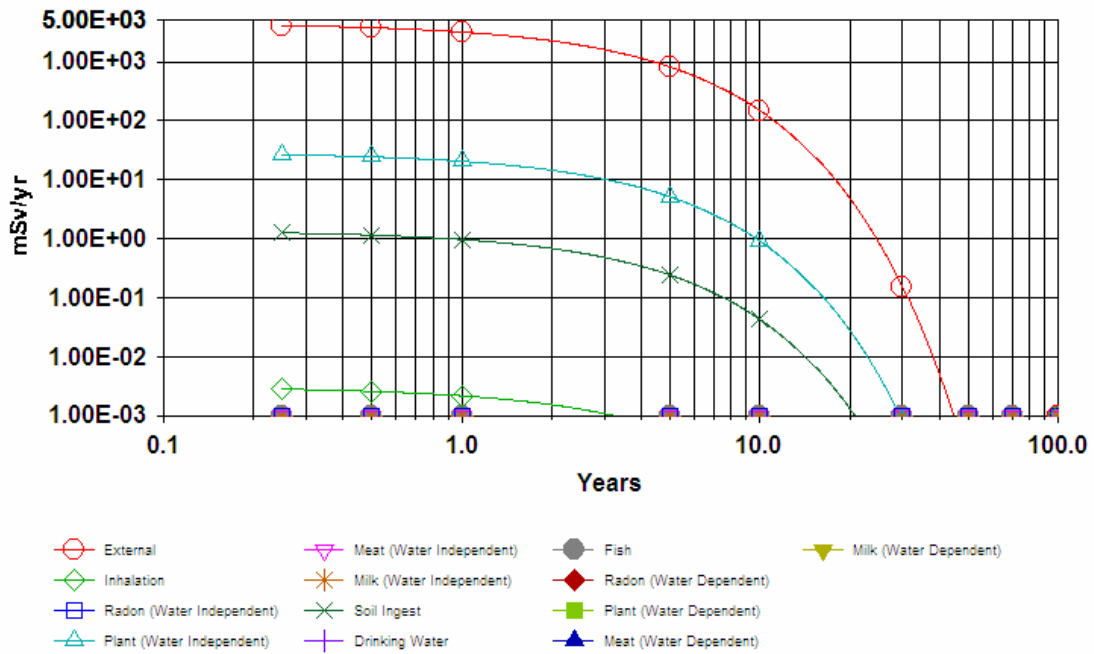


Figure 4-30: <sup>134</sup>Cs dose contribution within 3.7 GBq m<sup>-2</sup> contour, urban scenario.

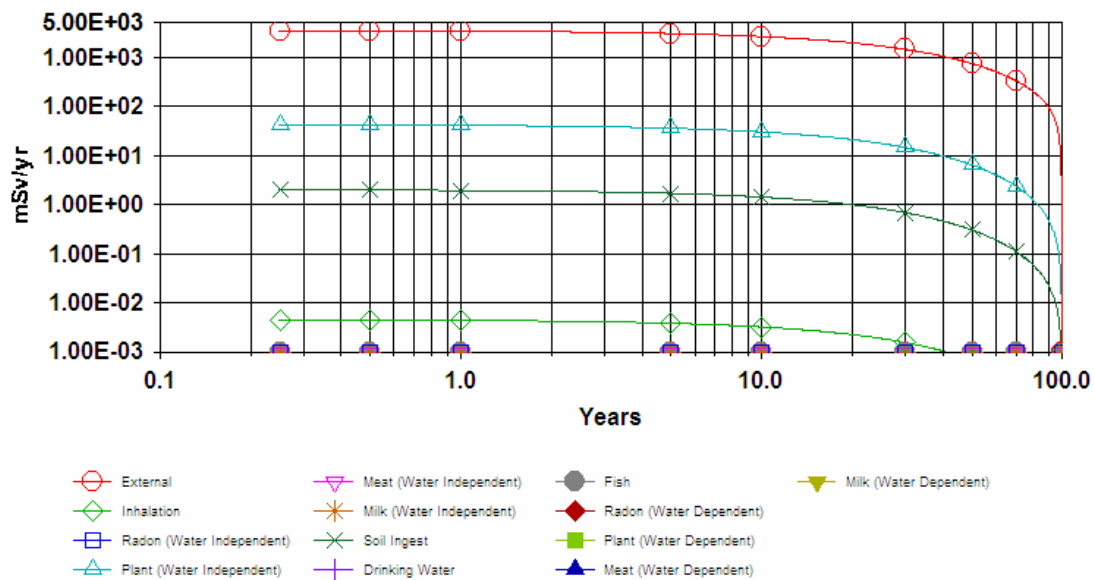


Figure 4-31:  $^{137}\text{Cs}$  dose contribution within  $3.7 \text{ GBq m}^{-2}$  contour, urban scenario.

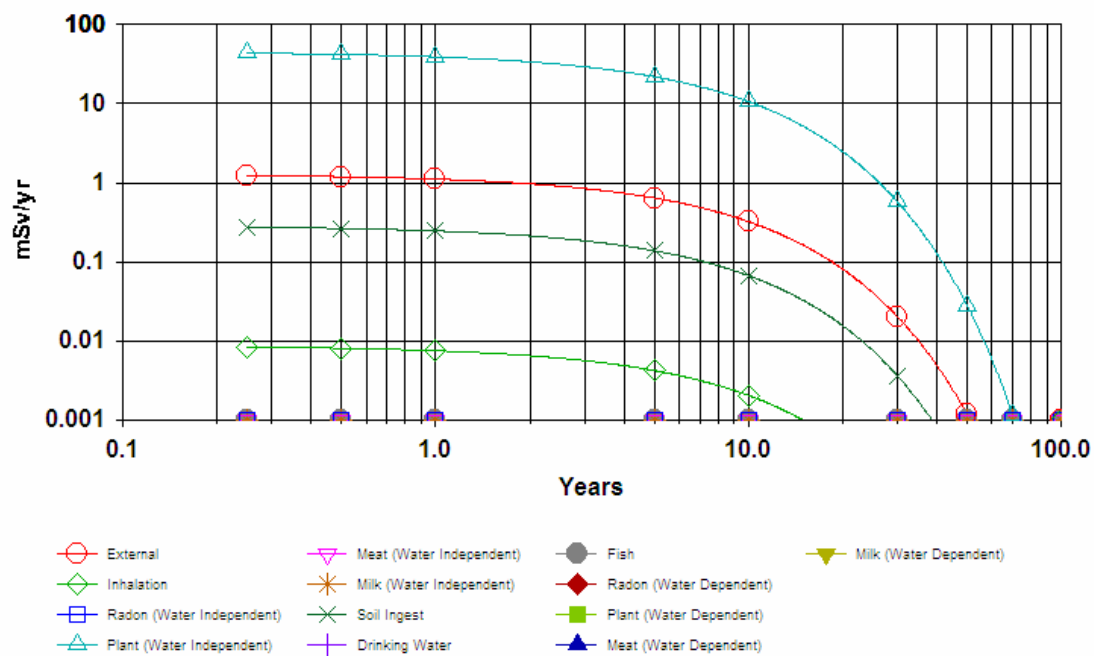


Figure 4-32:  $^{90}\text{Sr}$  dose contribution within  $3.7 \text{ GBq m}^{-2}$  contour, urban scenario.

Figure 4-33 illustrates the radionuclide contributions to annual dose of the exposed population in the  $13.87 \text{ km}^2$  contour with a concentration of  $0.37 \text{ GBq m}^{-2}$  ( $0.01$

Ci m<sup>-2</sup>). Individual dose components for <sup>134</sup>Cs, <sup>137</sup>Cs, and <sup>90</sup>Sr by component pathway are illustrated in Figures 4-34 through 4-36, respectively.

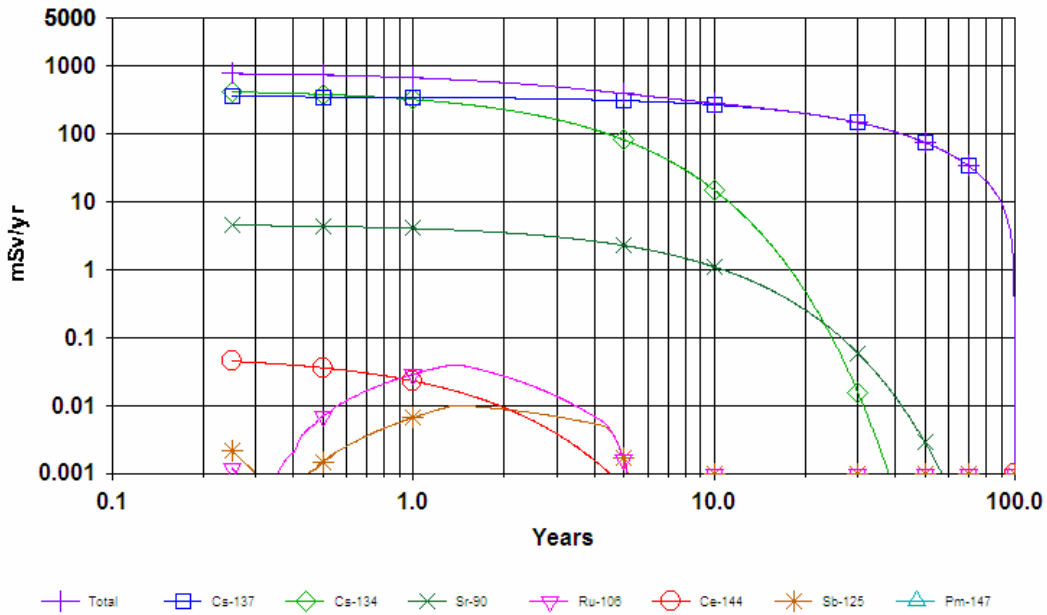


Figure 4-33: Annual dose from radionuclide contamination within 0.37 GBq m<sup>-2</sup> contour, urban scenario.

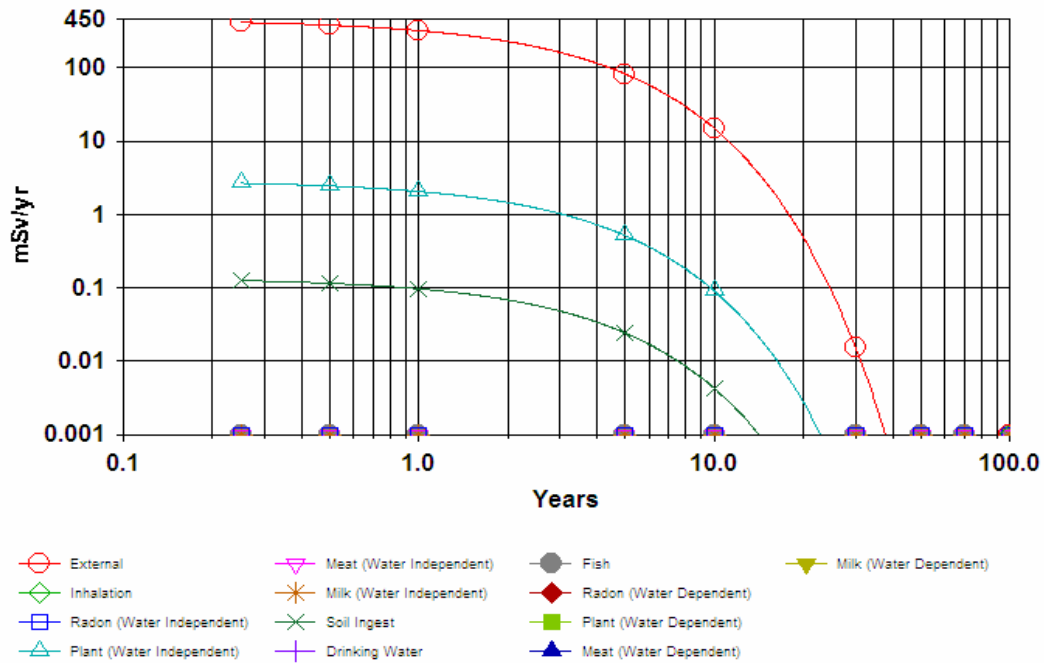


Figure 4-34: <sup>134</sup>Cs dose contribution within 0.37 GBq m<sup>-2</sup> contour, urban scenario.

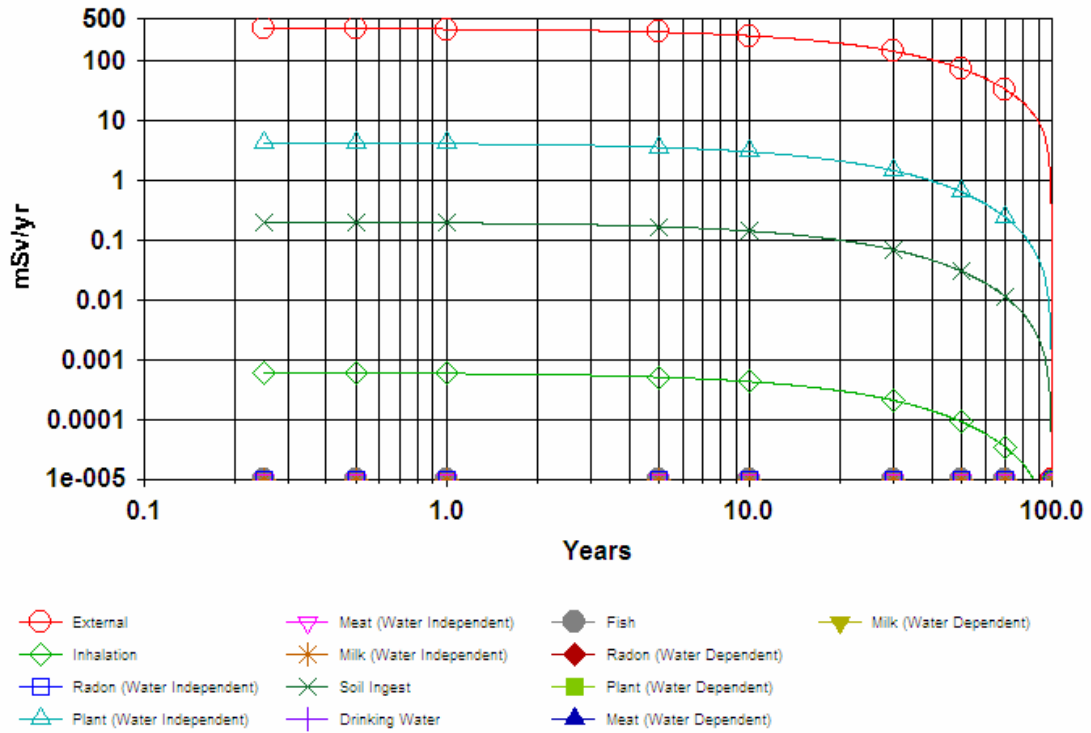


Figure 4-35:  $^{137}\text{Cs}$  dose contribution within  $0.37 \text{ GBq m}^{-2}$  contour, urban scenario.

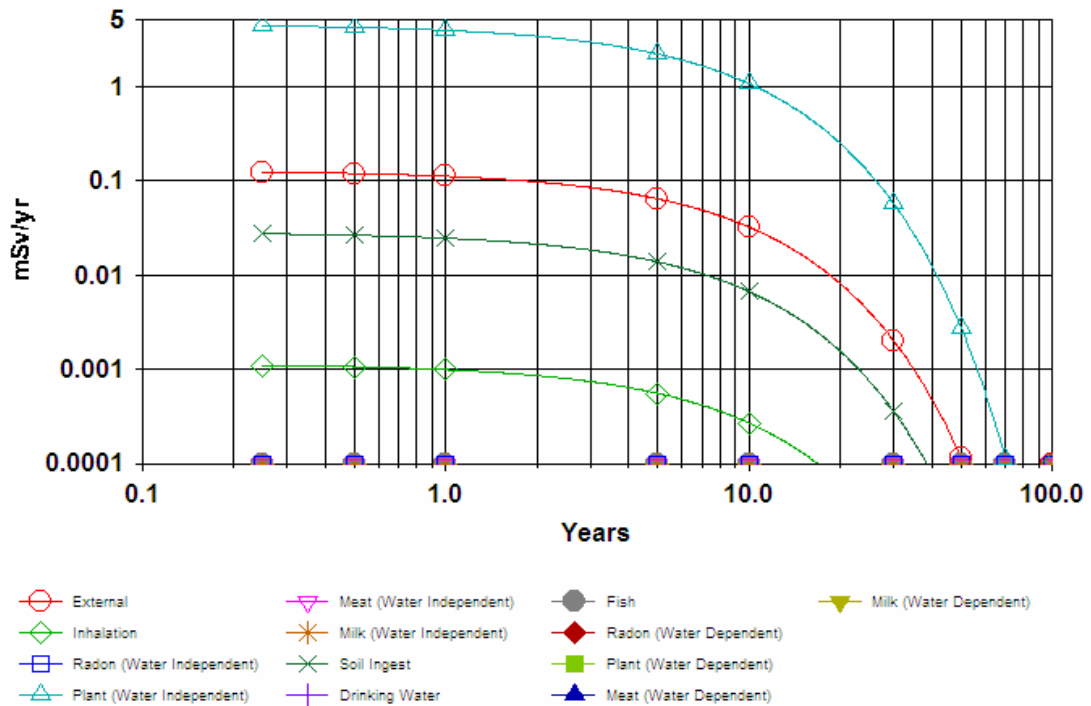


Figure 4-36:  $^{90}\text{Sr}$  dose contribution within  $0.37 \text{ GBq m}^{-2}$  contour, urban scenario.

Figure 4-37 illustrates the radionuclide contributions to annual dose of the exposed population in the 202.2 km<sup>2</sup> contour with a concentration of 0.037 GBq m<sup>-2</sup> (0.001 Ci m<sup>-2</sup>). Individual dose components for <sup>134</sup>Cs, <sup>137</sup>Cs and <sup>90</sup>Sr by component pathway are illustrated in Figures 4-38 through 4-40, respectively.

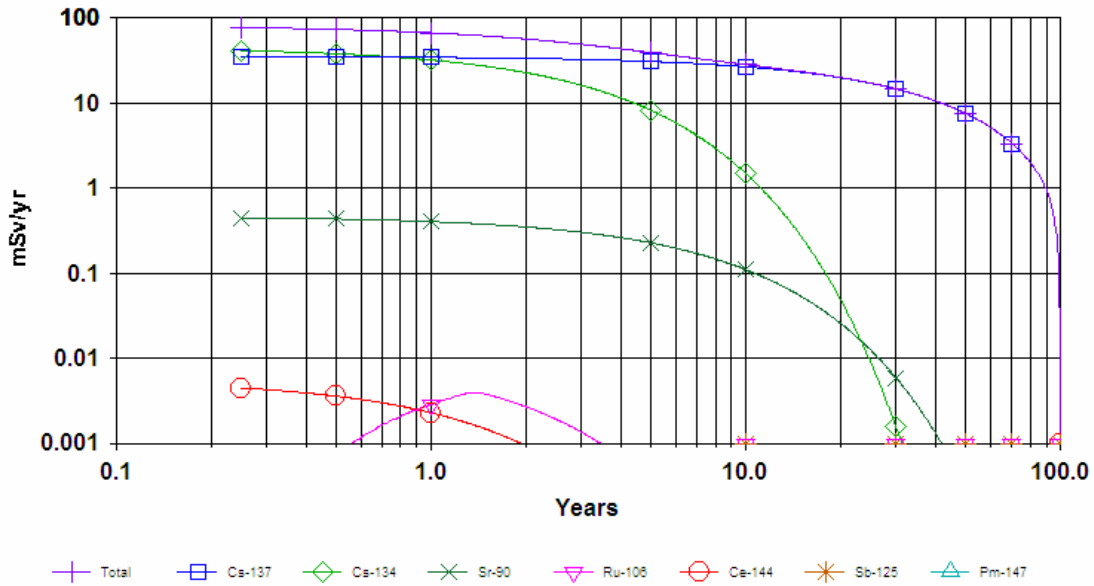


Figure 4-37: Annual dose from radionuclide contamination within 0.037 GBq m<sup>-2</sup> contour, urban scenario.

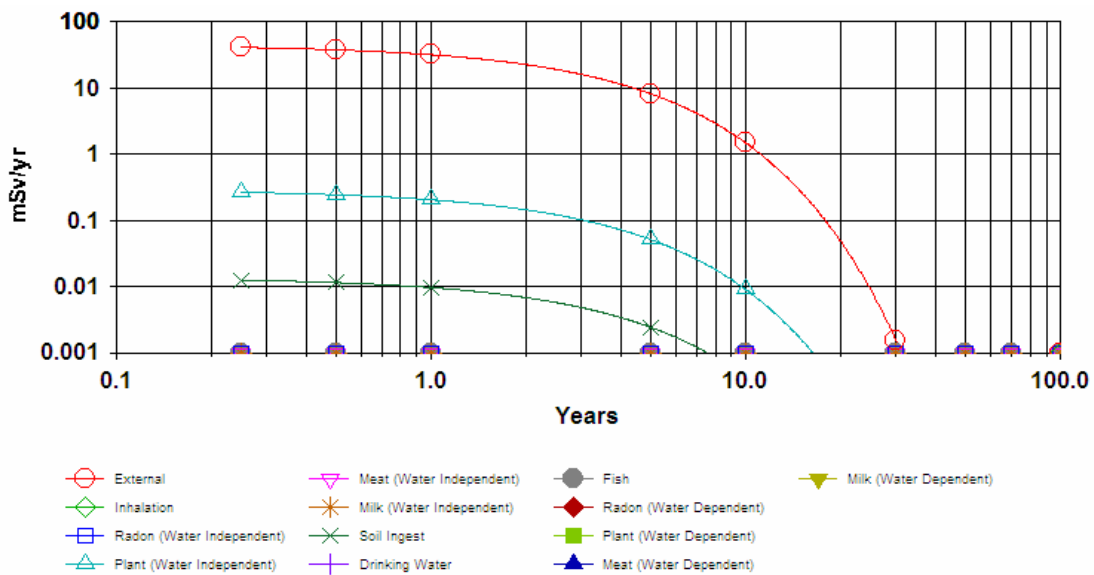


Figure 4-38: <sup>134</sup>Cs dose contribution within 0.037 GBq m<sup>-2</sup> contour, urban scenario.

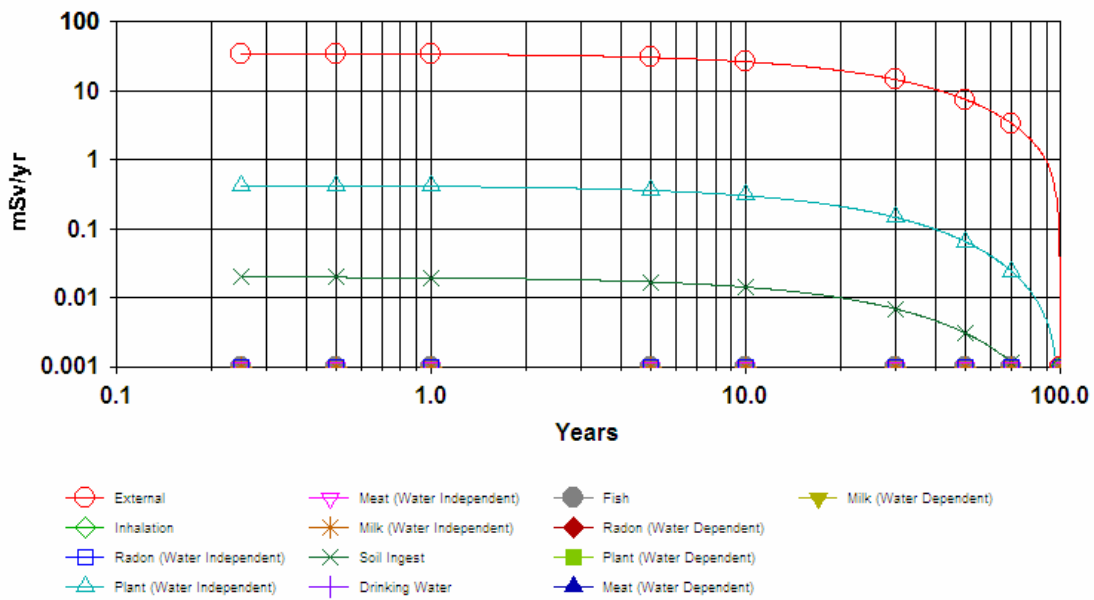


Figure 4-39: <sup>137</sup>Cs dose contribution within 0.037 GBq m<sup>-2</sup> contour, urban scenario.

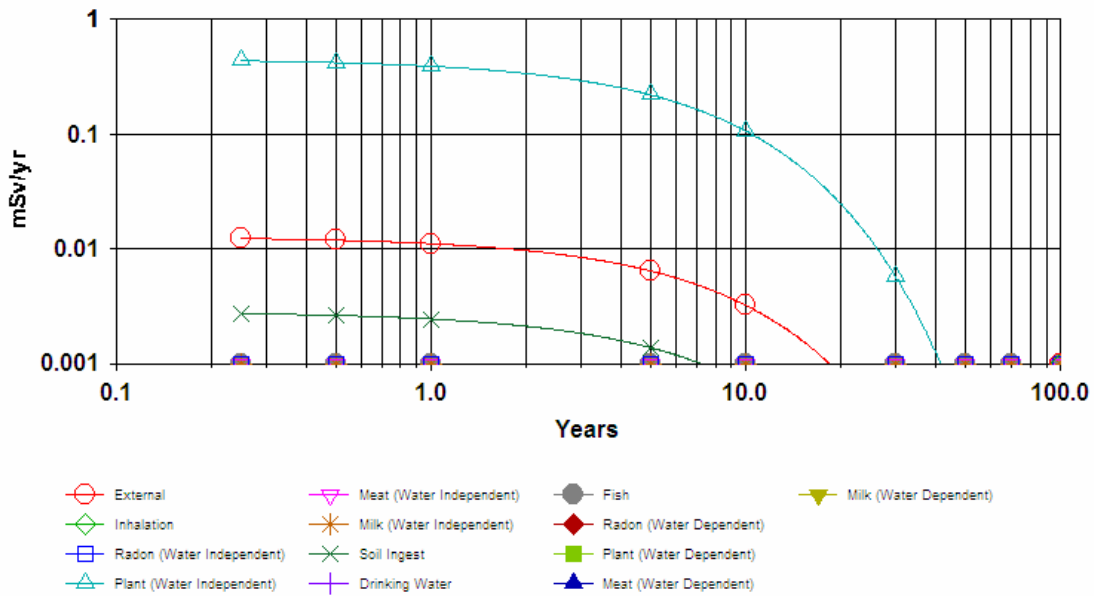


Figure 4-40: <sup>90</sup>Sr dose contribution within 0.037 GBq m<sup>-2</sup> contour, urban scenario.



## CHAPTER V

### DISCUSSION

A terrorist attack resulting in a dispersal of radioactive materials is fundamentally different from terrorist attacks employing conventional tactics. In a conventional attack such as the September 11 attacks, the event occurs, casualties are suffered, and survivors are rescued and treated. Those not killed or injured are usually free from further physical danger but are susceptible to psychological effects after the incident (i.e. post-traumatic stress disorder). The immediate area of the event can be secured as a crime scene and forensic investigation can be conducted in the usual manner employed in other crime scenes. In most cases, normal government services are continued with only minor or temporary interruptions.

In an unconventional terrorist attack (i.e. attacks on a SFP or attacks utilizing RDDs or improvised nuclear devices), the traditional aftermath discussed above will be complicated by many confounding factors. Treatment of casualties will be more difficult because of possible radioactive contamination. Of those not wounded by the terrorist attack, injuries and deaths could still occur from exposure to radiation. The debris from the event and other normally harmless materials may also be contaminated. As shown in this study, the affected area may be significantly larger than the immediate scene of the attack. Public fear and concern over exposure to radiation will cause a strain on normal government services. Forensic investigation of the crime scene will be complicated by the need to protect individuals from radiation exposure. Although only a partial list of

factors, these differences will significantly hamper the abilities of responders to restore order and return the affected areas to pre-incident conditions.

Radioactive materials released in a successful attack on a SFP may present both an immediate and long-term threat to public health and safety. In the time immediately following an incident (i.e. the early phase), decision makers will have to be concerned with protection of the responders and the general public to acute radiation effects and the decontamination and treatment of casualties. Although the basic tenets of radiation protection (i.e. increasing the distance from the source, limiting the time of exposure and utilizing intervening shielding) are more effective at reducing exposures, several countermeasures are also available to further reduce these subsequent exposures to personnel. The ability to enforce recommendations for sheltering or evacuations will depend on public participation as well as local and state laws. Restrictions on food and water will have both public health and economic implications. The immediate availability of radiation safety expertise, specialized equipment and supplies may also be limiting factors. Long-term considerations include public health, environmental, psychosocial and economic effects (NCRP, 2001).

### Human Health Effects

Routine practices and constraints will not be adequate in dealing with the human health effects in the aftermath of a terrorist attack. In the U.S., the EPA has derived projected dose level recommendations, called Protective Action Guidelines (PAGs), based on IAEA intervention levels to protect against acute (i.e. deterministic) effects and reduce the risk of chronic (i.e. stochastic) effects. These levels are intended to serve as a

threshold for initiating pathway-specific countermeasures. Table 5-1 illustrates the current PAG levels utilized in the U.S. (DHS, 2006).

Table 5-1: Protective Action Guidelines (DHS, 2006).

<b>Phase</b>	<b>Protective Action</b>	<b>PAG</b>
Early	- Limit Emergency Worker Exposure	0.05 Sv (5 rem)
	- Sheltering of Public	0.01-0.05 Sv (1-5 rem) projected dose
	- Evacuation of Public	0.01-0.05 Sv (1-5 rem) projected dose
Intermediate	- Limit Worker Exposure	0.05 Sv (5 rem) $y^{-1}$
	- Relocation of General Public	0.02 Sv (2 rem) projected dose 1 <sup>st</sup> year
Late	- Final Cleanup Actions	Based on "Optimization"

For emergency response personnel, the likelihood that the PAG listed in Table 5-1 will be met or exceeded in the early phase is exceptionally high. The NCRP has provided broad guidance for emergency responders in that only life saving actions justifies acute exposures that are significantly in excess of the PAG levels in Table 5-1. When this cannot be accomplished, the NCRP recommends that a limit of 0.5 Sv (50 rem) effective dose and an equivalent dose of 5 Sv (500 rem) to the skin be applied. For life saving or equivalent purposes, the equivalent dose may approach or exceed 0.5 Sv (50 rem) to a large portion of the body in a short time if the worker volunteers for the dose with full understanding of the possibility of acute effects and potential increase in lifetime risk of cancer (NCRP, 1993).

Results of this study indicate the area immediately around the SFP could produce dose levels in excess of the PAGs and the recommendations of the NCRP. In Figure 4-6, HPAC calculates a dose rate of 0.1-1 Sv h<sup>-1</sup> (10-100 rem h<sup>-1</sup>) in the vicinity of the SFP for

the rural scenario. Likewise, HPAC calculates a dose rate of  $> 0.1 \text{ Sv h}^{-1}$  ( $10 \text{ rem h}^{-1}$ ) for the urban scenario (see Figure 4-9). Without the application of countermeasures or other restrictions, the acute radiation effects discussed in Chapter II could be possible in these areas.

There are many practical ways to help minimize exposures to emergency workers, especially during the early phases. Some of these include: worker selection based on their experience in performing the required emergency tasks to reduce the exposure time, reducing the number of workers involved in a task as low as possible, use of older workers with low lifetime accumulated effective doses, etc. Pre-planning and training are key elements in ensuring emergency workers are equipped to respond to an incident of this nature.

Protection of the general public will require some form of “intervention” to regain control during and after the terrorist attack. In this case, an intervention consists of a set of pathway-specific countermeasures designed to avert as much of a projected exposure to the public as is practicable (NCRP, 2001). The pathways of importance include external exposure and internal contamination. External exposures can be received by persons located in the plume or persons exposed to surface or personal contamination as a result of the event. Internal exposures occur due to inhalation of particles in the plume or resuspended contamination, inhalation or ingestion of personal contamination, ingestion of contaminated foodstuffs, absorption through the skin or injection of contaminated material. Table 5-2 lists common countermeasures that can be employed to reduce external and internal exposures.

Table 5-2: Countermeasures to reduce external and internal exposures (NCRP, 2001).

<b>Exposure Pathway</b>	<b>Available Countermeasures</b>
External radiation exposure from nuclides in the plume	Sheltering, evacuation, control of access
Internal contamination due to nuclides in the plume	Sheltering, ad hoc respiratory protection, evacuation, control of access
External contamination from surface deposited contamination	Sheltering, evacuation, control of access, decontamination
External radiation from surface deposited contamination	Sheltering, evacuation, relocation, control of access, decontamination
Internal contamination due to resuspension	Evacuation, relocation, control of access, decontamination
Internal contamination due to personal contamination	Control of access, decontamination
Internal exposure due to ingestion of contaminated water and foods	Control of food and water and use of stored animal feeds

All countermeasures have associated risks that may supersede the risks from radiation exposure (i.e. evacuation of large populations could result in more casualties due to vehicle accidents than would be caused by radiation exposure). The use of countermeasures must involve consideration of the risks and benefits. Commonly, the upper end of the dose limit range, as listed in Table 5-1, is viewed as a value where a countermeasure is always justified. Conversely, the lower end of the dose limit range can be thought of as a value at which the countermeasure is not likely to be justified.

In the early phase (i.e. hours to days after the release), a projected dose of 0.01-0.05 Sv (1-5 rem) warrants the employment of countermeasures (see Table 5-1). Figure 4-6, for the rural scenario, and Figure 4-9, for the urban scenario, shows that either

external or internal exposure from nuclides in the plume could result in exposures in excess of the PAGs. As listed in Table 5-2, sheltering, evacuation, ad hoc respiratory protection and control of access are potentially suitable countermeasures for this mode of exposure.

RESRAD analysis of the surface contamination concentrations in both scenarios (Figures 4-11 – 4-40) shows that the PAGs in Table 5-1 could be exceeded in all contours during all phases (i.e. early, intermediate and late phases).

In the 3.7 GBq m<sup>-2</sup> contour (i.e. areas nearest the SFP) of both scenarios, RESRAD analysis indicates dose levels tremendously higher than the PAGs listed in Table 5-1. Figure 4-11 illustrates an initial annual dose rate of 7000 mSv y<sup>-1</sup>, due mainly from exposures to <sup>134</sup>Cs and <sup>137</sup>Cs. This equates to a dose rate of 0.8 mSv h<sup>-1</sup> with no countermeasures employed. Figures 4-12 and 4-13 show that the external pathway contributes the majority of the dose from the cesium radionuclides. Sheltering, evacuation, relocation, control of access and decontamination are all common countermeasures in dealing with external exposures. Analysis of Figures 4-14 – 4-16 reveals that the internal pathways could be controlled for <sup>90</sup>Sr, <sup>106</sup>Ru and <sup>125</sup>Sb, respectively, through employment of the common countermeasures listed in Table 5-2. However, the reduction in total dose rate would be relatively insignificant compared to the external contribution from <sup>134</sup>Cs and <sup>137</sup>Cs in this contour. Therefore, the only suitable countermeasure to employ in these areas would be a temporary evacuation of the public in the early phase and possible relocation in the intermediate and late phases. This recommendation would also apply to the urban scenario, as the total dose rate within the first year is essentially the same as the rural scenario (see Figures 4-29 – 4-32).

In the 0.37 GBq m<sup>-2</sup> contour of both scenarios, a dose rate of 0.08 mSv h<sup>-1</sup> is calculated before employment of countermeasures (see Figures 4-17 and 4-33). During the early phase, significant employment of in-place countermeasures (i.e. sheltering, ad hoc respiratory protection, decontamination and control of food and water use) to combat both external and internal exposures may reduce the projected dose to levels within, or slightly above, the PAGs listed in Table 5-1. Figures 4-18 – 4-22 (rural scenario) and Figures 4-34 - 4-36 (urban scenario) document the potential reduction of annual dose when employing internal exposure countermeasures. As shown in Figures 4-21 and 4-22, dose from <sup>106</sup>Ru and <sup>125</sup>Sb could be virtually eliminated by controlling food and water uses, as the doses are principally due to intake pathways. Similarly, dose from <sup>90</sup>Sr would also be reduced by employing this countermeasure. Since the external exposure from the cesium radionuclides still constitutes the majority of the total dose expected, evacuation, and temporary relocation, may be required in some areas but should only be determined after risk/benefit analysis is performed as discussed previously.

The largest contour for both scenarios, and thus largest populations which will be affected, is the 0.037 GBq m<sup>-2</sup> contour. With a dose rate of 8 μSv hr<sup>-1</sup>, the affected population would require continued exposure of over 6 hours without employment of controls or countermeasures to receive the 0.05 Sv PAG dose limit for sheltering or evacuation in the early phase. Therefore, employment of countermeasures already discussed would decrease the exposure rate to levels that may not require evacuation or temporary relocations for affected populations during the early phase. During the intermediate phase (i.e. days to months after the release), a projected dose of 0.02 Sv (2 rem) during the first year is the threshold for relocation of the general public. Once

again, a risk/benefit analysis would be required to determine if this action would be required. Long-term employment of controls may be adequate to protect the public in this area during the late phase (i.e. months to years after the release) until sufficient remediation efforts are undertaken.

To calculate the potential risk of developing cancer or severe genetic effects from continuous exposure within the contamination contours in this study, ICRP 60 risk coefficients (see Table 5-3) were utilized.

Table 5-3: ICRP Risk Coefficients (ICRP, 1991).

<b>Exposed Population</b>	<b>Fatal Cancer</b>	<b>Non-fatal Cancer</b>	<b>Severe Hereditary Effects</b>	<b>Total</b>
Adult Workers	0.040 Sv <sup>-1</sup>	0.008 Sv <sup>-1</sup>	0.008 Sv <sup>-1</sup>	0.056 Sv <sup>-1</sup>
Whole Population	0.050 Sv <sup>-1</sup>	0.010 Sv <sup>-1</sup>	0.013 Sv <sup>-1</sup>	0.073 Sv <sup>-1</sup>

An estimation of the risk to workers and emergency personnel cannot be performed in this study because uncertainties regarding the specific response to any given incident. In this case, risk calculations would be greatly affected by the factors discussed previously concerning minimizing exposures in the early phase. Regardless, based on the observed effects of Chernobyl responders, the estimation of risk in this case would probably coincide with published risk calculations discussed in Chapter II of this study.

Risk to the public however, can be estimated based on the population data incorporated in HPAC. Within each contour, the dose received by the affected population within the first year after the incident is multiplied by the risk coefficients in Table 5-3. The dose levels employed assume countermeasures would be employed to



reduce consumption of contaminated food and water and therefore correspond to external exposure only from the ground contamination.

In the rural scenario, an estimated total population of approximately 3500 people would be affected by the contamination. Based on the ICRP risk coefficients and the assumptions discussed above, a total of 18 fatal cancers, 3 non-fatal cancers and 6 severe hereditary effects are estimated. In the urban scenario, where the total population affected by the ground contamination is significantly higher (approximately 100,000), a total of 974 fatal cancers, 195 non-fatal cancers and 253 severe hereditary effects are estimated.

Considering the high degree of uncertainty in these calculations, the calculated fatal cancers in these scenarios, although lower, are roughly comparable to the 2200 calculated fatal cancers estimated as a result of the Chernobyl accident as discussed in Chapter II. Due to the nature of stochastic effects it will be impossible to discern the origin of an induced cancer. Radiation exposure is only one mode of cancer induction and all modes are indistinguishable from one another. Because these are theoretically calculated fatalities, the conclusion from these levels should be used as a guide to institution of countermeasures and other controls rather than determining the number of cancer patients to expect in the future.

The process of multiplying a chronic dose rate by a cancer risk factor and an exposed population, as done in this study, has been found to vastly overestimate the number of resulting cancers. Following the Chernobyl accident, one such study estimated that over 53,000 people in the US would die after exposure to low dose rates (i.e. 4.6  $\mu$ Sv per person) from fallout material (Jaworowski, 1999). Not only has there

not been an observable increase of cancer induction in the US from this source over the past 20 years, there has been no evidence of a major public health impact, increase in overall cancer incidence or increase in non-malignant disorders, attributable to radiation exposure in populations around Chernobyl. Additionally, the risk of leukemia, one of the main concerns owing to its short latency time, does not appear to be elevated, not even among the recovery operation workers (UNSCEAR, 2000a.).

Also, attempts to quantify the lifetime cancer mortality risks resulting from medical procedures have generated similar overestimates. A study performed at Columbia University determined the potential risks of low radiation doses from computed tomography (CT) scans will result in cancers proportional to those experienced in the atomic bomb populations (i.e. the theory of LNT). The theory of LNT presumes that the detrimental effects of radiation are proportional to dose. In this report, the authors applied this theory to their study and estimated the lifetime cancer mortality risk from a single abdominal CT examination in a 1 year old child to be approximately 1 in 550 and 1 in 1500 for a head CT examination (Brenner et al., 2001). In fact, similar lifetime cancer mortality risk estimates, based on this Columbia University study, have been published in national papers. Overestimates such as these have been found to significantly contribute to the public misconception about the hazards of radiation. To date, no measurable increases in cancers in children undergoing CT procedures have been measured in the US, and it is likely that some truly needed CT images were refused by parents worried about the associated radiation exposures.

Certainly, the study of the human health effects resulting after an event of this nature is critical to evaluations involving the health and safety of the public. Similarly,

the environmental concerns must be analyzed and understood in order to restore the affected areas to conditions at or similar to those present before the incident.

### Environmental Effects

The environmental concerns resulting from a dispersal of spent fuel will result in substantial decontamination and remediation as well as possible long-term monitoring. Similarly to the human exposure effects, actions taken in the early and mid phases of the response are likely to have a profound impact on site restoration. Additionally, responsible officials will have to take into consideration the restoration of confidence of local residence, potential economic partners, and customers upon whom their future economy will depend.

As listed in Table 5-4, the mean  $^{134}\text{Cs}$  and  $^{137}\text{Cs}$  release activity generated in this study exceeds the Chernobyl release by approximately 47% and 74%, respectively. Conversely, the mean  $^{90}\text{Sr}$  activity estimated in these scenarios is approximately 30% less than the activity released after the Chernobyl accident.

Table 5-4: Comparison of released activities for select radionuclides.

Radionuclides	Rural Scenario Radionuclide Released (GBq)	Urban Scenario Radionuclide Released (GBq)	Mean HPAC Radionuclide Release (GBq)	Chernobyl Radionuclide Released (GBq)	Percent Difference (HPAC vs Chernobyl)
$^{134}\text{Cs}$	8.51E+07	7.40E+07	7.96E+07	5.40E+07	147.31%
$^{137}\text{Cs}$	1.59E+08	1.37E+08	1.48E+08	8.50E+07	174.12%
$^{90}\text{Sr}$	7.40E+06	6.66E+06	7.03E+06	1.00E+07	70.30%

A comparison of the contamination contours generated in this study and the Chernobyl exclusion zone characterization by UIAR also highlights the potential magnitude of contamination requiring remediation.

As a result of the UIAR characterization as stated previously, approximately 4000 TBq (~ 0.11 MCi) of  $^{137}\text{Cs}$  contamination and 810 TBq (~ 0.022 MCi) of  $^{90}\text{Sr}$  contamination were measured in the exclusion area around Chernobyl approximately 12 years after the accident. Corrected for physical decay only, these results increase to 5278 TBq (~ 0.14 MCi) and 1082 TBq (~ 0.029 MCi), respectively and is an estimate of the activity of each radionuclide in the contaminated area within the first year following the accident. Based on these results and the current estimates of the total radionuclides released as a result of the accident (see Table 2-3), only approximately 6% of the  $^{137}\text{Cs}$  and 11% of the  $^{90}\text{Sr}$  released was deposited within the exclusion area.

Within the exclusion zone, the average density of  $^{137}\text{Cs}$  contamination ranges between 0.75 and > 20.0 MBq m<sup>-2</sup> (see Table 4-1). Correcting for physical decay of each isotope over the subsequent 12 years, the original density of contamination in 1986 can be estimated at between 1.0 and 26 MBq m<sup>-2</sup>. Assuming a similar soil density as used in this study (1.5 g cm<sup>-3</sup>), along with the majority of contamination remaining within the top 30 cm of soil (Kasparov, 2001), the  $^{137}\text{Cs}$  soil concentration after the accident is estimated to be between 2.2 and 59 Bq g<sup>-1</sup>. The upper limit of this range is slightly below the  $^{137}\text{Cs}$  soil concentrations estimated in the 0.037 GBq m<sup>-2</sup> (0.001 Ci m<sup>-2</sup>) contour in this study (81.8 and 82.9 Bq g<sup>-1</sup> respectively) as listed in Table 4-5 for the rural scenario and Table 4-7 for the urban scenario.

Similarly, the  $^{90}\text{Sr}$  contamination range in the immediate vicinity of Chernobyl (see Table 4-2) is shown to be approximately between 0.75 and 7.50 MBq m<sup>-2</sup>. After decay correction, this activity range increases to between 1.0 and 10 MBq m<sup>-2</sup>. Under the same assumptions used in the previous paragraph, the  $^{90}\text{Sr}$  soil concentration directly after the Chernobyl accident is estimated to be between 2.2 and 22 Bq g<sup>-1</sup>. As listed in Table 4-5 and Table 4-7, the  $^{90}\text{Sr}$  soil concentration estimated in the 0.037 GBq m<sup>-2</sup> (0.001 Ci m<sup>-2</sup>) contour in this study (3.81 and 4.03 Bq g<sup>-1</sup> respectively) are within this range.

Although the contamination in this study results from a NRC-regulated site, the question of which agency (NRC or EPA) has final decision-making authority in determining remediation levels would be an important concern in the intermediate and late phases of the incident. The NRC/EPA MOU (see Chapter 2) suggests that the EPA would probably enforce its decision-making rights at this site because of the three conditions in the agreement. Even with this MOU, the nature and size of this incident would probably cause these agreed-upon procedures to be re-evaluated. Also, the MOU refers to the decommissioning and decontamination of NRC-licensed sites. An argument could be made that the situations suggested in this study do not constitute traditional NRC-licensed sites and thus the MOU would not be applicable.

Assuming this to be the case and each agency applies their own criteria for remediation of the affected areas, the increases in cancer risk is minimal as determined by the RESRAD modeling parameters utilized in this study. This is illustrated in Figure 5-1 as the total cancer risk estimated in this study differs only slightly within the first years after an incident when both criteria are applied.

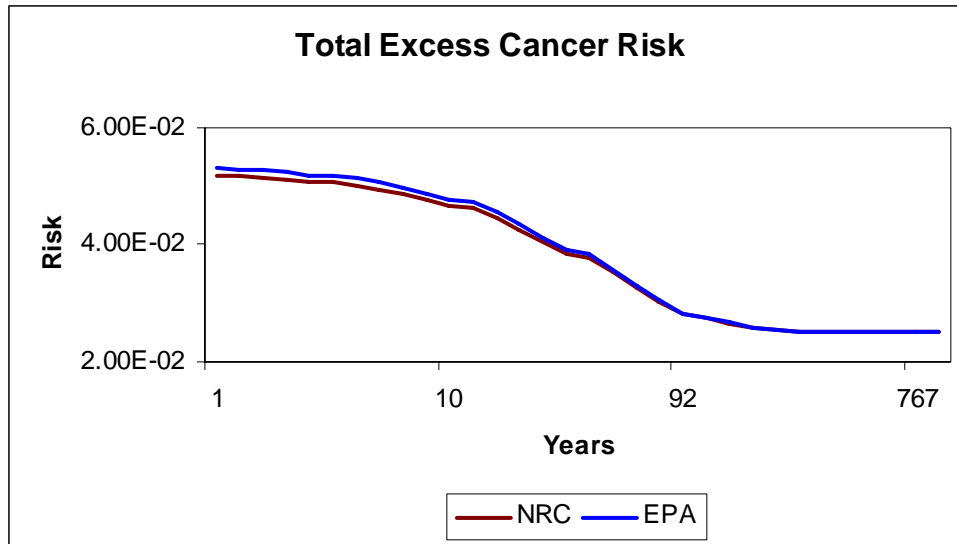


Figure 5-1: Comparison of NRC and EPA Remediation Criteria.

Without question, the various contaminated areas will require differing levels of remediation. The results of this study, and the example discussed below, suggest that determination of a final approach should not be a limiting factor in the intermediate or late response.

In 2002, the ITRC Radionuclides Team released a document summarizing the various regulatory standards used to develop cleanup levels, as well as 12 case studies that demonstrate these standards. This document, entitled “Determining Cleanup Goals at Radioactively Contaminated Sites: Case Studies,” examines the context in which cleanup levels have been developed at various radioactively contaminated sites and identifies common themes and lessons that could improve future decision making.

As described previously, calculation of cleanup levels vary due to site authority (i.e. NRC or EPA) and subsequent methodology. Under both criteria, many parameters are utilized to ultimately determine the remediation goal applied to a site. Although use

of parameters may differ, both approaches require selecting appropriate scenarios, models/equations, and site-specific input parameters.

Of the case studies presented by ITRC, a majority utilized EPA methodologies for determining site remediation goals which is commonly believed to result in lower radiation exposures to affected populations. At the Rocky Flats site, summarized below, it was shown that the dose approach resulted in the lowest exposures.

The Rocky Flats Environmental Technology Site, about 16 miles northwest of Denver, was previously a fabrication site for nuclear weapons components and involved the use of plutonium, uranium and tritium. Large releases of radioactive materials to the environment occurred because of fires and storage leaks during the time of site operation.

In 1972, the Colorado Board of Health was asked to determine levels of plutonium in soil below which construction activities could safely occur. In response, the board approved a standard that required “special techniques of construction” in areas where plutonium contamination exceeded  $0.033 \text{ Bq g}^{-1}$  ( $0.9 \text{ pCi g}^{-1}$ ). By approving this standard, they created an ARAR for this site.

In 1996, the DOE, EPA, and the Colorado Department of Public Health and Environment signed the Rocky Flats Cleanup Agreement (RFCA). Within the RFCA, an enforceable attachment, the Action Levels and Standards Framework (ALF), included a list of soil contaminant levels that trigger remedial or managerial actions. Risk based PRGs were calculated for nonradioactive hazards and radiation dose-based values were considered more appropriate and useful for radionuclides. For determining remediation levels for radionuclides, the RFCA prescribed two future land users: an office worker to represent potential reuse of the industrial area and an open-space user. The soil activity

equivalent to a 0.15 mSv (15-mrem) annual dose was back calculated for both scenarios using the latest RESRAD code at the time, version 5.61. To comply with the then-proposed Radiation Site Cleanup Regulations (40 CFR 196), these levels were then compared to an activity level calculated for a 0.85 mSv (85 mrem) annual dose to a resident. As Table 5-5 illustrates, a 0.15 mSv (15 mrem) dose to an office worker was calculated to be more conservative than the 0.85 mSv (85 mrem) dose to a suburban resident. For the open-space user however, the 0.85 mSv (85 mrem) dose to a suburban resident was more restrictive. Therefore, these respective activities were adopted as upper level, or Tier 1, values corresponding to  $10^{-4}$  risk and values exceeding these levels generally required remedial actions. The 0.15 mSv (15 mrem) annual dose to residents was adopted as lower level, or Tier 2, values corresponding to  $10^{-6}$  risk and required an evaluation to determine whether potential impacts to surface water or ecological resources would require an action.

Table 5-5. Radionuclide Surface Soil Action Levels for Rocky Flats, in pCi/g (ITRC, 2002)

Radionuclide	Rural Resident		Office Worker 15 mrem <sup>c</sup>	Open-Space User 15 mrem
	15 mrem <sup>a</sup>	85 mrem <sup>b</sup>		
Americium-241	38	215	209	1,283
Plutonium-239/240	252	1,429	1,088	9,906
Uranium-234	307	1,738	1,627	11,500
Uranium-235	24	135	113	1,314
Uranium-238	103	586	506	5,079

<sup>a</sup> Applied as Tier II action levels.

<sup>b</sup> Applied as Tier I action levels.

<sup>c</sup> Applied as Tier I action levels for industrial reuse.

This example presented illustrates that direct comparisons of NRC's annual dose criterion with EPA's lifetime cancer risk criterion for the purposes of determining which criterion would be more protective of the public can be misleading. The level of health



protection that is achieved by applying either criterion depends on many site specific assumptions and not simply the general assumption that a lower dose criterion provides greater protection.

Further complicating this overall process is the designation of the “Lead Federal Agency” (LFA). The LFA is defined as the agency designated by the President to lead and coordinate the overall federal response (NCRP, 2001). The designated agency may change over time as the FBI typically assumes this role in large scale incidents during the “crisis management” phase (i.e. addressing the causes of a terrorist event) and many agencies, including the NRC and EPA, assume this role during the “consequence management” phase (i.e. addressing how the incident will affect public health, safety, and the environment).

Even with a clear line of authority, organizations in a supporting role will respond pursuant to their own responsibilities and authorities. Organizations with similar responsibilities will inevitably clash over authority or procedures. For example, the EPA has independent statutory authority to respond to threats to humans and the environment. Similar statutory authority exists at state and local levels. With multiple authorities responding independently, great efforts must be taken to facilitate effective coordination between these agencies to ensure overall command and control is not affected.

### Psychosocial and Economic Impacts

Although beyond the scope of this study, it is essential to recognize the psychosocial and economic impacts of a successful attack at a SFP as they may be turned out to be more important to the overall well-being of the public than the human health effects from radiation exposure.

Acts of conventional terrorism have been found to produce especially high levels of psychosocial morbidity. Based on recent studies, civilian terrorist attacks have been found to produce high rates of post traumatic stress disorder as well as elevated risks of depression, self-medication and substance abuse (NCRP, 2001). Acts of terrorism resulting in radiation exposure may cause to increase these effects as many in the general public are exceptionally fearful of radiation.

Additionally, as witnessed after the Chernobyl accident, the relocation of residential populations proved to be a deeply traumatic experience in itself. Furthermore, poverty, “lifestyle” diseases (i.e. alcoholism, sexually transmitted diseases, etc.) and mental health problems pose a far greater threat to local communities than radiation exposure. As previously discussed, the results of the radiation exposure analysis in this study also suggest temporary relocations could be required if the benefit of such an act outweighs the corresponding risk.

The economic impacts of a SFP incident in the U.S. and the Chernobyl accident in the former Soviet Union would be vastly different. The economic foundations of the respective areas, along with the economic changes over the past 20 years, prevent a direct comparison of events for the purposes of this study. There is no question that the costs of responding to, operating in and restoring the affected area would be tremendous. Some reports estimate the property losses from the deposition downwind of the <sup>137</sup>Cs released by a spent-fuel-pool fire would likely be hundreds of billions of dollars (Alvarez, 2003).

This level of economic loss has been experienced in the U.S. as recently as 2005 after hurricane Katrina. There has been tremendous criticism of the Federal Government’s immediate response to this disaster. Although many people worked hard

to help mitigate the disaster in its aftermath, as a whole, the government was criticized for not being prepared for the events. The economic impacts have been far-reaching. As of April 2006, the Bush Administration has sought \$105 Billion for repairs and reconstruction in the region, making it the costliest natural disaster in US history. Current estimates have determined the total cost could approach \$200 billion (Wikipedia, 2006).

Utilizing the models employed in this study, the movement of older spent fuel out of SFPs to alternative storage, as suggested by Alvarez et al., was studied to determine the magnitude of ground contamination resulting. By simply reducing the spent fuel inventory to the 3 batches that produce adequate decay heat to ignite zirconium while maintaining all other parameters, areas of contamination are significantly reduced. In the rural scenario, the area of contamination for the  $0.037 \text{ GBq m}^{-2}$  ( $0.001 \text{ Ci m}^{-2}$ ) contour is reduced from  $555 \text{ km}^2$  to  $2.5 \text{ km}^2$ . In the  $0.370 \text{ GBq m}^{-2}$  ( $0.01 \text{ Ci m}^{-2}$ ) contour, this area is reduced from  $55 \text{ km}^2$  to  $0.11 \text{ km}^2$ . Similarly, the areas of contamination in the urban scenario are reduced from  $160 \text{ km}^2$  to  $38 \text{ km}^2$  and  $8 \text{ km}^2$  to  $2 \text{ km}^2$ , respectively. Furthermore, the number of people that would be located within the contamination contours of the urban scenario reduces from approximately 100,000 to 20,000. Economically, this reduction of possible victims would be substantial. Although further analysis of this must be completed, these preliminary results provide an encouraging means of protecting people and property from the effects of a successful spent fuel attack.

## CHAPTER VI

### CONCLUSION

Utilizing the HPAC model, under the estimated worst-case conditions presented in this study, dispersal of radionuclides as a result of a zirconium fire in a SFP result in contamination levels similar to those measured after the Chernobyl accident in 1986. As this is a general study with many assumptions taken, careful analysis of individual SFPs using site-specific parameters (i.e. SFP inventory, weather, etc.) could easily be accomplished to better determine a potential dispersion of radionuclides.

This study does not endorse either point of view in regards to the controversies regarding the probability of a successful SFP incident. At this time, there are groups performing intricate studies to help answer this question. These, and other studies, should provide considerable insight into the likelihood of a successful SFP attack. This study does provide analysis as to the potential magnitude of a successful SFP incident however. Although some studies have suggested that a zirconium fire in a SFP could release up to 20 times the amount of  $^{137}\text{Cs}$  than released from the Chernobyl accident or that areas up to 75% the size of New York State could be rendered inhabitable (Riverkeeper, 2004), the results of this study suggest that these predictions are perhaps overstated. As discussed previously, comparison of  $^{137}\text{Cs}$  and  $^{90}\text{Sr}$  releases from Chernobyl and this study show the levels to be generally similar. Additionally, HPAC results demonstrate that the size of an exclusion zone may be relatively small.

The RESRAD analysis performed here shows that areas close to the SFP would require at least a temporary relocation of the residential population, but the areas included may not be as large as the Chernobyl exclusion zone. In these contaminated areas, the potential for receiving exposures at levels that could produce deterministic effects is possible, but would be manageable with strict adherence to access control and other safety procedures.

In areas further from the SFP, a risk/benefit analysis on the use of countermeasures and other controls, especially in the early phases, is needed to determine whether or not the affected populations would be better protected by remaining in place. The long-term health effects expected would be similar to those measured after the Chernobyl accident as presented in this study. Similarly, a site-specific analysis at each SFP to better determine the environmental parameters utilized in the model would significantly reduce the uncertainty in the results presented in the study.

The list of documents addressing response to RDDs or similar radiological and nuclear devices, many of which are utilized in this study, is growing. Although the actions required in the aftermath of each event are similar in many ways, few documents exist that specifically address large releases of spent fuel. The Federal, State, and local governments, and their many agencies, must ensure a response to a terrorist attack of this nature does not suffer from the failures witnessed after Hurricane Katrina. In all phases of response, the lines of authority must be clearly drawn so that all agencies know their roles and responsibilities. Careful planning should be accomplished to ensure conflicts and duplication of resources is minimized while standardizing decision-making thresholds (i.e. PAGs) so there are no questions or debates at the time of a crisis. The

levels of training and equipping of responders since 9/11 must continue to ensure an ever-ready core of competence.

Psychosocial and economical issues arising from a large-scale terrorist attack of this nature are not fully understood and must be analyzed further. Many lessons have been learned from various natural and man-made disasters regarding psychosocial issues that arise in their aftermath. Continued research in both short-term and long-term effects will help responders mitigate such consequences. A thorough study of the economic considerations of shifting to alternate storage should be accomplished, as discussed previously, to determine the economic costs of finding alternative storage solutions outweigh the economic costs of a potential incident.

## REFERENCES

- Alvarez, Robert, et al., *Reducing the Hazards from Stored Spent Power-Reactor Fuel in the United States*. Science and Global Security 11 (2003): 1-51.
- Alvarez, Robert, et al., Response by the Authors to the NRC Review of “Reducing the Hazards from Stored Spent Power-Reactor Fuel in the United States.” Science and Global Security 11 (2003): 213-223.
- Argonne (2005a.), Argonne National Laboratory, *Human Health Fact Sheet: Cesium*, Aug. 2005. 15 Nov. 2005 <<http://www.ead.anl.gov/pub/doc/cesium.pdf>>.
- Argonne (2005b.), Argonne National Laboratory, *Human Health Fact Sheet: Strontium*, Aug. 2005. 15 Nov. 2005 <<http://www.ead.anl.gov/pub/doc/strontium.pdf>>.
- Argonne (2005c.), Argonne National Laboratory, *Radiological Dispersal Device*, Aug. 2005. 31 Jan. 2006 <<http://www.ead.anl.gov/pub/doc/rdd.pdf>>.
- Brenner D.J., et al. *Estimated Risks of Radiation-Induced Fatal Cancer from Pediatric CT*, American Journal of Roentgenology 176 (2001): 289-296.
- Cember, Herman., *Introduction to Health Physics*, 3<sup>rd</sup> Edition. McGraw-Hill, 1996.
- CRS (2005), Congressional Research Service, *Nuclear Power Plants: Vulnerability to Terrorist Attack*, CRS Report for Congress, 4 Feb. 2005. 9 Dec. 2005 <<http://www.fas.org/irp/crs/RS21131.pdf>>.
- DHS (2006), U.S. Department of Homeland Security, *Protective Action Guides for Radiological Dispersal Device and Improvised Nuclear Device Incidents*, Federal Register Volume 71, No. 1. 3 Jan 2006. 5 May 2006. <<http://www.ostp.gov/html/RDDIND1-3-06.pdf>>.
- EPA (1990). U.S. Environmental Protection Agency. “40 CFR Part 300 – National Oil and Hazardous Substance Pollution Contingency Plan,” Final rule, 55 FR 8666-8865 (U.S. Government Printing Office, Washington).
- EPA/NRC (2002). U.S. Environmental Protection Agency/U.S. Nuclear Regulatory Commission. *Memorandum of Understanding Between the Environmental Protection Agency and the Nuclear Regulatory Commission. Consultation and Finality on Decommissioning and Decontamination of Contaminated Sites* (October 9), June 2005 <<http://www.epa.gov/superfund/resources/radiation/pdf/mou2fin.pdf>> (U.S. Environmental Protection Agency, Washington).
- Gonzalez, A.J. (2005), *Lauriston S. Taylor Lecture: Radiation Protection in the Aftermath of a Terrorist Attack Involving Exposure to Ionizing Radiation*, Health Physics 89.5 (2005): 418-446.

- Gustafson, P.F., Nelson, D.M., Brar, S.S., and Muniak, S.E. (1971). "Recent trends in radioactive fallout," page 245 in *Radiological Physics Division Annual Report*, ANL-7760-III (Argonne National Laboratory, Argonne, Illinois).
- Hall, E.J., *Radiobiology for the Radiologist*, 5<sup>th</sup> Ed. Philadelphia: Lippincott Williams & Wilkins, 2000.
- HPAC, *Hazard Prediction Assessment Capability, Version 4.04*, CD-ROM. Defense Threat Reduction Agency, 2004.
- HEAST (2001). *Health Effects Assessment Summary Tables*, August 2005 <<http://www.epa.gov/radiation/heast>> (U.S. Environmental Protection Agency, Washington).
- InfoUkes (1997), InfoUkes Inc., *The Chernobyl Nuclear Accident and it's Ramifications*, 24 Apr. 1997. 15 Nov. 2005 <<http://www.infoukes.com/history/chornobyl/>>.
- IAEA (1988), International Atomic Energy Agency, *The Radiological Accident at Goiania*, September 1988, 4 Apr. 2006 <[http://www-pub.iaea.org/MTCD/publications/PDF/Pub815\\_web.pdf](http://www-pub.iaea.org/MTCD/publications/PDF/Pub815_web.pdf)>.
- ICRP (1979). International Commission on Radiological Protection. *Limits for Intakes of Radionuclides by Workers*, ICRP Publication 30, Supplement to Part 1, Ann. ICRP 3 (1-4).
- ICRP (1991). International Commission on Radiological Protection. *Recommendations of the International Commission on Radiological Protection*, ICRP Publication 60, Ann. ICRP 21(1-3).
- ICRP (1996). International Commission on Radiological Protection. *Age-Dependent Doses to Members of the Public from Intake of Radionuclides: Part 5: Compilation of Ingestion and Inhalation Dose Coefficients*, ICRP Publication 72, Ann. ICRP 26(1).
- ICRP (2003). International Commission on Radiological Protection. *A Framework for Assessing the Impact of Ionising Radiation on Non-human Species*. ICRP Publication 91, Ann. ICRP 33,3.
- INESAP (2005), International Network of Engineers and Scientists Against Proliferation, *Radiological Terrorism: Sabotage of Spent Fuel Pool*, Bulletin 22. 24 Oct. 2005 <<http://www.inesap.org/bulletin22/bul22art30.htm>>.
- ITRC (2002), Interstate Technology and Regulatory Council, *Determining Cleanup Goals at Radioactively Contaminated Sites: Case Studies*, 14 Oct. 2004. <<http://www.itrcweb.org/user/RAD-2.pdf>>.



- Jaworowski, Z., *Radiation Risk and Ethics*, (1999). 17 July 2006.  
<<http://www.riskworld.com/nreports/1999/jaworowski/NR99aa01.htm>>.
- Kashparov, V.A., et al., *Soil Contamination with <sup>90</sup>Sr in the near zone of the Chernobyl accident*, *Environmental Radioactivity* 56 (2001) 285-298.
- Lamarsh, John R., and Antony J. Baratta. *Introduction to Nuclear Engineering*. 3<sup>rd</sup> ed. New Jersey: Prentice-Hall, Inc., 2001.
- Mycio, M., *Wormwood Forest: A Natural History of Chernobyl*, Washington: John Henry Press, 2005.
- NAS (1996), National Academy of Sciences, *Radiochemistry in Nuclear Power Reactors*, Washington D.C.: The National Academies Press, 1996.
- NAS (2006), National Academy of Sciences, *Safety and Security of Commercial Spent Nuclear Fuel Storage: Public Report*, Washington D.C.: The National Academies Press, 2006.
- National (1971), National Research Council Panel on Radioactivity in the Marine Environment, *Radioactivity in the Marine Environment* (National Academy of Sciences, Washington).
- NCRP (2004). National Council on Radiation Protection and Measurements. *Approaches to Risk Management in Remediation of Radioactively Contaminated Sites*, NCRP Report No. 146 (National Council on Radiation Protection and Measurements, Bethesda, Maryland).
- NCRP (2001). National Council on Radiation Protection and Measurements. *Management of Terrorist Events Involving Radioactive Material*, NCRP Report No. 138 (National Council on Radiation Protection and Measurements, Bethesda, Maryland).
- NCRP (1991). National Council on Radiation Protection and Measurements. *Some Aspects of Strontium Radiobiology*, NCRP Report No. 110 (National Council on Radiation Protection and Measurements, Bethesda, Maryland).
- NCRP (1977). National Council on Radiation Protection and Measurements. *Cesium-137 From the Environment to Man: Metabolism and Dose*, NCRP Report No. 52 (National Council on Radiation Protection and Measurements, Bethesda, Maryland).
- NEA (2002), Nuclear Energy Agency, *Chernobyl: Assessment of Radiological and Health Impact*, 8 Jan. 2006 <<http://www.nea.fr/html/rp/chernobyl/c02.html>>.

- NRC (2001), U.S. Nuclear Regulatory Commission, *NUREG-1738: Technical Study of Spent Fuel Accident Risk at Decommissioning Nuclear Power Plants*, (Office Nuclear Reactor Regulation, U.S. Nuclear Regulatory Commission, Washington).
- NRC (2003), U.S. Nuclear Regulatory Commission, *Spent Fuel Pool*, 23 Jun. 2003. 16 Nov. 2005 <<http://www.nrc.gov/waste/spent-fuel-storage/pools.html>>.
- NRC (2005), U.S. Nuclear Regulatory Commission, *Fact Sheet: The Accident at Three Mile Island*, 31 Mar. 2005. 15 Mar 2006. <<http://www.nrc.gov/reading-rm/doc-collections/fact-sheets/3mile-isle.html>>.
- NWS (2005), National Weather Service, *NWS Support During Hazardous Materials Emergencies*, 2005. 30 May 2006 <[http://meted.ucar.edu/dispersion/disp\\_ops/index.htm](http://meted.ucar.edu/dispersion/disp_ops/index.htm)>.
- ORNL (1994), Oak Ridge National Laboratory, *U.S. Spent Nuclear Fuel and Radioactive Waste Inventories, Projections, and Characteristics*, Integrated Database Report, 1994. 25 Oct. 2005 <<http://www.davistownmuseum.org/cbm/RadXIntegratedDatabase.html>>.
- PSR (2005), Physicians for Social Responsibility, *Preventing Nuclear Terrorism: Nuclear Power and the Terrorist Threat*, Factsheet. Sep. 2005. 24 Oct. 2005 <[http://www.psr.org/home.cfm?id=factsheets\\_nuc\\_power](http://www.psr.org/home.cfm?id=factsheets_nuc_power)>.
- RADAR, The Radiation Dose Assessment Resource, Stanford Dosimetry, LLC. 3 Mar 2006 <<http://www.doseinfo-radar.com/RADARHome.html>>.
- REAC/TS (2002), Radiation Emergency Assistance Center/Training Site, *Insoluble Prussian Blue*, Informational Material Package Insert. 14 Nov. 2002. 18 Jan. 2006 <<http://www.orau.gov/reacts/prussian.htm>>.
- Riverkeeper (2002), Riverkeeper, Inc., *Chernobyl-On-The-Hudson: The Indian Point – Chernobyl Comparison*, Issue Brief. 2002. 12 Jan. 2006. <[http://riverkeeper.org/document.php/320/ISSUE\\_BRIEF\\_\\_TH.doc](http://riverkeeper.org/document.php/320/ISSUE_BRIEF__TH.doc)>.
- Shlyakhter, Alexander, and Richard Wilson, *Chernobyl: the inevitable results of secrecy*, Public Understand. Sci. 1, (1992) 251-259.
- Turner, J.E., *Atoms, Radiation, and Radiation Protection*, McGraw-Hill, 1970.
- UIAR (2001), *Contamination of the ChNPP 30-km Zone*, CD-ROM. Ukrainian Institute of Agricultural Radiology, 2001.
- UNSCEAR (2000a.), United Nations Scientific Committee on the Effects of Atomic Radiation, *Sources and Effects of Ionizing Radiation*, 2000 Report to the general assembly, Volume 1, 9 Jan. 2006 <[http://www.unscear.org/reports/2000\\_1.html](http://www.unscear.org/reports/2000_1.html)>.

- UNSCEAR (2000b.), United Nations Scientific Committee on the Effects of Atomic Radiation. *Sources and Effects of Ionizing Radiation*, 2000 Report to the general assembly, with scientific annexes, Volume 2, Annex J., 9 January 2006 <<http://www.uic.com.au/unsearcherno.htm>>.
- WHO (2005a.), World Health Organization. *Health Effects of the Chernobyl Accident and Special Health Care Programs*, Report of the UN Chernobyl Forum Expert Group “Health”, Working Draft. 31 August 2005. 12 January 2006 <[http://www.who.int/ionizing\\_radiation/a\\_e/chernobyl/-EGH%20Master%20file%202005.08.24.pdf](http://www.who.int/ionizing_radiation/a_e/chernobyl/-EGH%20Master%20file%202005.08.24.pdf)>
- WHO (2005b.). World Health Organization. *Chernobyl: The True Scale of the Accident*, Joint News Release WHO/IAEA/UNDP, 5 September 2005. 10 March 2006 <<http://www.who.int/mediacentre/news/releases/2005/pr38/en/print.html>>.
- Wikipedia (2005), *Radiation Hotspots Resulting from the Chornobyl Nuclear Power Plant Accident*, Map., Wikipedia: The Free Encyclopedia. 15 Nov. 2005 <[http://upload.wikimedia.org/wikipedia/en/0/07/Chornobyl\\_radiation\\_map.jpg](http://upload.wikimedia.org/wikipedia/en/0/07/Chornobyl_radiation_map.jpg)>.
- Wikipedia (2006a.) *Compilation of atmospheric dispersion models*. Wikipedia: The Free Encyclopedia. 2 May 2006. 30 May 2006 <[http://en.wikipedia.org/wiki/Compilation\\_of\\_atmospheric\\_dispersion\\_models](http://en.wikipedia.org/wiki/Compilation_of_atmospheric_dispersion_models)>.
- Wikipedia (2006b.), *Economic effects of Hurricane Katrina*. Wikipedia: The Free Encyclopedia. 23 May 2006. 25 May 2006 <[http://en.wikipedia.org/wiki/Economic\\_effects\\_of\\_Hurricane\\_Katrina](http://en.wikipedia.org/wiki/Economic_effects_of_Hurricane_Katrina)>.
- WNA (2005a.), World Nuclear Association, *Chernobyl Accident*, September 2005. 2 November 2005 <<http://www.world-nuclear.org/info/chernobyl/inf07.htm>>.
- WNA (2005b.), World Nuclear Association, *Processing of Used Nuclear Fuel for Recycle*, December 2005. 14 March 2006 <<http://www.world-nuclear.org/info/inf69.htm>>.
- Yu, C. et al., *Users Manual for RESRAD Version 6*, Jul. 2001. Illinois: Argonne National Laboratory, 12 Oct. 2005. <<http://web.ead.anl.gov/resrad/documents/resrad6.pdf>>.